EUROPEAN SCHOOL OF MOLECULAR MEDICINE (SEMM)
CAMPUS IFOM-IEO
MILAN

SHEDDING LIGHT ON GLIOBLASTOMA AND DERIVED EXTRACELLULAR VESICLES IN ONE CLIC

PhD in Molecular Medicine

Setti Matteo

Supervisor: Pelicci Giuliana MD PhD
Department of Experimental Oncology
IEO (European Institute of Oncology)

Co-Supervisor: Rolf Bjerkvig PhD
Department of Biomedicine
University of Bergen

TABLE OF CONTENTS

LIST OF ABBREVIATIONS

ALIX	Apoptosis-linked gene 2-interacting protein X
Amp	Amplified
BMP	Bone Morphogenic Protein
BSA	Bovine Serum Albumin
CDK	Cyclin-Dependent Kinase
CGH	Comparative Genomic Analysis
Chk	Checkpoint Protein
CLIC(1-6)	Chloride Intracellular Ion Channel (1-6)
CNS	Central Nervous System
CSC	Cancer Stem Cell
Ct	Computer Tomography
DAPI	4,6-diamidino-2-phenylindole
DIDS	4,4'-Diisothiocyano-2,2'-stilbenedisulfonic acid
DNA	Desoxyribonucleic acid
EDTA	Ethylenediaminetetraacetic acid
EGF(R)	Epidermal Growth Factor (Receptor)
EV	Extracellular vesicle
FACS	Fluorescence Activated Cell Sorting
FFPE	Formalin-Fixed Paraffin-Embedded
FGF	Fibroblast Growth Factor
FSC	Forward Scatter
GBM	Glioblastoma
G-CIMP	Glioma-CpG Island Methylator Phenotype
GFP	Green Fluorescent Protein
GM130	cis-Golgi Matrix 130
GSC	Glioma Stem Cell
H&E	Hematoxylin and Eosin
HGF(R)	Hepatocyte Growth Factor (Receptor)
HPRT1	Hypoxanthine PhosphoRibosylTransferase 1
IAA-94	Indanyloxyacetic acid–94
IDH	Isocitrate Dehydrogenase
IGF	Insulin-like Growth Factor
LOH	Loss Of Heterozigosity
mAb	monoclonal Antibody
MAPK	Ras-Mitogen-Activated Protein Kinase
MDR	Multi-Drug Resistance
MGMT	O-6-MethylGuanine-DNA MethylTransferase
MRI	Magnetic Resonance Imaging
mRNA	Messenger Ribonucleic Acid
mTOR	Mammalian Target Of Rapamycin
MTT	3-(4, 5-dimethylthiazol-2-yl)-2, 5-diphenyltetrazolium bromide
Mut	Mutated
ND	Not Determinated
NF	NeuroFibromatosis
NSC	Neural Stem Cell
NT	Not Targeting
OE	Over-Expressed
PBS	Phosphate Buffered Saline
PDGF(R)	Platelet-derived Growth Factor (Receptor)
PET	Positron Emission Tomography
PFA	ParaFormAldehyde

PI3K	PhosphatidylInositol 3-Kinase
PLA	Proximity Ligation Assay
PTEN	Phosphatase and Tensin Homologue
qRT-PCR	Quantitative Reverse Transcription-Polymerase Chain Reaction
Rb	Retinoblastoma
RTK	Receptor Tyrosine Kinase
Sh	Short Harpain
Shh	Sonic Hedgehog
TBP	Tata Binding Protein
TCGA	Total Cancer Genome Atlas Research Network
TSG101	Tumor susceptibility gene 101
VEGF(R)	Vascular Endothelial Growth Factor (Receptor)
WHO	World Health Organization

FIGURES INDEX

TABLES INDEX

ABSTRACT

The treatment of glioblastoma (GBM) still represents a tremendous clinical challenge, with the average survival that is not exceeding 14 months. Given the lack of reliable prognostic markers and druggable targets in GBM, several years ago our lab's interest focused on Chloride intracellular channel-1 (CLIC1), a protein belonging to a class of chloride channels that does not fit the classical paradigm of ion channels proteins. CLIC1 proteins can exist as both soluble globular protein and integral membrane protein with ion channel function. Upon oxidative stress, CLIC1 translocates from the cytoplasm to the plasma membrane where it exerts its function as a chloride (Cl^-) channel. CLIC1 is overexpressed in several human solid tumors, including gliomas. In this study we demonstrated that CLIC1 silencing in cancer stem cells (CSCs) isolated from human GBM patients negatively influences both proliferative capacity and self-renewal properties *in vitro* and impairs the *in vivo* tumorigenic potential. Moreover, CLIC1 expression inversely associates with GBM patient survival, thus suggesting a potential exploitation of CLIC1 as a new molecular therapeutic target and a possible outcome predictor. CLIC1 has been identified as a secreted protein and detected in exosomes released from different cell types, including primary tumors. Extracellular vesicles (40-1000 nm) (EVs) are secreted by virtually all cell types that arise from the invagination and the budding of the limiting membrane of late endosomes (hence called multivesicular bodies, MVB). We showed that CLIC1 is a protein localized within EVs isolated by GBM cell lines and GBM-derived CSCs and by tuning CLIC1 expression within EVs it is possible to modulate cellular response to EVs both *in vitro* and *in vivo*.

Taken together, our data suggest that CLIC1 plays an important role in regulating GBM proliferation and tumorigenic status, experimental evidences hint the possible transmission of these features to recipient cells by EV secretion.

1. INTRODUCTION

1.1. Brain tumors

The World Health Organization (WHO) classification system groups gliomas into 4 histological grades defined by increasing degrees of undifferentiation, anaplasia and aggressiveness (Table 1) (Louis D.N. et al., 2007). Malignant gliomas (WHO III-IV) are a group of oncological diseases characterized by heterogeneous cellular composition and diffuse invasiveness. These tumors diffusely infiltrate the surrounding normal tissue and have a high tendency for malignant progression making them fatal. Over the last years our knowledge about brain tumors has increased significantly, especially important progresses have been made by research on glioblastoma (GBM), the most aggressive among brain tumors, and unfortunately the most common (Dolecek T.A. et al., 2012). The demonstration of the existence of cancer stem cells has focused scientific community's attention on some issues such as the identification of the cell of origin of these tumors and the characterization of cells resistant to conventional therapies. The development of new animal models and large-scale genomic analyses of these tumors allowed the identification of mutations that drive tumor development. International organizations that join institutes around the world, such as the Cancer Genome Atlas (TCGA), were created with the mission of understanding 'the molecular basis of cancer through the application of genome analysis technologies' and selected GBM as the first cancer type for study, based on its uniformly poor prognosis and limited treatment options (Brennan C.W., TCGA Research Network, 2013). TCGA permitted collection of huge amount of data on brain tumors and the creation of web-tools freely accessible by the entire scientific community. Sadly, despite some advances in treatment, the overall survival of GBM cases is still not that different than it was several years ago.

Table 1. Classification of Malignant Gliomas and Survival According to the Surveillance, Epidemiology, and End Results (SEER) Program Registry[2]

	Survival, %	
	1-Year	5-Year
WHO grade IV tumors[a]		
Glioblastoma and variants[b]	35.7	4.7
WHO grade III tumors[a]		
Anaplastic astrocytoma	60.1	25.9
Anaplastic oligodendroglioma	81	49.4
Anaplastic oligoastrocytomas	NA	NA

Abbreviations: NA, not available (diagnosis not captured in this database); WHO, World Health Organization.

[a] The WHO classification groups gliomas into 4 grades based on increasing degree of anaplasia and aggressiveness. Malignant gliomas comprise WHO grades III and IV tumors.

[b] Gliosarcoma, giant cell glioblastoma, and small cell glioblastoma.

1.1.1. Epidemiology of gliomas

Gliomas are the most common primary tumors of the central nervous system, they account for the 77% of primary malignant brain tumors with approximately 10'000 deaths and 13'000 new cases annually occurring in the US (Central Brain Tumor Registry of the United States); the 60-70% of this enormous social burden is represented by GBMs. Individuals of all ages can be afflicted but they are most common among elderly adults with a peak around 50 - 55 years. Men are slightly more prone to these neoplasms. Furthermore, the incidence is 2 - 3 times higher in white than in black people (Wen and Kesari, 2008). Prognosis is poor and the median survival is 14.6 months (Stupp R. et al., 2007); only few patients survive for three or more years. Main risk factors are high dose radiation, hereditary syndromes and increasing age. Only 5% of patients have a family history of gliomas: in most cases they are affected by rare genetic syndromes, such as neurofibromatosis type 1 and 2, the Li-Fraumeni syndrome and Turcot's syndrome. However the genetic bases of malignant gliomas have not been identified yet.

1.1.2. Morphological classification of gliomas

Gliomas are classified according to the WHO guidelines (Louis D.N. et al., 2007). This classification system is based mainly on histopathology, according to morphological similarities between tumor cells and normal glial cells, cytoarchitecture and

immunohistological marker profile. The WHO divides the diffuse gliomas into three main categories: astrocytomas (related to astrocytes), oligodendrogliomas (related to oligodendrocytes) and oligoastrocytomas (related to a mixture of these two cell types). Furthermore, a grading system was created as a scale of malignancy. Four grades (I, II, III, and IV) distinguish astrocytomas and two grades (II and III) oligodendrogliomas and oligoastrocytomas. Lower grade astrocytomas (grade I-II) are well differentiated, have increased cell density and some cellular anomalies or atypias, but in general they resemble the non-neoplastic tissue. These gliomas are biologically indolent. Tumors of higher grade (grade III tumors) are anaplastic with nuclear atypia, increased vessels and cell density and elevated mitotic activity. The grade IV astrocytoma, also known as GBM, exhibits the additional presence of microvascular proliferation, necrosis and diffuse infiltration throughout the brain parenchyma, which denote the fully malignant state. The moniker "multiforme" derives from the varied morphological features of this tumor, in which heterogeneous cell populations with high degree of cellular and nuclear polymorphism and numerous giant cells coexist with area of high cellular uniformity.

GBM can be divided into two main subtypes on the basis of clinical presentation and biological and genetic differences (Furnari F.B. et al., 2007, Ohgaki H. et al., 2007) (Figure 1). Primary GBMs occur *de novo* with no antecedent lower grade pathology, typically in patients older than 50 years of age. On the contrary secondary GBMs are quite rare and are manifested in younger patients as low grade or anaplastic astrocytomas that transform over a period of 5-10 years into GBM. Late-stage mixed gliomas or oligodendrogliomas can also resemble GBM (Miller C.R. et al., 2007). Primary and secondary GBMs present distinct genetic alterations affecting similar molecular pathway. Primary GBMs are characterized by Epidermal growth factor (EGFR) amplification and mutations, loss of heterozygosity of chromosome 10q, deletions of Phosphatase and tensin homolog (PTEN) and p16. Secondary GBMs are more frequently characterized by mutations in p53 tumor suppressor gene, over-expression of Platlet-derived growth factor receptor (PDGFR),

abnormalities in the p16 and retinoblastoma (Rb) pathways, and loss of heterozigosity of chromosome 10q. Despite the genetic differences and their distinct clinical course, primary and secondary GBMs are morphologically indistinguishable and respond similarly to conventional therapy, but they may respond differently to targeted molecular therapy (Wen P.Y. and Kesari S., 2008; Stupp R. et al., 2007) (Figure 1).

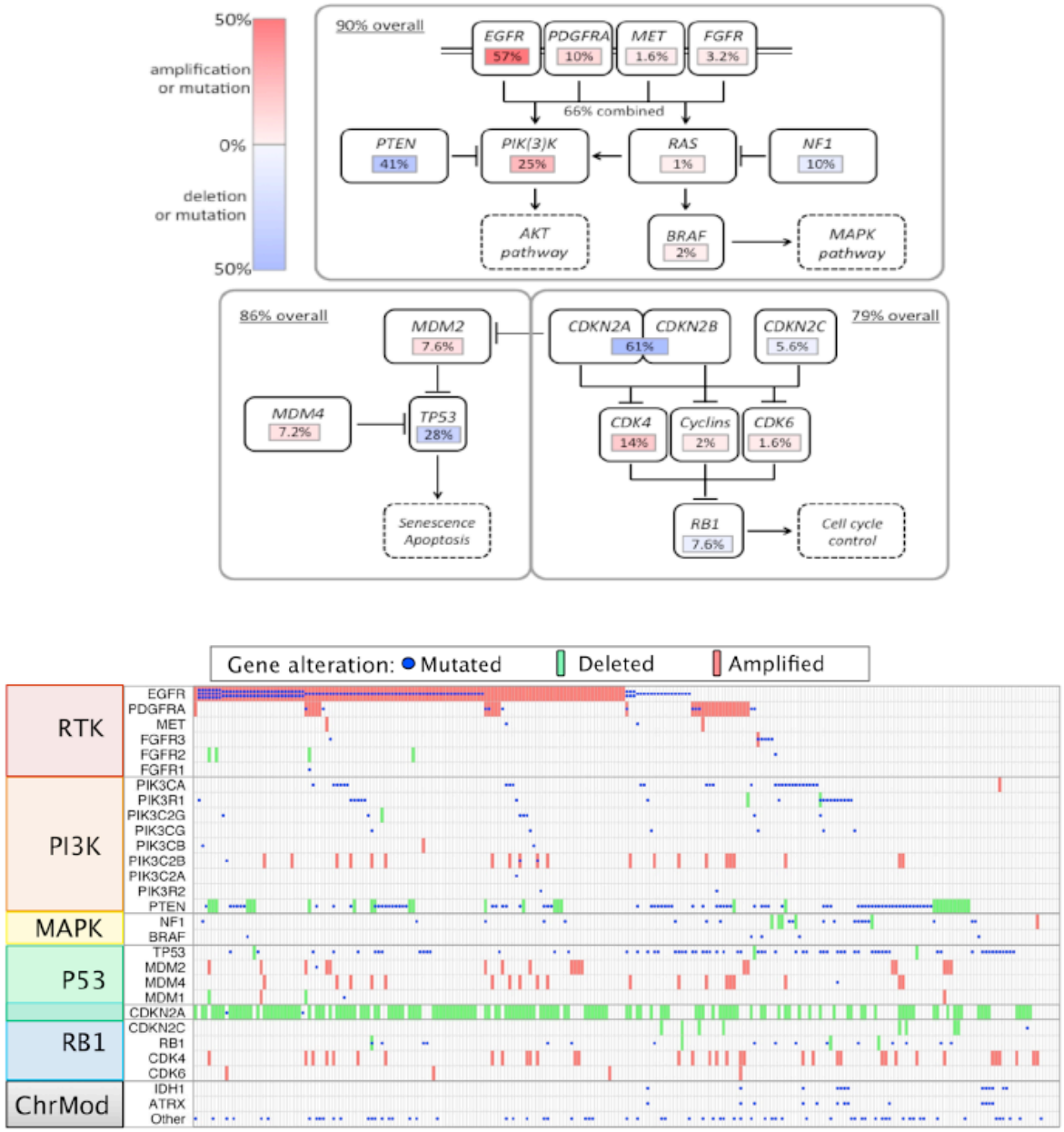

Figure 1. Landscape of Pathway Alterations in GBM. Alterations affecting canonical signal transduction and tumor suppressor pathways are summarized for 251 GBM with both exome sequencing and DNA copy number data. (A) Overall alteration rate is summarized for canonical PI3K/MAPK, p53 and Rb regulatory pathways. (B) Per-sample

expansion of alterations. Mutations (blue), focal amplifications (red) and homozygous deletions are selected and selected by function. Missense, nonsense and frame-shift mutations are included. (Adapted form Brennan C.W. et al., 2013)

1.1.3. Genetic abnormalities in gliomas

Numerous molecular abnormalities are linked to the pathogenesis of different glioma variants. The comparative genomic analyses (CGH) and the large-scale integrated genomic analyses (Cancer Genome Atlas Research Network 2008; Parsons D.W. et al., 2008) have resulted in more comprehensive analyses of the molecular aberrations underlying gliomagenesis. TCGA has so far accumulated expression, copy number alterations and sequencing data from hundreds of histologically confirmed GBMs and has comprehensively catalogued the genomic anomalies associated with GBM. Furthermore, the biological relevance of many of these molecular abnormalities to the process of gliomagenesis has been confirmed by mouse modeling studies (Huse J.T. and Holland E.C. et al., 2009). Genetic alterations characteristic of astrocytic glioma lead to aberrant activation of key signaling pathways mainly those involved in mitogenic signaling and cell cycle control.

1.1.3.1 Growth factor pathways

Alterations of the receptor tyrosine kinases (RTKs) and their associated downstream pathways occur in a large percentage of diffuse gliomas and appear to be critical to oncogenesis in these tumors. Genomic amplification and activating mutations in the EGFR locus occur almost exclusively in primary GBMs and represent the most prevalent RTK-associated molecular abnormality in malignant glioma (~45% of GBM). About half of the tumor with EGFR amplification express a constitutively autophosphorylated variant of EGFR, known as EGFRvIII, that lacks the extracellular ligand-binding domain (exon 2 through 7) (Libermann et al., 1985; Frederick L. et al., 2000; Pelloski C.E. et al., 2007; Furnari F.B. et al.,2007).

Enhanced PDGF signaling, either through receptor (PDGFRA) amplification/mutation or through ligand over-expression has been found to be a common feature of low grade glioma along with a significant subset of GBMs (Westermark B. and Nistlér M., 1995). Although activating mutations in PDGFRA are uncommon (Clarke I.D. and Dirks P.B., 2003), frequent co-expression of both the receptor and its ligand, most commonly PDGFB indicates the potential for autocrine or paracrine loops boosting oncogenic signaling through the PDGF network. Hepatocyte growth factor (HGF) and its RTK MET (also known as HGFR) appear to operate in a smaller subset of GBMs (Abounader R. and Laterrra J., 2005), as does the RTK ligand insulin-like growth factor 2 (IGF2) (Soroceanu L. et al., 2007). Common signal transduction pathways activated by growth factors are the mitogen-activated protein kinase (MAPK) pathway, which is involved in proliferation and cell cycle progression, and the PI3K-Akt-mTOR pathways, which are involved in the inhibition of apoptosis and cellular proliferation. Further dysregulation of the downstream Phosphoinositide 3-kinase (PI3K) – Akt – mammalian target of rapamycin (mTOR) and Ras-MAPK signaling pathways also exists in the majority of malignant gliomas (Cairncross et al., 1998). Mutations in the catalytic or regulatory domain of PI3K that are hypothesized to lead to its constitutive activation occur in 15% of GBMs (Cancer Genome Atlas Research Network, 2008). Notably, PTEN and neurofibromin 1 (NF1), important negative regulators of the PI3K-AKT-mTOR and Ras-MAPK networks, respectively, are frequently mutated or deleted in GBM (36% and 18%, respectively), and loss of PTEN at the protein level is found in more than 80% (Cancer Genome Atlas Research Network, 2008).

1.1.3.2 Cell cycle regulators

P53 and RB functions are inhibited by mutations or copy number alterations in at least 87% and 78% of GBM, respectively (Cancer Genome Atlas Research Network 2008). Additionally, mutations in the TP53 gene frequently characterize low-grade astrocytomas

and the secondary GBMs into which they evolve (Louis 1994). The Rb tumor suppressor pathway has been shown to be defective in a significant number of high-grade gliomas of both astrocytic and oligodendroglial lineage, either by inactivating mutations in RB1 itself or amplification of its negative regulators cyclin-dependent kinase 4 (CDK4) and, less frequently, CDK6 (Costello J.F. et al., 1997, Henson J.W. 1994). Analogously, amplification of the p53 antagonists mouse double minute 2 homolog (MDM2) and MDM4 have also been found in distinct subsets of Tp53-intact GBMs (Halatsch M.E. et al., 2006), as mutations and/or deletions in the CDKN2A locus that encodes both INK4A and ARF, which are crucial positive regulators of RB and p53, respectively (Kraus J.A. et al., 2000).

1.1.3.3. Other genetic alterations

Integrated genomic analysis has facilitated the identification and characterization of additional genes involved in glioma pathogenesis. Missense mutations in isocitrate dehydrogenase 1 (IDH1) are found in a significant number of GBMs that tend to occur mostly in younger patients with more protracted clinical courses (Parsons D. et al., 2008). These point mutations are restricted exclusively to the R132 residue in the active site region of the protein in which they disrupt hydrogen bonding with its substrate (Parsons D. et al., 2008, Bredel 2009, Yan H. et al., 2009). Interestingly, a separate group of gliomas harbour mutations in the IDH1 homologue IDH2 at the analogous residue (R172). Further investigations have shown that mutations in IDH1 and IDH2 are present in high proportions of grade II and III astrocytic and oligo dendroglial tumours (72–100%) along with secondary GBMs (85%), but are largely absent in primary GBMs (5%) (Yan H. et al., 2009, Hartmann C. et al., 2009). Furthermore, across all histological types of diffuse glioma, IDH mutations tend to segregate with other low-grade glioma-associated genomic abnormalities, such as TP53 mutations and 1p/19q deletion, and are not associated with EGFR amplification and chromosome 10 loss, anomalies occurring frequently in primary

GBM (Yan H. et al., 2009). These findings define an oncologic pathway for low-grade gliomas and the malignant tumors into which they evolve, which is distinct from that used by de novo primary GBM. The IDH1 mutation is associated with longer survival (Hartmann C. et al., 2010) of patients with secondary GBM and thus may be a highly valuable prognostic biomarker (von Deimling A. et al., 2011). IDH mutational status has also been linked with DNA methylation profiles in diffuse glioma. Recent analysis by TCGA has demonstrated a small subset of GBM (8.8%), which exhibit a CpG island methylator phenotype (G-CIMP) characterized by stereotyped hypermethylation of CpG islands in over 1,500 loci across the genome (Noushmehr H. et al., 2010). G-CIMP-positive GBMs exhibit increased frequency of characteristic copy number alterations (CNAs) in 8q and 10p and are highly enriched for IDH mutations (Turcan S et al., 2012). By report, approximately 87% of G-CIMP-positive versus 5% of G-CIMP-negative tumors were IDH-mutant, combining TCGA data with a validation tumor set. The striking correlation between G-CIMP and IDH mutation tracks across all diffuse glioma variants, especially in lower-grade astrocytomas and oligodendrogliomas.

1.1.4. Molecular classification of gliomas.

The WHO histological classification of gliomas has shown a high prognostic power, however considerable variability in clinical outcome among patients within each individual diagnostic category still exists. This is mainly due to the molecular complexity of gliomas and it has created the need of a more accurate classification of gliomas. The identification of prognostically distinct molecular subtypes within morphologically undistinguishable glioma subsets is also crucial. Gene expression profiling studies have been used to identify subclasses of gliomas based on transcriptional signatures. Earliest studies identified gene expression differences among morphologically defined gliomas. Differentially expressed genes were found among GBMs and lower grade gliomas (Rickman D.S. et al 2001; Nutt C.L. et al 2003; Shirahata M. et al 2007; Fuller G.N. et al 2002; Shai R. et al 2003; Li A. et

al, 2009), primary and secondary GBMs (Godard S. et al., 2003; Shai R. et al., 2003), adult and pediatric brain tumors (Faury 2007) or a variety of morphologically defined glioma subtypes (Godard S. et al., 2003; Shai R. et al., 2003; van den Boom J. et al., 2003). These studies confirmed that morphological differences among gliomas are reflected at the mRNA level. In some cases gene expression profiles classify diagnostically challenging malignant gliomas in a manner that better correlates with clinical outcome than standard pathology does (Nutt C.L. et al 2003, Shirahata M. et al 2007). Several schemes for classifying GBM subtypes based on expression signatures have been proposed in the past several years (Freije W.A. et al., 2004; Nigro J.M. et al., 2005; Phillips H.S. et al., 2006; Verhaak R.G. et al., 2010; Vital A.L. et al., 2010). The first relevant study carried out by Phillips and colleagues divides a cohort of malignant gliomas, comprised of both WHO grade III and IV, into three molecular subtypes named Proneural, Proliferative, and Mesenchymal in recognition of the key features of the molecular signatures associated with each group (Figure 2). The proneural subtype is defined by genes implicated in neurogenesis. It is associated with better outcome than either of the other two tumor subtypes. In contrast, the proliferative and mesenchymal gene signatures are defined by proliferation- and extracellular matrix/invasion-related genes, respectively, and are both associated with poor outcome. GBMs with Proliferative signatures have an elevated proliferation index (MIB-1) in tumor cells, whereas GBMs of the Mesenchymal subtype show evidence for increased angiogenesis.

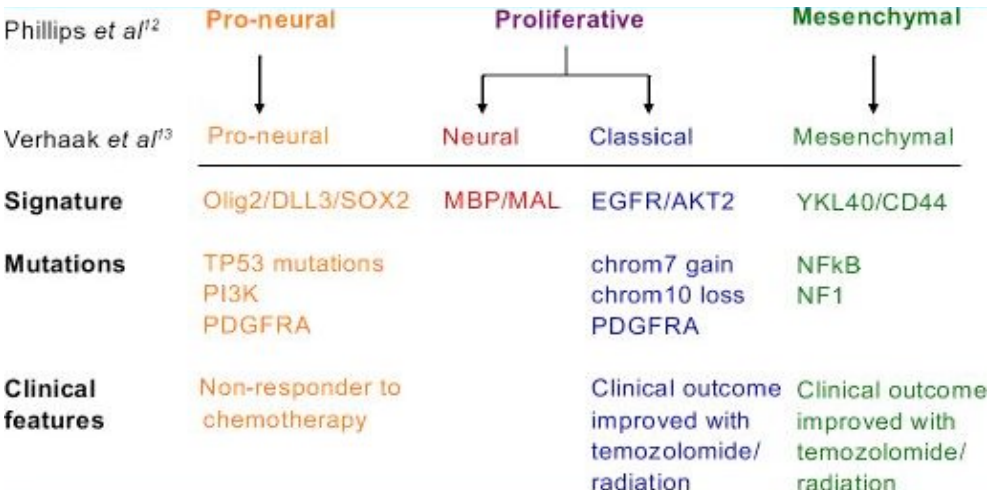

Figure 2. Molecular signature of different subclass of gliomas. Adapted from J Neurol Neurosurg Psychiatry 2012

The authors speculated that poor outcome of Proliferative and Mesenchymal tumors may be differentially associated with a high rate of tumor cell proliferation or angiogenesis, respectively. Prognostic significance of molecular subtype was validated in an independent cohort of 184 gliomas of various histological types. Remarkably, nearly all WHO grade III tumors (65 out of 73 gliomas) fell into the proneural subgroup, along with a subset of GBMs occurring in younger patients with prolonged disease courses. Moreover recurrent tumors, although mostly retaining their initial transcriptional subclassification, seemed to significantly shift their mRNA signatures towards the mesenchymal profile. On note, a recent work has identified a set of master regulator transcription factors, the most important of which are the signal transducer and activator of transcription 3 (STAT3) and CCAAT/enhancer-binding protein beta (C/EBP β), which seem to mediate the expression of the mesenchymal phenotype and so enhance GBM aggressiveness (Carro M.S. et al., 2010). An additional clustering analysis using transcriptional data obtained by the TGCA on 200 primary GBMs has established four distinctive GBM subtypes, namely Proneural, Neural, Classical, and Mesenchymal (Verhaak R.G. et al., 2010). Significant similarities, but not entirely overlap, were found between the mesenchymal and proneural phenotypes described in Phillips' and Verhaak's works. Unlike previous studies, the TCGA proneural subtype is not associated with improved prognosis in the TCGA data set consisting solely of grade IV astrocytoms, but it is in the validation of the data sets (Phillips H.S. et al, 2006; Madhavan S.Z.J. et al., 2009) containing lower-grade gliomas. Conversely, re-analysis of the TCGA data using Phillips' molecular subtype designations confirmed a slightly more favorable prognosis of the "Phillips-proneural" relative to "Phillips-mesenchymal/proliferative" GBMs. Because of the huge amount of molecular data available for these tumors (TCGA, 2008) recurrent genomic aberrations in each molecular

subtype were identified. The proneural subtype is more diffused in younger patients, as found in previous studies (Phillips H.S. et al., 2006; Lee J. et al., 2008), and harbours frequent PDGFRA amplification and point mutations in IDH1, TP53 mutations and loss of heterozigosity, PIK3CA/PIK3R1 mutations. The proneural group shows high expression of oligodendrocytic development genes (such as PDGFRA, NKX2-2 and oligodendrocyte transcription factor 2 [OLIG2]) and this signature contained several proneural development genes as well as doublecortin (DCX), delta-like 3 (DLL3), aschaete-scute homolog 1 (ASCL1) and transcription factor 4 (TCF4) (Phillips H.S. et al., 2006). The neuronal subtype was characterized by the expression of neuron markers such as NEFL, GABRA1, SYT1 and SLC12A5. The classical subtype was characterized by frequent EGFR amplification and EGFRvIII mutations and a distinct lack of TP53 mutations and CDKN2A deletion. The mesenchymal subtype was typified by deletion of NF1, TP53, and PTEN genes and displayed expression of mesenchymal markers, such as CHIL3 (also known as YKL40) and MET, as described elsewhere (Phillips H.S. et al., 2006). Moreover, higher overall necrosis, microvascular proliferation and inflammatory infiltrates are frequent in mesenchymal GBM, while necrosis typically lacks in the proneural subtype. Using a proteomic analysis three proteomically-defined subclasses of GBM have been identified. These subclasses are characterized by protein- and phosphorylation-level signaling abnormalities in the EGFR, PDGFR, and NF1 pathways and correspond to classical, proneural, and mesenchymal subtypes of GBM, respectively (Brennan C.W. et al., 2009). Analysis of epigenetic changes from TCGA GBMs identified a distinct subset of samples with characteristic promoter methylation alterations, indicating the existence of a G-CIMP (Noushmehr H. et al 2010). G-CIMP tumors were mainly secondary or recurrent GBMs and were tightly associated with IDH1 mutations and displayed distinct copy-number alterations. Patients with G-CIMP positive tumors were younger and survived longer than G-CIMP negative GBM patients. Integration of DNA methylation data with gene expression data showed that G-CIMP positive tumors represented a subset of

proneural tumors. In the end, G-CIMP could be used to further refine the expression-defined groups into an additional subtype with clinical implications.

Several studies have been published on the identification of glioma subtypes based on gene expression profiles, but no consensus gene expression profile in malignant gliomas reproducibly associates with patient outcome across independent datasets. However, the first gene expression profile based diagnostic test is currently being evaluated in two prospective, randomized clinical trials (Colman H. et al., 2010). A 9-gene profile (AQP1, CHI3L1, EMP3, GPNMB, IGFBP2, LGALS3, OLIG2, PDPN, and RTN1) predictive of clinical outcome was identified for the development of a qRT-PCR assay performed on FFPE samples. On the basis of the logistical difficulties in obtaining fresh frozen tumors for DNA microarray based assays, such an assay is absolutely critical for successful clinical implementation with FFPE GBMs, which constitute the vast majority of clinical samples. In summary, molecular sub-typing now has the potential to become a readily implemented clinical test that may guide future treatment decisions.

1.1.5. Brain tumor therapy

1.1.5.1 Glioma diagnosis

Patients with a malignant glioma may present a variety of symptoms including headache, confusion and loss of memory, neurological deficits and personality changes. The diagnosis of malignant gliomas is usually made by magnetic resonance imaging (MRI), computer tomography (CT) or positron emission tomography (PET). The images typically show an enhancing mass surrounded by edema. GBMs frequently have central areas of necrosis and more extensive peritumoral edema than those associated with anaplastic gliomas.

1.1.5.2. Glioma prognosis

Despite decades of research and clinical trials, life expectancy for glioma patients has not improved considerably and is only about 2-3 years for anaplastic astrocytoma and 15 months for GBM (Stupp R. et al., 2007). There are several reasons why it has been so difficult to find new effective therapies against glioma. First, drug delivery is limited by the blood-brain-barrier impediment and the distorted glioma vessels (Weis S.M. and Cheresh D.A., 2005). Second, the invasive nature of gliomas makes the complete surgical resection of the tumor impossible. Third, tumor cells also have a strong intrinsic attitude for malignant progression and some cells, supposedly the cancer stem cells, are resistant to therapy. Lastly, over-expression of proteins involved in DNA repair machinery could dampen the effects of radio- and chemotherapy (Bao S. et al., 2006).

1.1.5.3 Treatment

The standard treatment for gliomas is the surgical resection, radiotherapy and chemotherapy using alkylating agents. The size and localization of the tumor is important for the possibility to perform optimal surgery (Bergenheim et al. 2007). Due to their invasive growth, gliomas indeed are impossible to completely resect. Surgical elimination of the tumor reduces the symptoms caused by mass effect and seems to give a modest survival advantage to the patient. For patients with GBM, the median survival from time of diagnosis is about three months without treatment. After treatment with surgery and postoperative temozolomide and radiotherapy, the survival increases to 14.6 months (Stupp R. et al., 2007). O-6-methylguanine-DNA methyltransferase (MGMT) is an important repair enzyme that contributes to resistance to temozolomide. Methylation of MGMT promoter silences the gene, decreasing DNA repair activity and increasing the susceptibility of the tumor cells to temozolomide. Treatment with temozolomide in GBM patients with MGMT promoter methylation prolonged the survival to 2 years (Hegi M.E. et al., 2005). For oligodendrogliomas, PCV chemotherapy (procarbazine, lomustine and vincristine) treatment after surgery and radiation is the more commonly used (Cairncross

G. et al., 2006). Several approaches have been used to target individual signaling molecules involved in gliomagenesis. Particular interest has focused on inhibitors of RTKs and their downstream effectors and on inhibitors of angiogenesis. EGFR is one of the most widely expressed RTK in human gliomas, so several EGFR inhibitors have been developed (Castillo et al. 2004). Gefitinib (ZD1839, Iressa™) (Rich J.N. et al., 2004) and erlotinib (Tarceva®) (Prados M.D. et al., 2006) have been investigated in recurrent gliomas with limited activity. An alternative approach has been developed based on a vaccination strategy against the constitutively activated EGFRvIII (Sampson J.H. et al., 2008). CDX-110™ is a peptide-based vaccine that targets the tumor specific mutated segment of EGFRvIII (Heimberger A.B. and Sampson J.H., 2009), it is currently in phase II/III randomized studies with radiation and temozolomide. Therapies directed towards the PDGFR pathway include many different putative targets (Grossman S.A. et al., 2001; Kilic T. et al., 2000). Imatinib (Gleevec®), a tyrosine kinase inhibitor specific for Abl kinase, c-KIT and PDGFR, has been demonstrated to have only limited anti-tumor activity in patients with recurrent malignant glioma (Raymond E. et al., 2008; Wen P.Y. and Kesari S., 2008). PDGFR antagonists might target the pericytes to preferentially block angiogenesis in established tumors (Sennino B. et al., 2007). Since angiogenesis is a hallmark of malignant glioma and affects drug delivery, anti-angiogenic treatment could be of value in combination with already existing treatment modalities. The VEGF signalling pathway is the cornerstone in angiogenesis, so most anti-angiogenic therapies target VEGF or VEGFR. Bevacizumab (Avastin®) is a humanised anti-VEGF165 mAb. Promising results from a phase II study with bevacizumab in combination with irinotecan was reported in patients with recurrent high-grade glioma (Vredenburgh J.J. et al., 2007). However, there are emerging problems with both developing treatment-resistance and adverse effects associated with anti-VEGF therapy such as disturbance of VEGF-dependent physiological functions and homeostasis in the cardiovascular and renal systems, wound healing and tissue repair. This promotes the search for novel

antiangiogenic therapies. VEGF-trap (aflibercept) is a soluble VEGF receptor binding VEGF-A, -B, and PDGF and has been shown to be effective in both initial and advanced phase of tumor development in a preclinical tumor model (Gomez-Manzano C. et al., 2008). This substance is now in phase II trial in recurrent glioma that is not responding to temozolomide. Cediranib (AZD2171, Recentin™) is a RTK inhibitor of VEGFR 1-3, PDGFR and c-KIT. It is currently in phase III clinical study in recurrent GBM where patients are randomised between treatment with cediranib alone, cediranib in combination with lomustine (an alkylating agent) or lomustine with placebo. Using MRI, it is also shown that cediranib normalizes tumor vessels in GBM and alleviates edema (Batchelor T.T. et al., 2007). Other VEGFR inhibitors that may be active against malignant glioma include the VEGFR/PDGFR inhibitors vatalanib (PTK 787), pazopanib (GW 786034), sorafenib, and sunitinib; the VEGFR/EGFR inhibitor vandetanib (ZD6474); the adnectin-based CT 322; and the VEGFR/c-Met kinase inhibitor XL 184 (Norden A.D. et al., 2008).

A huge amount of signaling pathways and potential targets in malignant glioma has been described. Many clinical studies are ongoing. For summary of potential targets see Figure 3.

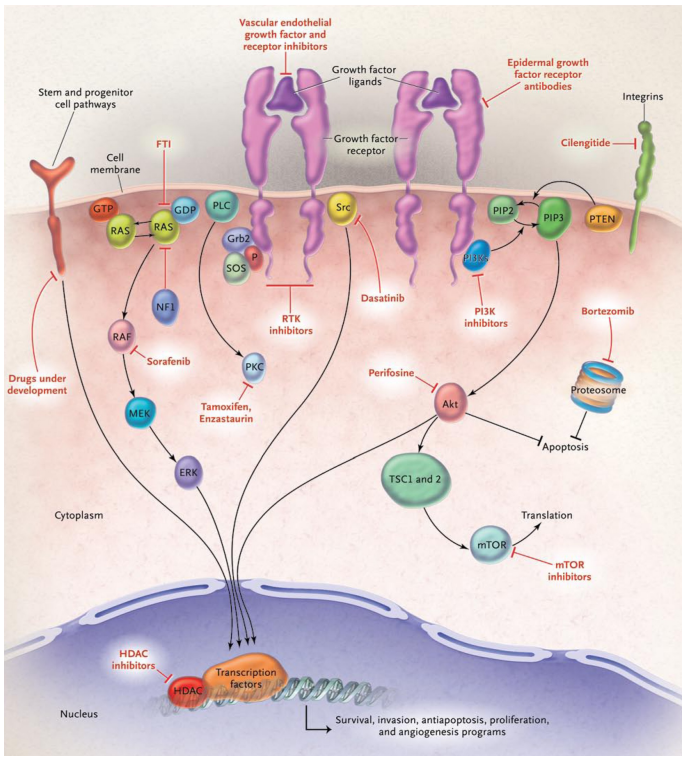

Figure 3. Major signaling pathways in malignant gliomas and the corresponding targeted agents in development for GBM. Adapted from Wen and Kesari, 2008.

It is naive to believe that there will be one single treatment to cure all gliomas; rather the combination of multiple treatment strategies will have the best effect. Possibly, future patients will be given selected and individually targeted treatments based on the expression/mutation analysis of that particular patient's tumor. Ideally, treatment could be tailored to achieve highest possible efficacy depending on expression of growth factors and mutated genes. Strong efforts are made to effectively target tumor stem cells that will be discussed in the next chapter. These cells are believed to survive both radiation and chemotherapy and can generate new tumor cells during recurrence.

1.2. Cancer stem cells in solid tumors

Tumors are composed of a heterogeneous population of cells that exhibit different states of differentiation and proliferation capacity. At least two models have put forward to account for heterogeneity: the "cancer stem cell" (Bonnet D. and Dick J.E., 1997; Reya T. et al., 2001) and the "clonal evolution" (Nowell P.C., 1976; Campbell L.L. and Polyak K., 2007) models (Figure 4).

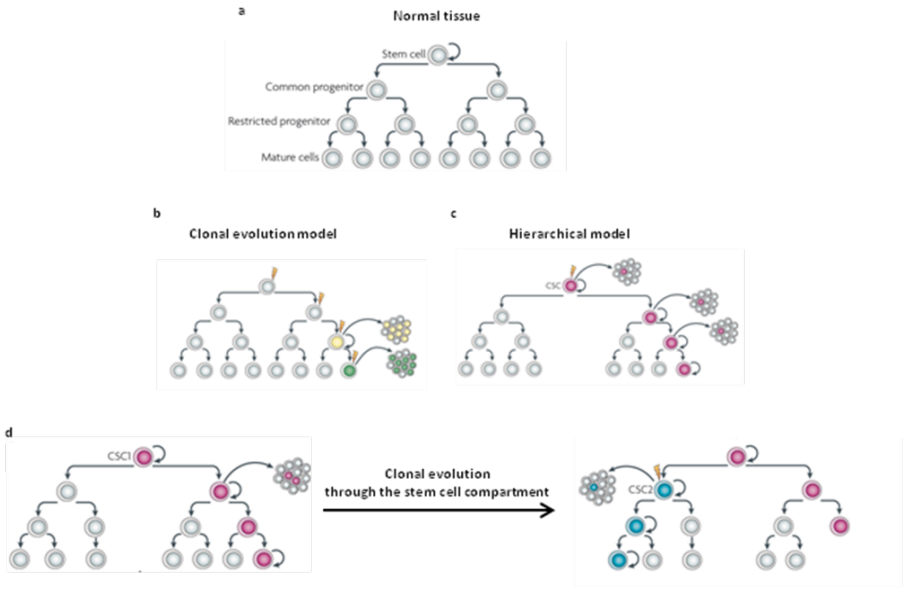

Figure 4. Cancer stem cells and clonal evolution models.
(a) In a normal tissue the cellular hierarchy comprising stem cells, which progressively generate more restricted progenitor cells and ultimately all the mature cell types that constitute the tissue. **(b)** In the clonal evolution model all undifferentiated cells have similar tumorigenic capacity. **(c)** In the cancer stem cell model, only the CSC can generate a tumor, based on its self-renewal properties and proliferative potential. **(d)** The two tumor models are not mutually exclusive- Initially, tumor growth is driven by a specific CSC (CSC1). With tumor progression, another distinct CSC (CSC2) may arise due to clonal evolution of CSC1. This may result from the acquisition of an additional mutation or epigenetic modification. This more aggressive CSC2 becomes dominant and drives tumor formation. Adapted from Visvader and Linderman, 2008.

The "cancer stem cell" model proposes that the growth and progression of many tumors are driven by a small subpopulation of cancer cells with stem-like features. These cells share important properties with normal tissue stem cells, including self-renewal (by symmetric and asymmetric division) and differentiation capacity, albeit aberrant. This implies that many cancers are hierarchically organized in much at the same manner as normal tissues. Just as normal stem cells differentiate into phenotypically diverse progeny with limited differentiation potential, CSCs also differentiate into phenotypically non-tumorigenic cells that compose the bulk of the cells in the tumor. The CSC model posits that differences in tumorigenic potential among cancer cells from the same patient are largely epigenetically determined, because it is implausible that only rare cancer cells have a genotype permissive for extensive proliferation. However, there is no direct evidence that tumorigenic cells differ from non-tumorigenic cells as a result of epigenetic rather than genetic differences (Shackleton M. et al., 2009). In the "clonal evolution" model all the cells have similar tumorigenic capacity. The mutated cells with a growth advantage are selected and expanded, with the cells in the dominant clone having a similar potential for generating tumor growth. The clonal evolution model holds that genetic and epigenetic changes occur over time in individual cancer cells. If such changes confer a selective advantage they will allow individual clones of cancer cells to out-compete with other clones. Clonal evolution can lead to genetic heterogeneity, conferring phenotypic and functional differences among the cancer cells within a single patient (Shackleton M. et al.,

2009). It is important to note that the clonal evolution and the cancer stem cell model are not mutually exclusive in cancers that follow a stem cell model, as cancer stem cells would be expected to evolve by clonal evolution (Barabe F. et al., 2007). Thus, if a mutation conferring self-renewal or growth properties advantages occurs, a more dominant cancer stem cell may emerge among the others. For example, the leukemic stem cells that maintain chronic myeloid leukemia despite imatinib therapy would be selected to develop imatinib resistance mutations over time by clonal evolution (Shah N.P. et al., 2007).

The first evidence for the existence of CSCs came from acute myeloid leukemia (Bonnet D. and Dick J.E., 1997; Lapidot T. et al., 1994), in which a rare subset of cells comprising 0.01-1% of the total population could induce leukemia when transplanted into immunodeficient mice. These concepts and experimental approaches were then applied to solid tumors such as breast (Al-Hajj M. et al., 2003), brain (Singh S.K. et al., 2004) and colon (Dalerba P. et al., 2007; Ricci-Vitiani L. et al., 2007) cancers.

Most studies on cancer stem cells follow a common scenario: a marker or a combination of markers is found to be expressed in a heterogeneous fashion in a certain tumor type. On the basis of this marker heterogeneity or using markers of normal stem cells of the same organ, subpopulations of cells are sorted from primary tumors and transplanted into immunodeficient mice by limiting dilution; then, that tumor growth is scored some weeks or months later. Different capacity for tumor initiation between tumor cell subsets can be interpreted as evidence for the presence of CSCs in the primary tumor (Figure 5).

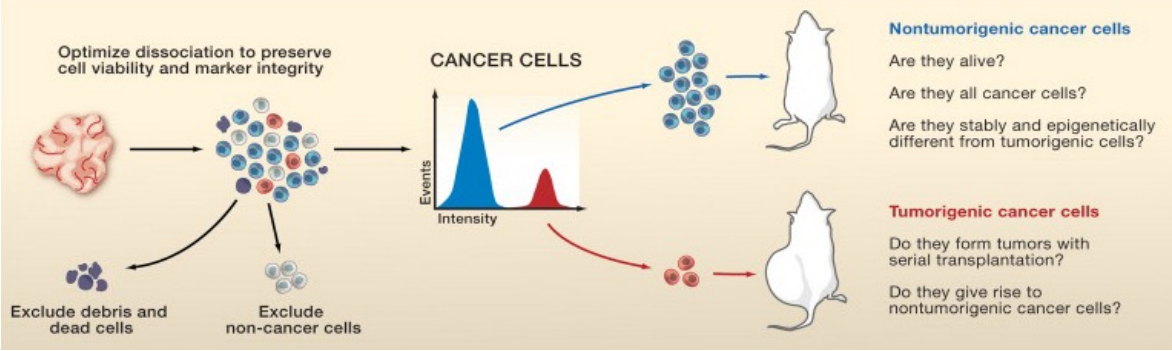

Figure 5. Testing the Cancer Stem Cell Model.
The tumor is dissociated into single cells using conditions optimized to maximize the preservation of cell viability and surface marker expression. The cells are sorted by flow cytometry using specific cell surface markers. The tumorigenicity of all cells is tested using xenotransplantation assays in immunocomprpmised mice. Adapted from Shackleton M. et al., 2009.

According to the CSC model only a specific subset of cancer cell population should be able to sustain in vivo tumor growth, whether all other subsets should not. The transplanted tumors contain mixed populations of tumorigenic and non-tumorigenic cancer cells, thus recapitulating at least some of the heterogeneity of the parental tumor. However, the most convincing demonstration of CSC identity comes from serial transplantation of a cellular population into the animal model, which is the only true demonstration of self-renewal ability of a cancer cell. The frequency of cancer stem cells is highly variable between solid tumors of the same type.. Recent mathematical analyses have further indicated that CSCs in advanced tumors may not occur as a small fraction (Kern S.E. and Shibata D., 2007). Extensive in vivo limiting dilution analyses are required to determine the frequency of CSCs within solid tumors (Bonnefoix T. et al., 1996). This may eventually allows correlation between CSCs frequency, tumor grade and clinical outcome. It is also important to note that the nature of the xenograft model used and the site of transplantation influence the determination of stem cell frequency. The efficiency of human cell engraftment can be significantly influenced by the presence of residual immune effector cells in recipient mice (Quintana E. et al., 2008). The xenogeneic immune response that mice mount against human cells can reduce the ability of human cancer cells to engraft in mice, underestimating the frequency of human cancer cell with tumorigenic potential. On the other hand it is also clear that immune cells have a role in the progression of many tumors and this highly artificial animal model may not represent the true in vivo niche. The activity of tumor cells can also be influenced by an altered vascular environment, which creates the stem cell niche. Thus, the development of orthotopic transplantation assays is

crucial. The concept that cancer growth can be sustained by cancer stem cells leads to the necessity of new and more effective antitumor treatments. According to the CSC model, therapeutic approaches that do not eradicate the CSC compartment are likely to achieve little success; they might kill the majority of tumor cells and induce temporary regression of gross tumor lesions but fail to prevent disease relapse and metastatic dissemination (Figure 5).

1.2.1 Neural Stem Cells

Neural stem cells (NSCs) are multipotent cells within the brain capable of self-renewal and differentiation into all major cell types of the central nervous system (neurons, astrocytes and oligodendrocytes) (Mayer-Proschel M. et al., 1997; Rao M.S. et al., 1998) (Figure 6). During development NSCs are found in the ventricular zone of the central nervous system. In the adult brain, NSCs are primarily restricted to two areas: the subependymal zone of the lateral ventricles and the subgranular zone of the dendrite gyrus within the hippocampus. In the hippocampus, NSCs integrate functionally into the granule cell layer (Cameron H.A. and McKay R.D., 2001). In the rodent brain, progeny from neural stem cells of the subventricular zone migrate along the rostral migratory stream to the olfactory bulb to differentiate into local interneuron (Luskin M.B., 1993; Lois C. et al., 1996). In the human brain, migration of neuroblasts toward the olfactory bulb may occur via alternate routes (Sanai N. et al., 2004; Curtis M.A. et al., 2007). Persistence of NSCs in the adult reflects their role in endogenous repair mechanisms and maintenance of normal brain functions. Adult neurogenesis is likely to have a crucial role in the neurobiological basis of learning and memory (Aimone J.B. et al., 2006).

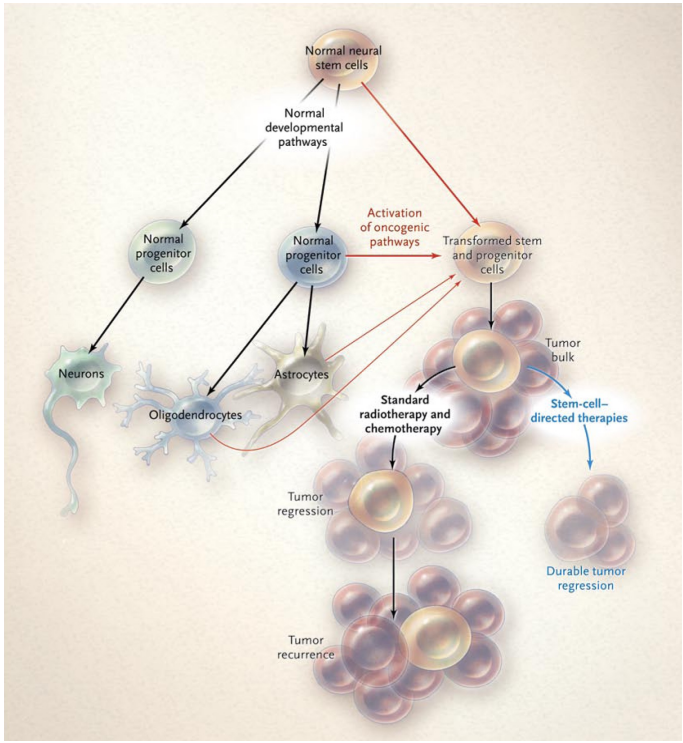

Figure 6. Resistance Mechanisms in Glioma Cells.
Normal neural stem cells self-renew and give rise to multipotential progenitor cells that form neurons, oligodendroglia, and astrocytes. Glioma stem cells arise from the transformation of either neural stem cells or progenitor cells (red) or, less likely, from differentiation of a oligodendrocytes or astrocytes (thin red arrows) and lead to malignant gliomas. Glioma stem cells are relatively resistant to standard treatments such as radiation and chemotherapy and lead to re-growth of the tumor after treatment. Therapies directed at stem cells can deplete these cells and potentially lead to more durable tumor regression (blue). Adapted from Wen P.Y. et al., 2008.

1.2.3 Glioma stem cells (GSCs)

The presence of stem cells in brain tumors has been demonstrated in several studies (Singh S.K. et al., 2003 and 2004; Galli R. et al., 2004; Hemmati H.D. et al., 2003; Ignatova T.N. et al., 2002; Yuan X. et al., 2004). However the isolation of brain tumor cells with tumorigenic capacity, tested in vivo using the xeno-transplantation assay, was initially reported independently by two groups (Singh S.K. et al., 2004; Galli R. et al., 2004). Although they arrived at similar conclusions, they used different approaches for isolating brain tumor stem cells: the cell sorting based on selection for the cell surface marker CD133 (Singh S.K. et al., 2004) and the neurosphere assay (Galli R. et al., 2004).

1.2.3.1 Isolation of glioma stem cells using cell surface markers

The first prospective in vitro and in vivo identification and characterization of a putative CSC from human brain tumors was based on cell sorting for the neural stem cell surface marker CD133 (Singh S.K. et al., 2003, 2004). Uchida and colleagues sorted human fetal brain cells for CD133 expression highly enriching for stem cell properties in vitro and in vivo (Uchida N. et al., 2000). Then CD133 was used to sort fresh human brain tumors. In vitro, CD133-positive cells formed clonogenic neurosphere colonies, proliferated and could be induced to differentiate into mature neural cell lineages that were characteristic of the mature lineages seen in the patient's original tumor (Singh S.K. et al., 2003). Moreover CD133-positive brain tumor cells were highly enriched for tumor initiating activity in vivo. As few as 100 CD133-positive cells were able to initiate fatal infiltrative tumors in immunocompromised NOD/SCID mice after orthotopic transplantation. Injection of 100000 CD133-negative cells did not lead to tumor formation, although viable human tumor cells could be identified in the mouse brains four months after transplantation, suggesting that these cells were viable, but were no longer be able to initiate tumor formation. Serial passage of CD133-positive cells re-isolated from the primary transplant and injected into secondary recipient was also shown. It is important to note that sorting for CD133 enriches for cancer stem cells and does not definitively identify them. Furthermore several studies have questioned the utility of CD133 in the isolation of glioma stem cells (Brescia P. et al., 2013). Hence, a number of cell surface markers have been proved useful for the isolation of GSCs, including CD15 (Son M.J. et al., 2009), CD44 (Anido 2010), Integrin-α6 (Lathia J.D. et al., 2010), ABCB5 as well as Hoechst33342 exclusion by the side population cells (Harris M.A. et al., 2008, Bleau A.M. et al., 2009). Notably none of these markers are exclusively expressed by the GSCs and in all the tumor samples, highlighting the necessity of additional and more specific markers or the use of combinatorial markers.

1.2.3.2 Isolation of glioma stem cells using the neurosphere assay

In serum-free culture, in the presence of mitogens including epidermal growth factor (EGF) and fibroblast growth factor (FGF), human brain tumor stem cells can be grown as single cell–derived colonies, namely neurospheres (Singh S.K. et al., 2003; Hemmati H.D. et al., 2003; Galli R. et al., 2004; Ignatova T.N. et al., 2002; Yuan P.Y. et al., 2004). The neurosphere assay was initially used by Reynolds and Weiss in 1992 to isolate neurospheres from the mouse striatum (Reynold 1992) and was subsequently used to successfully enrich tumor-initiating cells from brain tumors (Singh S.K. et al., 2003; Hemmati H.D. et al., 2003; Galli R. et al., 2004; Ignatova T.N. et al., 2002; Yuan P.Y. et al., 2004). These assays are currently used as the standard *in vitro* method for identifying the presence of stem cells derived from both tumor and non-tumor tissues (Chaichana K. et al., 2006; Reynolds B.A. and Rietze R.L., 2005; Vescovi A.L. et al., 2006). Similar sphere-forming assays are also used in other stem cell systems, including skin (Toma J.G. et al., 2001), breast (Matsuda M. et al., 2004) and pancreas (Seaberg R.M. et al., 2004). The selective serum-free conditions, in which the neurosphere assays is carried out, allow the stem-like cells to continually divide and form multipotent clonal spheres, while the more differentiated cells incapable of self-renewal and multipotency die off with serial passages (Chaichana K. et al., 2006; Hemmati H.D. et al., 2003; Reynolds B.A. and Rietze R.L., 2005) (Figure 7).

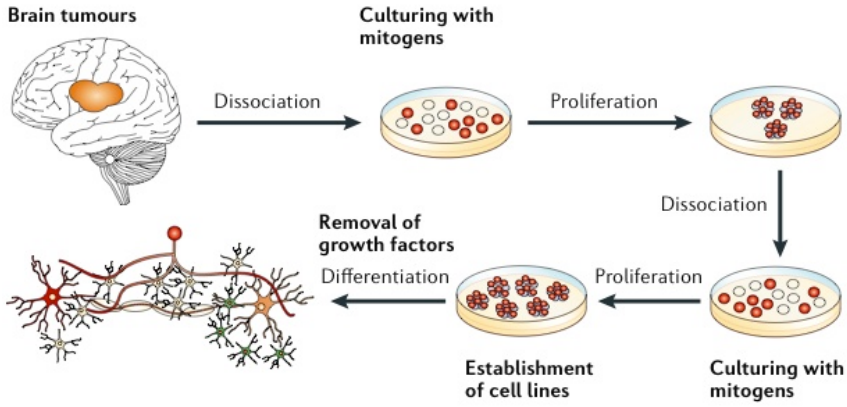

Figure 7. Isolation, perpetuation and differentiation of brain tumor stem cells in culture. The neurosphere assay in a serum-free culture system that allows the isolation of stem cells based on their exclusive and extensive self-renewal potential. Adapted from Vescovi A.L. et al., 2006.

Notably, on mitogen removal and in addition of serum the cells can be differentiated into neurons, astrocytes and oligodendrocytes. The assay thus provide culture conditions that permit competent cells to exhibit the cardinal stem cell property of self-renewal over an extended period of time, so generating a large number of progeny that can differentiate into the primary cell types of the tissue from which they were obtained (Louis S.A. et al., 2008). Neurosphere initiating cells isolated from adult human GBM had stem-cell characteristics: extensive self-renewal, multipotency and the capacity both to initiate new tumors that recapitulate the histological features of the parental tumor, when transplanted into the brain of immunodeficient mice (Galli R. et al., 2004). Most importantly, *in vivo* studies have shown that neurosphere formation is a significant predictor of clinical outcome in glioma patients, independent from Ki67 proliferation index, and is a robust, independent predictor of glioma tumor progression (Larks D.R. et al., 2004). Hence the neurosphere assay has become the method of choice to study neural and brain tumor stem cell populations in vitro. However, it is associated with some limitations. Neurospheres are composed by a heterogeneous cell population that consists of stem cells, together with progenitors and more differentiated cells (Reynolds B.A. et al., 1996; Suslov O.N. et al., 2002). Only the stem cells can exhibit extended self-renewal over serial passages (Louis S.A. et al., 2008), while the progenitor cells may not be able to form neurospheres for more than six passages (Chaichana K.L. et al., 2006) and the terminally differentiated cells are not able to form any sphere. Several evidences have indicated that the majority of spheres are derived from progenitor cells with limited self-renewal capabilities which do not generally survive beyond six passages (Louis S.A. et al., 2008; Reynolds B.A. et al., 1996). Cultures that fail to survive more than six passages are more likely to be derived from progenitor cells (Reynolds B.A. et al., 2005), as suggested by the finding that spheres differentiated prior to

establishing clonal ability (>6 passages) typically only display astrocyte characteristics (Louis S.A. et al., 2008). However, a true separation of stem cells and progenitor cells in the neurosphere assay remains problematic. Thus, the use of sphere cultures for elucidating and interpreting the biological and molecular characteristics of GSCs could give rise to misleading results (Chaichana K.L. et al., 2009). It is notable that individual cells dissociated from neurospheres show distinct proliferative potentials: some form abortive colonies, whereas others form larger colonies of variable size (Liu Q. et al., 2009). Recent studies have found that spheres >2 mm in diameter show high proliferative potential and multilineage differentiation over time, whereas smaller spheres have limited proliferation potential and typically only differentiate into cells with an astrocyte phenotype (Louis S.A. et al., 2008). Thus, larger neurospheres (>2 mm) are more likely to be derived from stem cells, rather than from progenitor cells with limited proliferative and differentiating capacities (Louis S.A. et al., 2008). Besides being used to enrich GSCs, neurosphere assays are also widely adopted to estimate stem cell frequencies by counting secondary neurosphere formation (Reynolds B.A. et al., 2005), however an estimation of stem cell frequency based on the number of secondary neurospheres could significantly overestimate stem cell number because of the existence of confounding spheres derived from progenitors (Reynolds B.A. et al., 2005). The in vivo limiting dilution assay made inoculating progressive lower number of cells in the mouse brain, could be a more accurate assay to calculate the stem cell frequency in the neurosphere. Moreover, the transplantation of individual glioma spheres into mouse brains, and the serial transfer of the xenograft tumors through mice for several passages could demonstrate the *in vivo* self-renewal ability of GSCs (Harris M.A. et al., 2008). The ability to grow human brain tumor cells as neurospheres is variable. GBM cells are most easily grown in these conditions, but other types of brain tumors, such as medulloblastoma and ependymoma, can be grown only for short periods in neurosphere conditions. (Taylor R.E. et al., 2005). Nevertheless, application of serum-free growth conditions to GBMs has enabled growth of cell lines that

retain the same genotype of the patient's primary tumor (Vik-Mo E.O. et al., 2010), and which show stable stem cell properties in vitro and more faithful generation of models of the disease after xenotransplantation in vivo (Lee J. et al., 2006). These methods clearly show the advantages of serum-free–based culture methods for studying human brain tumor cells, and suggest that serum-based cultures have limited utility.

1.2.4 Cell of origin of gliomas

The term cancer stem cell does not imply that this tumor cell derives from a normal stem cell. It is not yet clear whether cancer-initiating events occur in NSCs, progenitors or differentiated cells. However, NSCs are reasonable candidates as cell of origin of brain tumor stem cells, because their long existence may subject them more easily to acquisition of multiple gene abnormalities necessary for tumorigenesis (Dalerba P. et al., 2007; Hanahan D. and Weinberg R.A., 2000). Currently there is experimental evidence in mouse brain tumors for cell of origin from stem cells and progenitor cells as well as more differentiated cells (Holland E.C. et al., 2000; Uhrbom L. et al., 2002; Bachoo R.M. et al., 2002; Liu C. et al., 2011) (Figure 5). It is also of relevant note that brain tumors of different phenotypes, in different locations, with different genetic mutations, may have different cell of origin (Stiles C.D. et al., 2008). Identifying the cell of origin of brain tumor may be important for several reasons. The particular cell in which an oncogene is expressed may determine the subsequent phenotype and resulting aggressiveness of the tumor, suggesting that different treatments could depend on the cell of origin of the tumor.

1.2.5 Glioma stem cell niche (Figure 8)

Stem cell biology is strongly supported by a specialized microenvironment or stem cell niche. Stem cell niches are complex dynamic entities that actively regulate stem cell function (Scadden D.T., 2006), in particular their self-renewal and fate. Calabrese and colleagues demonstrated that stem cells from various brain tumors, including GBM, are

maintained within vasculature niches that mimic the neural stem cell niche (Calabrese C. et al., 2007). Notably, co-transplanting brain tumor stem cells and endothelial cells into immunocompromised mice, the initiation and growth of tumors in the brain were accelerated by the endothelial derived factors. Brain tumor stem cells seem to have potent angiogenic properties and can recruit vessels during tumorigenesis. It was shown that CD133-positive human GBM produced high level of VEGF and formed highly vascular and hemorrhagic tumors in the brains of immunocompromised mice. Furthermore, treating CD133-positive cells with bevacizumab blocked their ability to induce endothelial cell migration and tube formation in culture, and initiate tumors in vivo (Bao S. et al., 2006). Moreover it was observed that GBM stem cells directly differentiate into endothelial cells lining tumor vessels (Ricci-Vitiani L. et al., 2010; Wang R. et al., 2010). As well as regulating stem cell proliferation and cell-fate decisions, niches also have a protective role defending stem cells from environmental insults (Moore K.A. and Lemischka I.R., 2006).

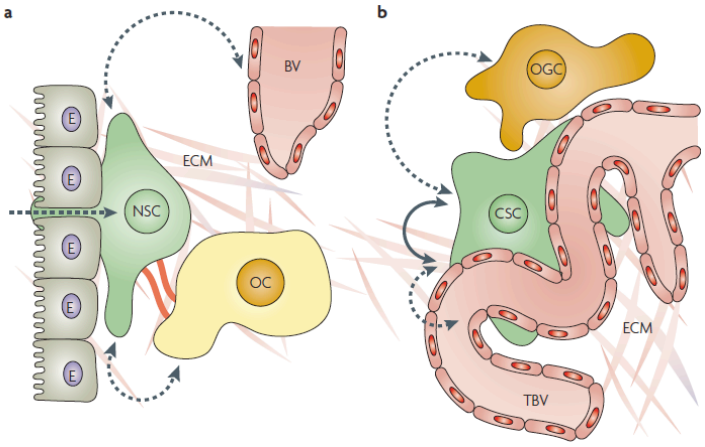

Figure 8. The normal and malignant stem cell niche. (A) Stylized view of the normal sub-ventricular zone (SVZ) neural stem cell niche. Neural stem cells (NSCs, type B cells) interact inti- mately with ependymal cells (E), blood vessels (BV) and various other cell types including progenitor and support cells (OC). NsC function may be regulated by various diffusible factors derived from the surrounding cells, as well as the cerebrospinal fluid (broken lines; for example, growth factors, pigment epithelium-derived factor (PEDF) and bone morphogenetic proteins (BMPs)). Additional regulation might be provided by direct cell contacts (red solid lines; for example, NOTCH receptor- ligand signals) and the extracellular matrix (ECM). (B) glioblastoma cancer stem cells (CSC) are found in intimate contact with the aberrant tumour vasculature (TBV). CSC can secrete diffusible factors such as VegF, which recruit TBV to the niche. In turn, TBV and other glioma cells (OGC) secrete factors that maintain aberrant CSC self-renewal. Mutations in CSC might also enable aberrant, intrinsic self-renewal (solid line). Adapted from Gilbertson RJ et al., 2007.

1.2.6 Implications of glioma stem cells in the therapy

From a clinical perspective, the cancer stem cell concept has significant implications, as these cells need to be eradicated in order to provide long-term disease free survival (see Figure 5). Cancer stem cells are thought to be resistant to chemotherapy and targeted therapy, through active mechanisms. They often express higher level of drug-resistance proteins such as ATP-binding cassette sub-family G member 2 (ABCG2) and ABCG5 and multidrug resistance protein 1 (MDR1) transporters. Human CD133-positive GBM cells were shown to be resistant to radiation therapy, retaining a clonogenic and tumorigenic potential, because of a more potent activation of DNA damage checkpoint mechanisms. This repair mechanism has been shown to be targetable through pharmacologic inhibition of the checkpoint kinases Chk1 and Chk2, which renders the CD133 GBM cells more radiosensitive (Bao S. et al., 2006). Glioma stem cells might be protected further from conventional therapies by factors within the vasculature niche. Treatments that disrupt aberrant vascular stem cell niches could therefore prove active against gliomas, because they might also function to disrupt stem cell maintenance. Calabrese and colleagues showed that treating GBM-bearing mice with bevacizumab depleted tumor blood vessels and caused a dramatic reduction in the number of GBM stem cells and the growth rate of the tumor (Calabrese C. et al., 2007). Also pathways regulating neural stem cell proliferation and differentiation might be targeted in brain tumor treatment. Promotion of tumor stem-cell differentiation may be an important strategy for treatment of brain tumor stem cells. Vescovi et al (Piccirillo S.G et al., 2006) have shown that BMPs, which normally induce astrocyte differentiation from normal neural precursors, have been shown to promote GBM cell differentiation in vitro and in vivo, reducing stem cell tumorigenicity in vivo. Another possibility is to target the process of GSC differentiation into endothelial cells in the tumor (Ricci-Vitiani L. et al., 2010; Wang R. et al., 2010). Signaling pathways that regulate stem-cell self-renewal and proliferation, such as Notch, Shh, and Wingless pathways are potentially important targets in the therapy against glioma stem cells.

1.3. Extracellular Vesicles

1.3.1. Microvesicles and Exosomes

Intracellular communication, a key element of multicellular organization, can occur either directly by cell-cell contact or by means of molecules secreted into the extracellular environment. In the last two decades, a third way of signalling emerged as equally prominent: Extracellular Vesicles (EV). The EV compartment encompasses two distinct groups of vesicular structures often classified for size, morphology and biogenesis: microvesicles (MVs) and exosomes (Figure 9). MVs are usually referred as vesicles deriving from plasma membrane (PM) domains that, after bending and consequent sealing of the membrane, are released into the extracellular environment as bilayered vesicles (Cocucci E. et al., 2009). Historically, exosomes were identified more than three decades ago as 40-100 nm vesicles of unkown origin produced by a variety of cell types (Trams E.G. et al., 1981). Years later, immunoelectron microscopy allowed the identification of these small vesicles inside large multivesicular endosomes (MVE) fused with the PM (Harding C. et al., 1983; Pan B.T. et al., 1985); this evidence gave rise to controversial reaction among the scientific community since MVE were long considered as pre-degradative compartments fated to full degradation by fusion with lysosomes. Ten years later, it was observed that even B lymphocytes and dendritic cells are able to release exosomes following the fusion of MVBs with the membrane (Raposo G. et al., 1996). Afterwards, MVE and exosomes were detected in a variety of other cell types including cytotoxic T lymphocytes, platelets, mast cells, neurons, oligodendrocytes, Schwann cells and intestinal epithelial cells (Simons M. and Raposo G. , 2009; Thery C. et al., 2009); in the end it is likely that virtually all cells are endowed with the capacity of producing and secreting exosomes. Vesicles with the characteristics of exosomes have been identified in body fluids as well: semen (Ronquist G. and Brody I., 1985), blood (Caby M.P. et al., 2005), urine (Pisitkun et al., 2004), saliva (Ogawa Y. et al., 2011), milk (Admyre C. et al., 2007), amniotic fluid (Asea A. et al., 2008), ascites (Andre et al., 2002), cerebrospinal fluid (Vella L.J. et al., 2007), and bile (Masyuk A.I. et al., 2010). The gold standard currently accepted for exosome purification

consists in collecting the serum-free medium of growing cells and performing serial steps of differential centrifugations aimed to separate low-density exosomes from protein aggregates and other non-membranous particles. Purified exosomes share the same size with intraluminal vesicles (ILVs) stored in the MVBs where they come from: 40-100 nm. Although MVs are generally bigger in size (up to 1 mm), MVs originating from the PM may also fall in the 40-100 nm range (Booth A.M. et al., 2006). Higher rates of purification can be achieved by immunoadsorption using an exosomal protein (usually a tetraspanin like CD63) as probe (Wubbolts R. et al., 2003).

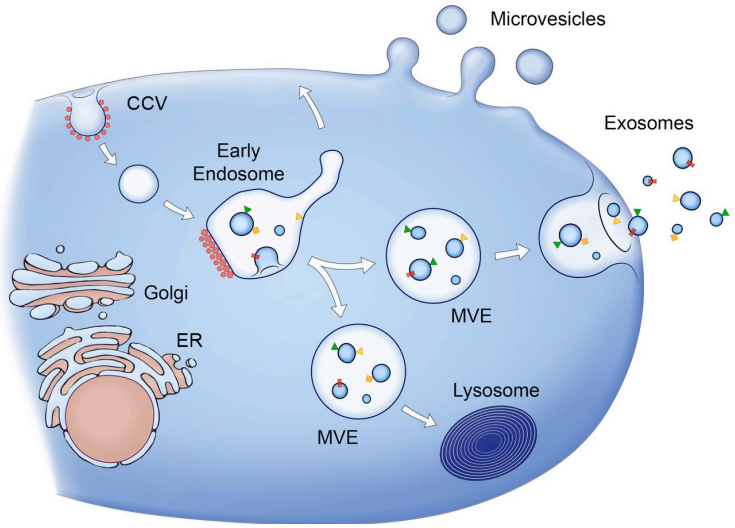

Figure 9. EV Biogenesis. Microvesicles (MVs) rise as outward buddings of the PM, conversely exosomes are inward buddings of the membrane of multivesicular endosomes (MVE) (Adapted from Raposo G. and Stoorvogel W., 2013)

1.3.2. Molecular Cargoes

As a product of the endocytic pathway, exosomes share with endosomes a variety of cargoes (e.g. Rab GTPase, SNAREs, Annexins and Flotillin), protein involved in endosomal maturation and in MVB biogenesis (e.g. Alix and Tsg101) (van Niel G. et al., 2006), and transmembrane proteins like tetraspanins (CD63, CD81, CD82, CD53 and CD37) (Hemler M.E., 2003; Zöller M., 2009). The lipidic structure of exosomes is also peculiar and different from the one of the PM, with a marked enrichment in cholesterol, sphingomyelin and ceramides at the expense of their phosphatidylcholine and phosphatidylethanolamine contents (Wubbolts R. et al., 2003).

Recent reports have shown that exosomes may also act as carriers of genetic information, transferring both messenger and micro RNAs to target cells (Ratajczak J. et al., 2006; Valadi H. et al., 2007; Skog J. et al., 2008). Recent studies have also suggested that T cells exosomes can selectively incorporate miRNAs that are subsequently conveyed to dendritic cells where they are able to act on their original targets (Mittelbrunn et al., 2011; Montecalvo A. et al., 2012); moreover analysis of vesicular RNA showed the presence of other non-coding RNAs in addition to mRNAs and miRNAs. Several RNAs were found enriched in exosomes compared to cellular RNAs thus leading to the possibility that RNAs could be actively selected for vesicular incorporation (Ratajczak J. et al., 2006; Valadi H. et al., 2007) (Figure 10). ExoCarta database (http://www.exocarta.org) comprehends a list of lipids, proteins and RNAs identified so far in EVs derived from different cell types; no distinction between MVs and exosomes has been made so far. General efforts are aimed to the standardization of protocols able to purify MVs and exosomes more and more efficiently, thus reaching deeper levels of comprehension.

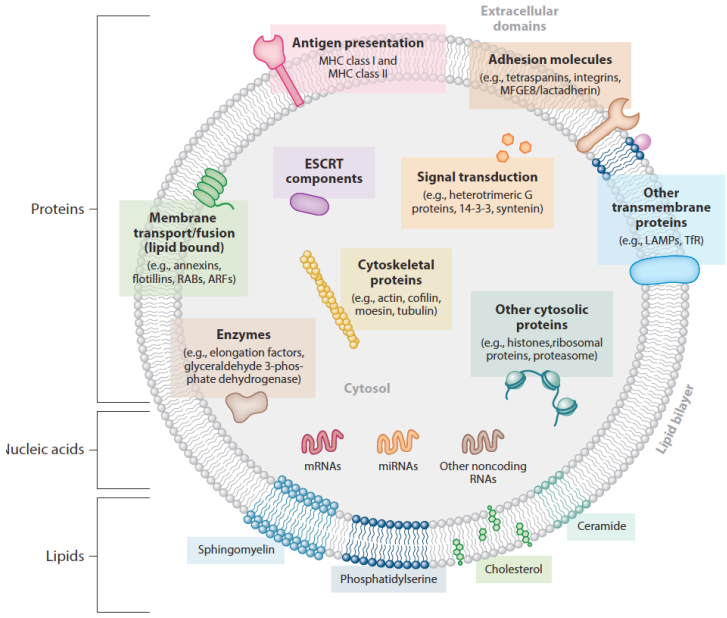

Figure 10. Schematic representation of exosome molecular cargoes. (Colombo M., Raposo G. and Thèry C., 2014)

1.3.3. Biogenesis of EVs and cargo incorporation

MVs and exosomes differ for both their entire biogenesis and mechanisms of secretion. MVs are formed and released at the level of the PM, where the process starts with a bending of the PM, followed by an active process that culminates with the narrowing of PM rim, the final seal and release of the vesicles (similar to what happen in cytokinesis during late stages of mitosis). There are actually membrane structural similarities between MVs and apoptotic vesicles, being both of them originated by PM curvature and shedding. Exosome formation starts at the surface where clathrin aggregates allow PM budding and the formation of clathrin-coated vesicles (CCVs) that following detachment and clathrin recycling become Early Endosomes (EEs). EE membrane undergoes structural rearrangements that ultimately lead to the inward invagination of the bilayer and the formation of ILVs in Late Endosome (LE) pouch that is hence called MVB. MVB can become secretory, by fusion with the PM and release of its content in extracellular environment, or be fated to ultimate degradation by lysosome mediated processing (Figure 11).

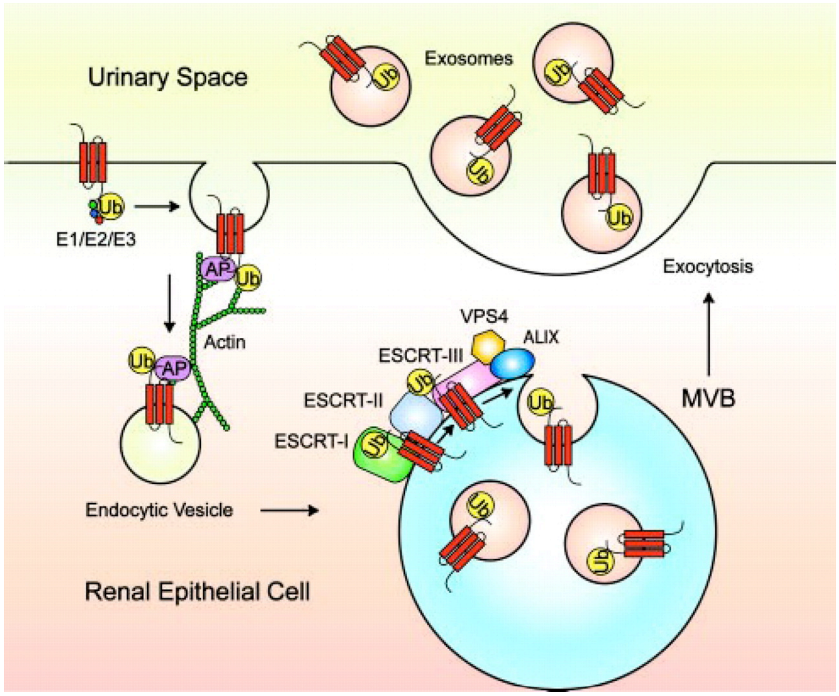

Figure 11. Process of exosome formation and release into the urine. Ub, ubiquitin; AP, adaptor protein; ESCRT, endosomal sorting complex required for transport; ALIX, ALG-2 interacting protein X. Adapted from Pisitkun T. et al., 2004

MVBs fated to secretion or degradation show some biochemical differences, since secretory vesicles are enriched in cholesterol (Möbius W. et al., 2002) while are depleted in their lysobiphosphatidic acid content (White I.J. et al., 2006). Behind exosome biogenesis resides the *endosomal sorting complex responsible for transport* (ESCRT) a highly conserved complex made up of a core of four multimers (ESCRT-0, -1, -2, -3) and accessory proteins (e.g. Vps4 and Alix). ESCRT-0, -1 and -2 are responsible for binding with ubiquitinated endosomal transmembrane proteins and their recruitment, while ESCRT-3 allows membrane invagination and ILV scission (Hurley J.H., 2010). However, ESCRT-mediated ILV formation is not the only mechanisms adopted by cells to produce exosomes; several studies have reported that in oligodendroglial cells exosome production is mediated by sphingomyelinase, an enzyme that converts sphingomyelin to ceramide and consequently can generate deformation of the membrane leading to ILV formation (Trajkovic K. et al., 2008). Nevertheless, in 2011 van Niel and colleagues observed exosome production in cells without ESCRT machinery and ceramide synthesis, thus suggesting an alternative way to produce and secrete ILVs. As for the loading of cytosolic proteins onto exosomal vesicles, it is supposedly linked to *chaperon proteins* (Thery C. et al., 2001). A small group of proteins has been identified to physically interact with exosomal tetraspanins and other transmembrane proteins like MHC II. Proteins like Hsp70, Hsp90, 14-3-3 e and PKM2 belong to this group and each one of them may play a role in the selection of molecules fated to be internalized within exosomes (Buschow S.I. et al., 2010). RNA loading onto exosomes is determined by specific sequences that specifically fate the RNA molecule to vesicular internalization (Batagov A.Q. et al., 2011); other studies suggest that ESCRT-2 might be responsible for loading RNA into exosomes, given its ability to bind RNA molecules (Irion U. and St Johnston D., 2007). Likewise, cargo internalization in MV is largely unknown; it is supposed that cytoplasmic proteins might undergo oligomerization and bind to PM proteins that recruit them within the new-formed MV (Shen B. et al., 2011).

The discovery of microRNAs (miRNAs) changed our understanding of the regulation of

gene expression. Distinct patterns of miRNA expression have been observed in many cancers, including GBMs, and the functional significance of some of these miRNA alterations is beginning to emerge. Only recently, researchers have focused on the possible role of miRNA in the microenvironmental communication of glioblastoma, primarily through the release and uptake of EVs. The analysis of EV/microRNA networks suggests that they can affect the tumor microenvironment in different ways (Figure 10): (i) direct reprogramming of cells in the tumor microenvironment (ii) indirect reprogramming of cells in the tumor microenvironment, or (iii) modification of the extracellular microenvironment. These mechanisms, separately or in combination, may be utilized for sensitization to therapy. EVs are avidly taken up by cells in culture where they can change such target cells' translational, transcriptional, and proteome profile. In fact it has been shown that the delivery of this tumor-derived EV cargo (Al-Nedawi K. et al., 2008) becomes functional in recipient cells (Montecalvo A. et al., 2012). EVs carrying oncogenic and tumor-suppressive proteins such as EGFR, EGFR variant III, PDGFRA, Met, and PTEN have been discovered in several models of high-grade gliomas (Bronisz A. et al., 2014). The contents of gliomas derived EVs also were found to be deregulated in hypoxia (Kucharzewska P. et al., 2012) and after radiation (Arscott W.T. et al., 2013). In these studies, hypoxia-inducible factor 1 or PDGFRA was found to be overexpressed. Likewise, pro-oncogenic and tumor-suppressive microRNAs (miR-34a, miR-128, miR-1, miR-26) directly targeting these and many other factors have been documented as deregulated in GBM cells (Li Y. et al., 2009). Therefore, EVs appear to provide a significant mode of communication between tumor cells (Figure 12).

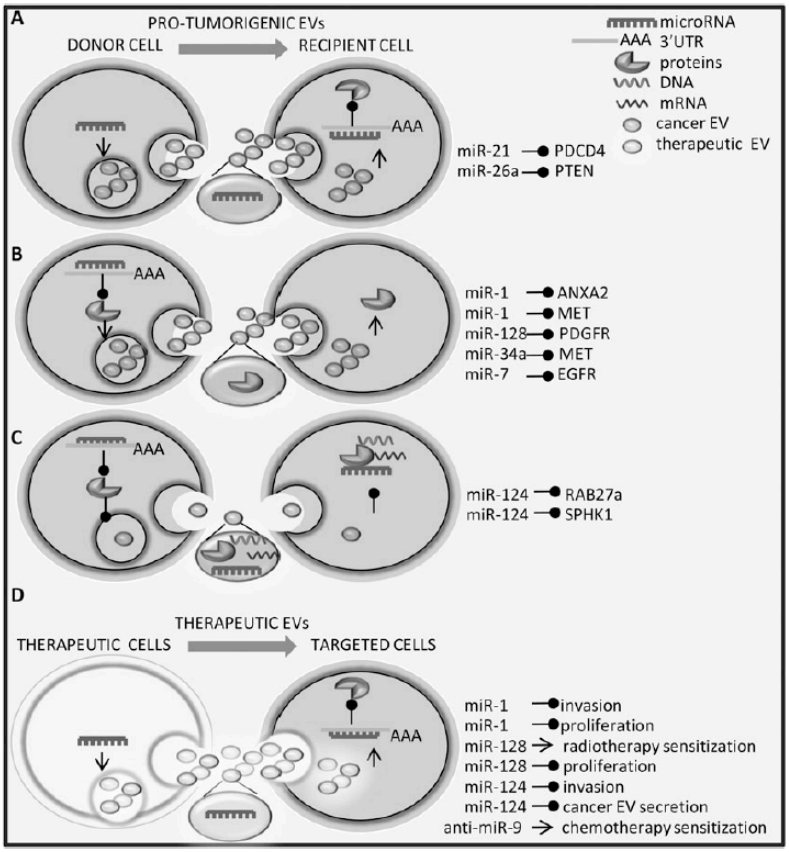

Fig. 12. The ways of action of EV/microRNAs in the microenvironment. (A) Direct reprogramming of cells in the tumor microenvironment by microRNA transfer, (B) indirect reprogramming of cells in the tumor microenvironment by miR-dependent targeting of EV cargo, (C) modification of extracellular microenvironment by miR-dependent alteration of EV release, (D) therapy sensitization by delivering therapeutic microRNA/anti-microRNA (Adapted from Godlewski J. et al., 2014)

1.3.3. Exosome-to-cell interaction

EV mechanism of action occurs by means of the physical interaction between the vesicle and target cell, with the former transferring cargo molecules, proteins, lipids and RNAs, within the host. Several studies reported this kind of interaction to be cell type specific, like in the case of B cell-derived exosomes showing a specific affinity for follicular dendritic cells harbouring lymphoid follicles (Denzer K. et al., 2000); analogously, intestinal epithelial exosomes preferentially interact with dendritic cells PM rather than with B or T lymphocytes (Mallegol J. et al., 2007). Exosome-cell specificity appears to rely on adhesion molecules expressed on the exosomal membrane, like integrins (Clayton A. et al., 2004). It has also been suggested that differences in tetraspanin levels on exosomal membrane could influence exosome-cell interaction and therefore explain exosome selectivity both in vitro and in vivo, by means of the

fine tuning of tetraspanin-associated proteins like integrins (Hemler M.E., 2003). Once stable interaction is established, exosomes can either merge with target cell PM and release their cargoes within or undergo internalization through the endocytic pathway; in this case exosomal membrane can fuse with endosome one, thus spreading molecular cargo within recipient cells.

1.3.4. EVs in physiologic and pathologic conditions

In the central nervous system (CNS), astrocytes, neurons and oligodendrocytes secrete exosomes that tightly regulate the chemical interaction among these different cell types (Lachenal G. et al., 2011). EVs actively induce neuron myelinisation, axon elongation and neuron survival (Wang Z. et al., 2011). EVs are also considered major players in the progression of several CNS disease driven by the aberrant accumulation of proteins: prions (Fevrier B. et al., 2004), b-amyloid peptides (Rajendran L. et al., 2006), superoxide dismutase (Gomes C. et al., 2007) and a-synucleins (Emmanouilidou E. et al., 2010) are secreted via the endocytic pathway within EVs. Alpha-synucleins were recently detected in patients plasma and cephalorachidian fluid thus paving the way to the opportunity to exploit EVs as a source of viable biomarkers in neurodegenerative disorders (Simpson R.J. et al., 2009). In 2008, Al-Nedawi and colleagues explored the possibility for a malignant cell to transfer oncogenes to target cells via EVs. Gliomas often express the constitutively active form of EGFR, called EGFRvIII; this truncated form of the receptor is capable alone of activating the whole pathway downstream to the EGFR. The authors treated glioma cells EGFRvIII-negative with EGFRvIII-expressing EVs with the resulting activation of the EGFR pathway downstream EGFR with MAPK and Akt pathway activation, morphology changes and increased proliferation capacity (Al-Nedawi K. et al., 2008). The same year, another lab showed that GBM cells secrete EVs containing angiogenic proteins, mRNAs and miRNAs; these vesicles interact with endothelial cells and stimulate their aberrant proliferation to support the growing of the tumor cells (Skog J. et al., 2008). Furthermore, fibroblast and normal epithelial cells treated with EVs isolated

from GBM cell lines are endowed with tumoral-traits, anoikis resistance and increased survival (Antonyak M et al., 2010).

1.3.5. EVs and clinical implications for GBM treatment

EVs are loaded with proteins, nucleic acids, lipids and metabolites reflecting their cell of origin. Since EVs can be detected and isolated from virtually every biological fluid, it is of notable interest the possibility to exploit EVs as carriers of a set of markers that may be indicative of GBM progression. While the concept of liquid biopsy is often associated to haematological tumors or to circulating tumoral cells, in GBM this is not an option, given the lack of circulating tumoral cells in patient blood stream; combining their relative abundance in GBM cells extracellular environment and their ability to cross the blood brain barrier (BBB), EVs can circumvent this limitation. Beyond their diagnostic value, it is also conceivable an exploitation of EVs for prognostic purposes, testing the expression of viable reliable prognostic markers like EGFRvIII and IDH1.

1.4. Chloride Intracellular Ion Channel – 1 (CLIC1)

1.4.1. Structure

The family of chloride intracellular ion channel (CLIC) is made up of small proteins with just a putative transmembrane domain. Proteins belonging to this group are widely and differently expressed. Even marked by intracellular localization, several of these proteins can be isolated from the plasma membrane. CLIC1, the first member of CLIC family, is a protein consisting of 241 amino acids. It has a molecular weight of 26.9 kDa and a pI of 4.85 as estimated by the DNAStar software (Lasergene) (Valenzuela M.S. et al., 1997). CLIC1 shows a 47.7% helical content and an 8.3% sheet content according to the crystal structure (Harrop S.J. et al., 2001); it contains six cysteine residues, one of which, Cys24, is found in the active site. Until the structure of CLIC4 was published in 2005 (Littler D.R. et al., 2005), CLIC1 was the only member of the CLIC family of proteins to have its crystal structure solved. CLIC1 is a

relatively flat protein that folds in two domains, a C-terminal and a N-terminal domain, linked by a proline-rich region that is thought to bestow an amount of plasticity upon the domain interface (Harrop S.J. et al., 2001). The N-terminal domain harbors a canonical thioredoxin region (bababba motif) (Martin J.L., 1995). The larger C-terminal domain is structurally all a-helical. CLIC1 forms a highly negatively charged loop between helix 5 and 6 (Pro147 – Gln164); this loop is extremely flexible and is supposed to play a central role in protein – protein interactions and membrane insertion (Harrop S.J. et al., 2001). The evidence that a region of CLIC1 was shielded from protein K digestion implied CLIC1 ability to span the membrane (Tulk B.M. and Edwards J.C., 1998). Harrop and colleagues were the first to hypothesize that CLIC1 forms a channel in plasma membranes, the N-terminal domain of the protein should undergo rapid unfolding and quick refolding to be properly inserted into the lipid bilayer. CLIC1 also harbors a glutathione (GSH) binding site within its N-terminal domain. GSH covalently binds Cys24 thus allowing the formation of a disulfide bond. Several studies reported CLIC1 to form a non-covalent dimeric entity following oxidation by means of hydrogen peroxide (Littler D.R. et al., 2004). This transition, reversible upon reduction, is due to the establishment of a disulphide bond between Cys24 and Cys59 of CLIC1 in its monomeric form and results in a major structural transition, particularly in the N-terminal domain, that ultimately leads to he exposure of a hydrophobic surface (Figure 13).

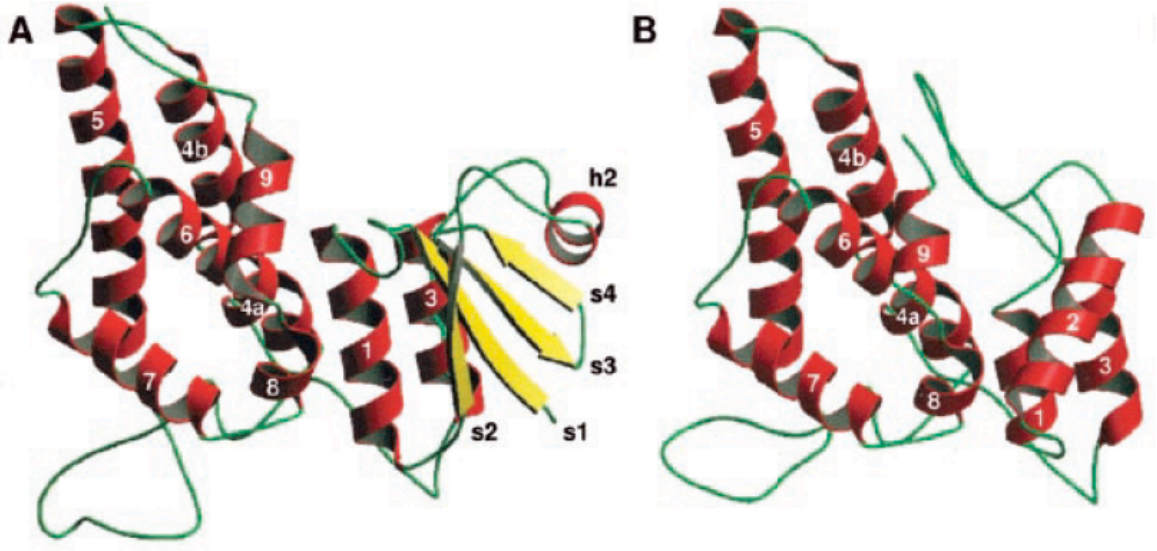

Figure 13. CLIC1 structural rearrangement. (A) Schematic representation of CLIC1 reduced form and (B) CLIC1 morphological change following oxidation. Adapted from Littler D.R. et al., 2005.

This hydrophobic surface may represent the membrane-docking interface in vivo where the monomer is believed to undergo similar alterations to its N-terminal domain before interacting with the membrane. CLIC1 dimer is less globular than the dimers formed by other members of the GST superfamily and can be compared with the unusual elongated dimer of the class Kappa enzyme (Ladner J.E. et al., 2004). The oxidized CLIC1 dimer can still form chloride channels as can the reduced protein, and both Cys24 and Cys59 were shown to be essential for CLIC1 channel formation (Littler D.R. et al, 2004). The only other member of the CLIC family that is known to form a homodimer is CLIC6 (Griffon N. et al., 2003). This protein dimerises in solution at its GST-like C-terminus but nothing else is known about the structure or properties of the CLIC6 dimer. CLIC4 has been shown to form a homotrimer under non-reducing conditions (Li Y. et al., 2006). This trimer is formed in the absence of disulphide bonds and proves that hydrogen bonds and hydrophobic contacts may be all that is required for a CLIC protein to muiltimerise.

1.4.2. Pathological role

CLIC1 appears to have a main role in all the diseases that involve oxidative stress (Averaimo S. et al., 2010). Indeed, CLIC1 was reported to contribute in activated microglia cells to the production of reactive oxygen species (ROS), a process well studied for its role in the progression of pathologies like Alzheimer (Milton R. et al., 2008). Since 2008, a series of publications started pointing out CLIC1 as a protein involved in different kinds of epithelial cancers: gastric carcinoma (Chen C.D. et al., 2007), colorectal cancer (Petrova D.T. et al., 2008), hepatocellular carcinoma (Huang J.S. et al., 2004) and more recently brain tumors (Kang M.K. et al., 2008; Setti M. et al., 2013). In these types of tumors CLIC1 is thought to play a major contribution in determining cell aggressiveness, regulating key-processes like proliferation, migration and metastatic behaviour. In 2000, one of the first electrophysiological studies carried out on this newly identified chloride ion channel identified CLIC1 on the PM of CHO-K1 cells in G2/M transition (easily identified for their round shape); moreover, CLIC1 inhibition by IAA-94 specific blocker led to global cell cycle lengthening (Valenzuela M.S. et al., 2000). Physiological fluctuation in ROS levels might explain this behaviour and partially explain CLIC1 involvement in regulating cell cycle progression (Menon S.G. and Goswami P.C., 2007). Several studies highlighted CLIC1 potential involvement in cellular migration and tumor metastatization, like in colorectial cancer and endothelial cells (Tung J.J. and Kitajewski J., 2010). CLIC1 could exert its control on cell motility by regulating either cellular volume or cytoskeletal dynamics. Other works have shown how several members of CLIC family seem to be capable of binding cytoskeletal elements: CLIC5A is tightly bound to cortical actin in placenta microvilli (Berryman M. and Bretscher A., 2000), CLIC4 interacts with both microtubules and actin-related elements (Berryman M. and Goldering, 2003), CLIC1 ion channel activity was found to be impaired by F-actin pointing out possible physical interactions (Singh S.K. et al., 2007).

1.4.3. Secreted CLIC1

Given the lack of proper peptides signalling for either PM insertion or secretion, CLIC1 tends to float into the cytoplasm in its soluble form. In 2007, Ulmasov and co-workers described CLIC1 intracellular localization in pancreatic and colorectal carcinoma cell lines (Panc1, T84 respectively). Immunofluorescence stainings showed CLIC1 distribution homogeneously scattered throughout the entire cell, with a more marked cytoplasmic rather than nuclear localization. Co-localization analyses showed no expression of CLIC1 in endoplamic reticulum and Golgi apparatus, in lysosomes and in trans-Golgi vesicular network; conversely, CLIC1 expression was appreciable in the endocytic and exosomal compartment (Ulmasov B. et al., 2007). CLIC1 has been detected in exosomes derived from renal tubular epithelial cells and urine (Pisitkun T. et al., 2004), mast cells (Valadi H. et al., 2007), B cells (Buschow S.I. et al., 2010), bladder carcinoma (Welton J.L. et al., 2010), breast carcinoma (Staubach S. et al., 2009), colorectal carcinoma (Mathivanan et al., 2009); CLIC1 is one of the top scoring proteins in ExoCarta database. In 2009, CLIC1 was detected by Enzyme-linked Immunosorbent Assay (ELISA) in the medium of nasopharyngeal carcinoma cell lines, and similarly CLIC1 was found at sensibly higher levels in the blood of patients affected by nasopharyngeal carcinoma thus proposing CLIC1 as a viable biomarker (Chang Y.H. et al., 2009). In 2012 Tang and colleagues exploited a murine model of ovarian carcinoma and detected CLIC1 in the serum of xenografted mice; they identified and increased expression of CLIC1 together with cathepsin D and peroxiredoxin in xenografted mice rather than healthy counterparts (Tang et al., 2012).

2. MATERIALS AND METHODS

2.1. Preparation of cell suspensions from patient tumors

This study was approved by the Ethical Committee for human experimentation of IEO (European Institute of Oncology) and all patients signed an approved consent document prior to surgery. Surgical specimens of tumors were collected at the Neurosurgery Dpt. at IRCCS Istituto Clinico Humanitas and examined by a neuropathologist to verify that each case met criteria for GBM and to select a tissue fragment with high content of viable tumor tissue. Each tissue specimen was minced in to small pieces and maintained in sterile saline at room temperature. One piece of the mincate was fixed in formaldehyde solution (38%) and successively paraffin-embedded; the remaining tissue was dissociated into single cell suspension in warmed EBSS (Earle's Balanced Salt Solution) containing papain (2 mg/ml) (Worthington Biochemical), EDTA (0.8 mg/ml) and L-Cystein (0.8 mg/ml) at 37C for 1-2 hours. The dissociated tumor was filtered through a 70 micron filter and washed a minimum of three times prior to culturing.

2.2. Neurosphere culture

Neurosphere cultures were maintained in neurosphere culture medium consisting of DMEM-F12 1:1 (Dulbecco's Modified Eagle Medium – Ham's F12 Nutrient Mixture) medium (Invitrogen) supplemented with B27 Supplement (Invitrogen), EGF (20 ng/ml), b-FGF (10 ng/ml) (PeproTech) and 2 ug/ml Heparin (Sigma), at 37°C in a 5% CO2 humidified incubator. All cultures were passaged by mechanically dissociation when spheres reached approximately 300-500 microns in diameter, and cell counts were performed at the time of passage. For cultures passaged at intervals longer than one week, media containing fresh growth factors was added twice weekly.

To established neurosphere cultures, dissociated tumor cells were seeded at an initial density of 1-2 x 10^5 cells/ml. Sorted populations from each tumor case were matched for plating density.

2.3. Lentiviral mediated CLIC1 silencing

Short hairpins specific for human CLIC1 (5'-GATGATGAGGAGATCGAGCTC-3') and for firefly luciferase (5'-CGTACGCGGAATACTTCGA-3') mRNA were cloned into XhoI/HpaI sites of PLentiLox 3.7 lentiviral vector. PLentiLox 3.7 and packaging plasmids (vpMDLg/pRRE, pRSV-REV and pMD2G) were amplified in the E.Coli-strain Top10, purified using a QUIAGEN MAXI KIT (Quiagen, Valencia, CA), and transfected in human HEK 293T cell line by calcium phosphate according to established procedures (TronoLab). After overnight transfection, the culture medium was replaced with DMEM supplemented with 10% FBS. Viral particles were collected 48h post transfection and concentrated using PEG-it (Mountain View, CA). Transducing unit (TU) concentration was then determined by Green Fluorescent Protein (GFP) expression. Single cell suspensions derived from GBM neurospheres were infected with 10^4 TU/ml. 72 hours after infection, transduced cells were selected with 1.5 mg/ml puromycine (Sigma-Aldrich, St. Louis, MO). Interference efficiency was evaluated 72 hours post selection by western immunoblot analysis.

2.4. Western blotting

Primary antibodies: CLIC1 (mouse monoclonal, 1:1000, clone CPTC-CLIC1-1 Millipore, Billerica, MA), Vinculin (mouse monoclonal, 1:10000, clone HVIN-1, Sigma Aldrich, St. Louis, MO), CD63 (mouse monoclonal, 1:50, clone FC-5.01 18-7300 Invitrogen), tsg101 (goat polyclonal, 1:1000, sc-6037 Santa Cruz, CA,USA), GM130 (mouse monoclonal, 1:500, 610822, Becton Dickinson, Franklin Lakes, NJ, USA).

Neurosphere and EV samples were lysated on ice in 50-100 ml of lysis buffer (50 mM Tris–HCl buffer [pH 8], 10 mM $CaCl_2$, 5mM EGTA [pH 8], 250 mM NaCl , Glycerol 10%, triton-x

100 1%) containing a cocktail of proteinase inhibitors (50 mM NAF , 10 mM NAPP ,10mM NaOrtoV , PMSF [0.1mg/ml], Leupeptin , Apoprotinin). Concentration of protein lysates was assessed by Bradford assay (Biorad, Hercules, CA). Each lysate (Whole cell extracts: 10 μg, EV lysates: 2 μg) was loaded onto a SDS-polyacrylamide gel electrophoresis (PAGE) under reducing conditions, and resolved proteins were transferred on to Nitrocellulose Transferring membranes (Protran ®, Indianapolis, IN) of 0.2 μm pore size. After blocking with 5% nonfat dry milk in Tris-Buffered Saline and Tween 20 (TBS-T [50mM Tris, 150mM NaCl, 0.05% Tween 20]), membranes were incubated overnight at 4°C with primary antibodies. Antibody binding was assessed by horseradish peroxidase (HRP)-conjugated secondary antibody (1:10000, Sigma Aldrich, St. Louis, MO). Immunoreactive bands were detected with ECL western blotting reagents (GE Healthcare Bio-Sciences, Pittsburgh,PA). Immuno-precipitation was carried out with 20 μg of anti-GFP antibody (sc-9996, Santa Cruz, CA, USA) on 2mg of whole cell extract overnight at 4°C. Membranes were blotted anti-CLIC1.

2.5. Quantitative RT-PCR analysis

Total RNAs from cell samples was isolated by RNAeasy Mini kit (Quiagen, Valencia, CA). Total RNAs from normal brain tissues (n=20) and astrocytic tumors of different grades (n=13 WHO grade II, n=28 WHO grade III and n=20 WHO Grade IV) were a generous gift of Maria Stella Carro (University of Freiburg, Germany). RNAs from each sample (1mg) were retrotranscribed using ImProm-II Reverse Transcriptase (Promega, Madison, WI) at the following temperature steps: 25°C for 5', 42°C for 60', 70°C for 10'. Quantitative real time PCR (qRT-PCR) analysis was then performed by 7,500 Fast Real-Time PCR System (Applied Biosystems, Foster City, CA) with Syber Green PCR Master Mix (Applied Biosystems, Foster City, CA). Threshold cycle (CT) values for each gene were normalized to TATA-Box Binding Protein expression levels (TBP) for cell samples and to Hypoxanthine PhosphoRibosylTransferase expression levels (HPRT1) for FFPE samples. The sequence of primers was the following: CLIC1 fw: 5'-GTTGACACCAAAAGGCGG-3', rev: 5'-

TCTCCAGATTGTCATTGAGTGC-3';TBP fw:5'-TGCACAGGAGCCAAGAGTGAA-3', rev:5'-CACATCACAGCTCCCCACCA-3' ; HPRT1 fw:5'-TGACCTTGATTTATTTTGCATACC-3',rev:5'-CGAGCAAGACGTTCAGTCCT-3'.

2.6. Clonogenic assay

The colony forming cell assay, also referred to as the methylcellulose assay, is an *in vitro* assay used in the study of stem cells. The assay is based on the ability of progenitors to proliferate and differentiate into colonies in a semi-solid media in response to growth factors stimulation. The colonies formed can be enumerated and characterized according to their unique morphology. The standard protocol was used with minor modifications. The cells were resuspended in D-MEM/F12 medium with growth factors and an equal volume of Methylcellulose (StemCell Technologies) was added; the methylcellulose concentration in the final cell mixture was approximately 1.27%. 1.5 mL (3000 cells) of the final cell mixture was added to a 35 mm culture plate with grid (at least three plates were prepared for each condition). The medium was spread evenly by gently rotating the plate. Three sample plates and an uncovered plate containing 3 - 4 mL sterile water, necessary to maintain the humidity necessary for colony development, were placed in a 100 mm culture plate and covered. The cells were incubated for 14 - 16 days at 37° C and 5% CO_2, avoiding disturbing the plate during the incubation period to prevent shifting of the colonies. The colonies were scored at the end of the incubation period. Individual colonies were identified and counted using an inverted microscope and the scoring grid. Colonies consisting of at least 40 cells were counted.

2.7. MTT Assay

U87MG were harvested in 96-well plates at the density of 3000 cells

U87MG and mechanically dissociated neurospheres were seeded in 96-well plates at the density of 3000 cells per well. 3-(4, 5-dimethylthiazol-2-yl)-2, 5-diphenyltetrazolium bromide (MTT, 50mg/ml) was added and, after incubation for 4 hours, crystals were dissolved in

DMSO. Cell viability was evaluated by CellTiter 96® AQueous Non-Radioactive Cell Proliferation Assay (Promega, Madison, WI). GBM cells were treated with EVs 50 mg/ml and cell viability was assessed after 120 hours of incubation.Three independent replicates were considered for each experiment.

2.8. Cell cycle analysis and apoptosis

For apoptosis analysis, infected cells (GFP+) were first fixed in 1% formaldehyde for 20 minutes on ice, washed once in PBS and fixed again in ethanol 75% for 30 minutes on ice. Fixed cells were incubated in Propidium Iodide (2.5 μg/ml) and RNAse (250 μg/ml) for 12 - 16 hours at +4^{o}C and analyzed by flow cytometry.

2.9. Immunofluorescence analysis

Primary antibodies: CLIC1 (mouse monoclonal, 1:1000, clone 356.1, Santa Cruz Biotechnology, Santa Cruz, CA), Sox2 (rabbit polyclonal, 1:500, ab15830, Abcam, Cambridge, UK), Nestin (rabbit polyclonal, 1:200, ABD69, Millipore, Billerica, MA), GFAP (rabbit polyclonal, 1:500, Z0334, DakoCytomation, Glostrup, Denmark), BrdU (mouse monoclonal, 5 mg/ml, BD Biosciences, Franklin Lakes, NJ), Cleaved Caspase-3 (rabbit polyclonal, 1:500, Cell Signaling, Danvers, MA). Confocal images and live-microscopy images were generated with a Leica SPII spectral confocal microscope (Leica Microsystems, Wetzlar, Germany). Neurospheres were mechanically dissociated until single cell suspension was achieved and let adhere onto Polysine Slides (Thermo Scientific, Waltham, MA) for 40'. Cells were fixed with 4% paraformaldehyde (PFA) in phosphate-buffered saline (PBS). Cells were then permeabilized with 0.1% Triton-X for 10' and blocked with a 5% Bovine Seum Albumin (BSA) in PBS for 30'. Primary antibodies were used at room temperature (RT) for 60'. Fluorescein isothiocyanate (FITC)-conjugated or cyanine dye (Cy3)-coniugated secondary antibodies were applied at RT for 60'. Nuclei were counterstained with DAPI (1:5000). The

quantitative comparison between CLIC1 expression and expression of other stem/progenitors and/or differentiated markers was performed independently by *two* blinded *operators.*

2.10. Proximity Ligation Assay (PLA)

Samples were processed for PLA according to manufacturer's instructions (OLink Bioscience, Sweden) using the DuoLink in situ Orange detection reagent. Then, for complete detection of the expression levels of the targeted molecules, coverslips were incubated with antibodies (see previous section). Primary antibodies employed for PLA were: CD63 (mouse monoclonal, 1:50, clone FC-5.01 18-7300 Invitrogen), CLIC1 (rabbit polyclonal, 1:500, sc-134859 Santa Cruz, CA, USA).

2.11. Immunohystochemistry (IHC)

All sections were counterstained with Mayer's haematoxylin and visualized using a bright field microscope. Tissue slices were incubated overnight at 4°C with the following primary antibodies: CLIC1 (mouse monoclonal, 1:1000, clone 356.1, Santa Cruz Biotechnology, Santa Cruz, CA), anti-Nuclei (mouse monoclonal, 1:1000, clone 3E1.3, Millipore, Billerica, MA), GFP (rabbit polyclonal, 1:1000, sc8334, Santa Cruz Biotechnology, Santa Cruz, CA)**.**

2.12. Isolation of EVs

GBM cell lines were grown in DMEM with 10% (vol/vol) FBS. Cultures were then washed in triplicate and grown in serum-free medium for 48 h. The same approach was adopted for GBM-derived CSC. These media were collected and treated according to standard procedures (Thèry et al., 2006); media underwent serial centrifugation (500g for 10', 1200g for 20', 10'000g for 30'), they were 0.22-**μ**m syringe filtered, and then, ultracentrifuged at 100'000g for 60'.

2.13. Electron microscopy (EM)

For routine electron microscopy (EM), purified exovesicles were fixed with 1% glutaraldehyde for 1 h, washed, post-fixed with 1% reduced osmium tetroxide for 1 h, washed, post-stained with 0,3% thiocarbohydrazide; refixed in the OsO4 and embedded into Epon. Ultrathin sections were placed on formvar-coated grids or slot-grids. Immune-EM analysis was performed as previously described (Polishchuk et al., 1999; Beznoussenko, et al., 2007). Briefly, purified exovesicles were fixed with 1% glutaraldehyde and centrifuged. The pellet of purified exovesicles was embedded into gelatine and cryo-sections were prepared according to the standard procedure and cryo-sections were placed on slot-grid and labelled with antibodies against CLIC1 and CD63 (KMC8, 10 mg/ml) with subsequent labelling with protein A conjugated with 10 and 15 nm gold particles (UMC Utrecht, 1:60). Grids were observed at 200 kV with a Tecnai 20 (FEI Company). Size of individual vesicles was measured on 5 different pictures taken at 10,000x magnification for each EV preparation, using the software integrated into the Tecnai20 electron microscope software. Primary antibodies: anti-CD63 (rabbit polyclonal, 1:1000, sc-15363, Santa Cruz, CA, USA), anti-CLIC1 (rabbit polyclonal, 1:500, sc-134859 Santa Cruz, CA, USA).

2.14. Nanoparticle tracking analysis (NTA)

We used the light-scattering characteristics of 488 nm laser light on microvesicle preparations undergoing Brownian motion injected by continuous flow into the sample chamber of an LM10 unit (Nanosight, Amesbury, UK). Three videos of 60-90 seconds were recorded of each sample. Data analysis was performed with NTA 3.0 software (Nanosight). The diffusion coefficient and hydrodynamic radius were determined using the Stokes–Einstein equation, and results were displayed as a particle size distribution. Data are presented as the average and standard deviation of the three video recordings. Since NTA is most accurate between particle concentrations in the range of $2x10^8$ to $2x10^9$/ml, when samples contained higher numbers of particles, they were diluted before analysis and the relative concentration calculated according to the dilution factor. Control 100 and 200 nm beads were supplied by Nanosight. NTA of a

small sample of any given preparation revealed that they were essentially monodisperse, excluding the problem of aggregation, which may significantly impact on a biological system.

2.15. Label-free Mass Spectrometry

Peptide mixtures were analyzed by online nano-flow liquid chromatography tandem mass spectrometry (LC-MSMS) using an EASY-nLC™ 1000 (Thermo Fisher Scientic, Odense, Denmark) connected either to an Q-Exactive (Thermo Fisher Scientific) or LTQ-OrbitrapVelos (Thermo Fisher Scientific) through a nanoelectrospray ion source. For nUHPLC, the nano LC system was operated in one column set-up with a 25 cm analytical column (75 μm inner diameter, 350 μm outer diameter) packed with C_{18} resin (ReproSil, Pur C18AQ 1.9 μm, Dr.Maisch, Germany) configuration. Solvent A was 0.1% FA in ddH2O and solvent B was 80% ACN with 0.1% FA. Samples were injected in an aqueous 1% TFA solution at a flow rate of 500 nl/min. Peptides were separated with a gradient of 5-40% solvent B over 200 min followed by a gradient of 40-60% in 5 min and 60-95% over 5 min at a flow rate of 250 nl/min in the EASY-nLC 1000 system. For HPLC analysis instrument connection, solvent composition and gradients were as described before but analytical column were packed with a different C_{18} resin (ReproSil, Pur C18AQ 3 μm, Dr.Maisch, Germany). The Q-Exactive instrument was operated in the data-dependent mode (DDA) to automatically switch between full scan MS and MSMS acquisition. Survey full scan MS spectra (from m/z 300-1150) were analysed in the Orbitrap detector with resolution R=35,000 at m/z 400. The five most intense peptide ions with charge states ≥2 were sequentially isolated to a target value of 3e6 and fragmented by Higher Energy Collision Dissociation (HCD) with a normalized collision energy setting of 25%. The maximum allowed ion accumulation times were 20 ms for full scans and 50 ms for MSMS and the target value for MSMS was set to 1e6. The dynamic exclusion time was set to 25s. Standard mass spectrometric conditions for all experiments were: spray voltage, 2.4 kV; no sheath and auxiliary gas flow. Raw data has been analyzed by label-free software MaxLFQ that is completely integrated into MaxQuant software

2.16. Animal experiments

An intracranial orthotopic model was utilized for evaluation of cell tumorigenicity (Uchida et al. 2000). Cells from dissociated neurospheres were resuspended in 2 µl of PBS and stereotaxically injected into the nucleus caudatus (coordinates: 0.7 - 1 mm posterior, 3 mm left lateral, 3.5 mm in depth from the dura) of 5-week-old female CD-1 nude mice. The mice were maintained until development of neurologic signs and then killed for the analysis of tumor histology and immunohistochemistry. CD-1 nu/nu mice were housed in plastic cages and were kept in a regulated environment (22 ± 1°C; 55 ± 5% humidity), with a 12 h light/dark cycle (lights on at 7:00 A.M.). Food and water were available *ad libitum*. T2-weighted MR images were obtained using a 9.4-T magnet (Varian) and tumor areas were calculated from resulting images on a single scan in 3 mice per group using ImageJ software. Experiments involving animals were performed in accordance with the Italian Laws (D.L.vo 116/92 and following additions), which enforces EU 86/609 Directive (Council Directive 86/609/EEC of 24 November 1986 on the approximation of laws, regulations and administrative provisions of the Member States regarding the protection of animals used for experimental and other scientific purposes).

2.17. Statistical Analysis

To determine differences within group pairings we used either Bonferroni's correction, when samples analyzed showed homogeneous variances, or Tamhane's test, to analyze samples with non-homogeneous variances. Co-localization analysis was studied using Cohen's test to determine inter-rater agreement between categorical items, in our case marker positivity. Significance of Cohen K index was obtained by applying a Chi-square test to positivity and negativity frequencies in compared conditions. In Kaplan-Meier curves, survival differences were compared by log-rank analysis. For the *in vivo* limiting dilution assay, tumor formation frequency and statistical significance were evaluated with the extreme limiting dilution analysis function (http://bioinf.wehi.edu.au/software/elda/).

3. RESULTS

3.1. CLIC1 expression in patients affected by Glioblastoma

CLIC1 has been proposed as an ion channel widely expressed in a variety of human cancers, so we wanted to look into CLIC1 expression in human glioblastomas (GBM) compared to the other members of CLIC family. To do that we analyzed the expression of CLIC family members in the National Cancer Institute's Repository for Molecular Brain Neoplasia Data (REMBRANDT) (Madhavan S et al., 2009) and we found CLIC1 and CLIC4 as the only members differentially expressed in GBM compared to healthy samples (Figure 14), with the former showing the greater difference between expression in gliomas and in control (non-tumor) samples (Figure 15) (F test for disomogeneous variances: F= 106.56; df=2 and 385; p << 0.001; ANOVA with Tamhane's multiple comparison test: Non-tumor vs Grade II-III p << 0.0001, Grade II-III vs Grade IV p << 0.0001).

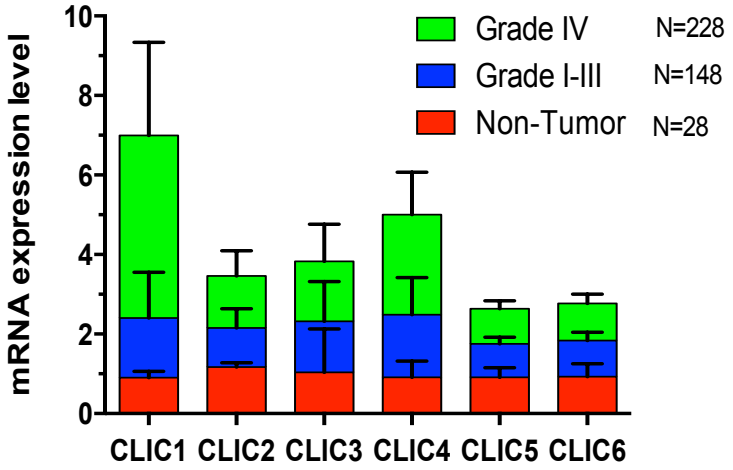

Figure 14. CLIC expression in brain tumors. mRNA levels of CLIC family members in control (non-tumor) brain tissues, astrocytomas (WHO grades I-III) and glioblastomas (WHO grade IV) derived from REMBRANDT database. Median values are depicted; Error bars represent 95% confidence intervals. ** $p < 0.001$ and *** $p < 0.0001$ of differences between averages of indicated pairs calculated by ANOVA with Tamhane's multiple comparison test; n.s.: not significant.

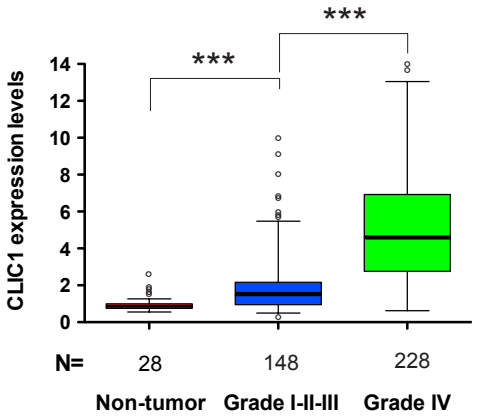

Figure 15. CLIC1 expression level in human gliomas. Box-plot showing CLIC1 mRNA levels in control (non-tumor) brain tissues, astrocytomas (WHO grades I-III) and glioblastomas (WHO grade IV) derived from REMBRANDT database. The solid lines within the boxes represent the median value; the boxes show the 25th and 75th percentile range of CLIC1 mRNA levels; maximum and minimum values are depicted as horizontal bars; circles represent outliers. ** $p < 0.001$ and *** $p < 0.0001$ of differences between averages of indicated pairs calculated by ANOVA with Tamhane's multiple comparison test; n.s.: not significant.

Analysis of CLIC1 transcript levels in relation to patient survival derived from REMBRANDT revealed that CLIC1 expression inversely associated with patient survival, suggesting a potential exploitation of CLIC1 as an outcome predictor ($CLIC1^{low}$ vs $CLIC1^{high}$ survival: Chi square= 74.35, d.f. = 1, log-rank p-value < 0.001) (Figure 16 A). Likewise, we obtained analogous results narrowing down the analysis to the subgroup consisting of GBM patients alone (Chi square= 10.99, d.f.= 1, log-rank p-value < 0.01) (Figure 16 B).

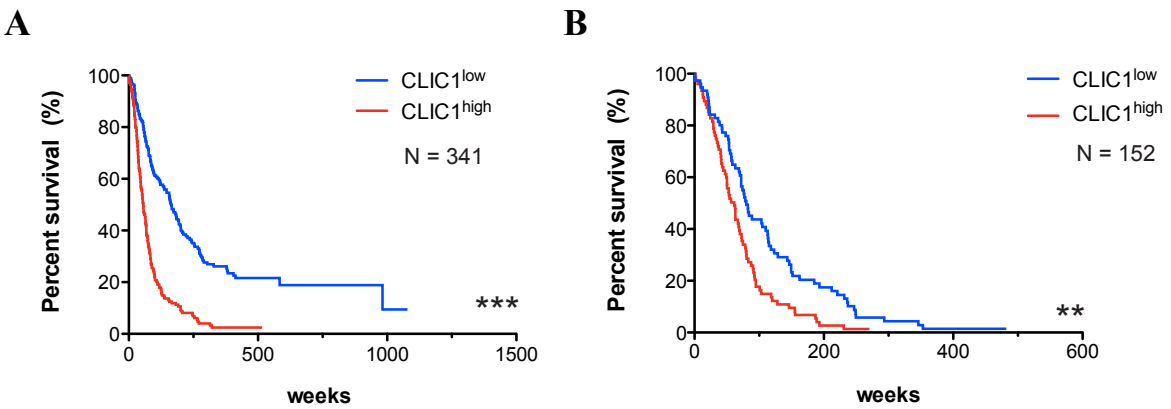

Figure 16. CLIC1 expression and patient prognosis. Association of CLIC1 mRNA expression with patient prognosis: (A) Kaplan-Meier survival plot based on patient data from REMBRANDT database. (B) Kaplan-Meier survival plot based on subgroup from REMBRANDT database comprising only GBM patients. In each graph, patient samples have been divided into CLIC1 low-expressing tumors ($CLIC1^{low}$, blue) and CLIC1 high-expressing tumors ($CLIC1^{high}$, red) based on whether the tumors had CLIC1 mRNA levels that were less than or grater than median levels. (WHO grade IV) derived from REMBRANDT database.

GBMs have been classified in molecular subtypes according to gene expression signatures (Phillips HS et al., 2006; Verhaak RG et al., 2010). Phillips et al. defined three sub-types (Proneural [PN], Proliferative [PROL], Mesenchymal [MES]) close to those described by Verhaak et al, who used data from The Cancer Genome Atlas (TCGA, Nature 2008) to describe four distinct subtypes (Proneural [PN], Neural [N], Classic [CL] and Mesenchymal [MES]).

Thus, we analysed CLIC1 expression using both Phillips' and Verhaak's microarray data sets. We found that CLIC1 expression was always significantly higher in the mesenchymal subtype compared to the others (Figure 17 A and B) (Phillips'.dataset – ANOVA with Tamhane's multiple comparison test: PN vs each of the others, always $p << 0.001$, PROL vs. MES $p = 0.002$. Verhaak's dataset –ANOVA with Tamhane's multiple comparison test: N vs. each of the others, always $p < 0.001$, MES vs. each of the others, always $p < 0.001$, N vs. CL $p = 0.990$).

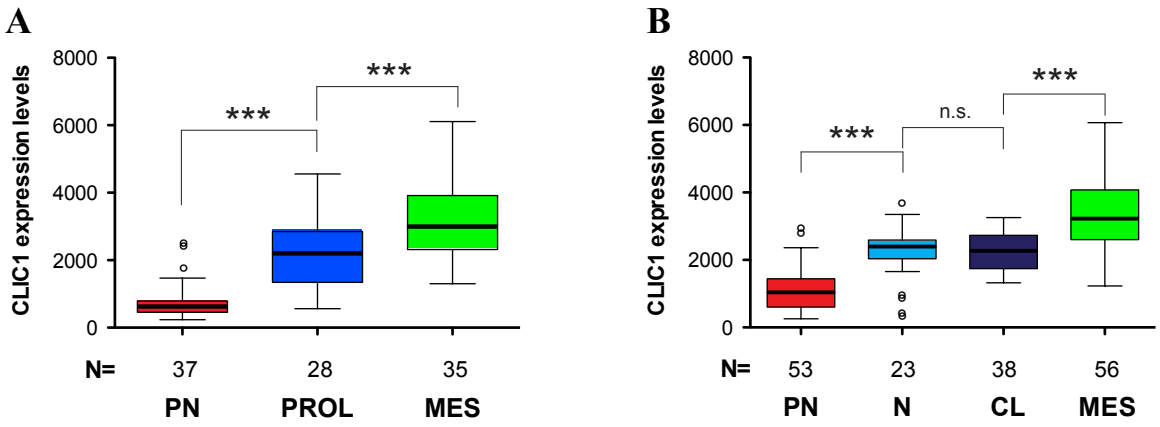

Figure 17. CLIC1 distribution in the different molecular subclasses. Association of CLIC1 mRNA levels with GBM subtypes (Proneural [PN], Proliferative [Prolif], Neural [N], Classical [CL] and Mesenchymal [MES]): microarray data set from Phillips' (A) and from Verhaak's works (B) were examined. In both panels the solid lines within the boxes represent the median value; the boxes show the 25th and 75th percentile range of CLIC1 mRNA levels; maximum and minimum values are depicted as horizontal bars; circles represent outliers. ** $p < 0.001$ and *** $p < 0.0001$ of differences between averages of indicated pairs calculated by ANOVA with Tamhane's multiple comparison test; n.s.: not significant.

3.2. Dissecting CLIC1 distribution within cancer stem / progenitor cells isolated by GBM samples

To further evaluate the extent of CLIC1 overexpression in human gliomas, we examined CLIC1 expression level in a distinct set of normal brain tissues (n=20) and astrocytic tumors of different grades (n=13 WHO grade II, n=28 WHO grade III and n=20 WHO Grade IV). CLIC1 was weakly expressed in normal brain specimens and its expression increased with tumor grade, reaching the highest levels in GBMs. Notably, GBM subgroup displayed a marked heterogeneity in CLIC1 expression (Figure 18).

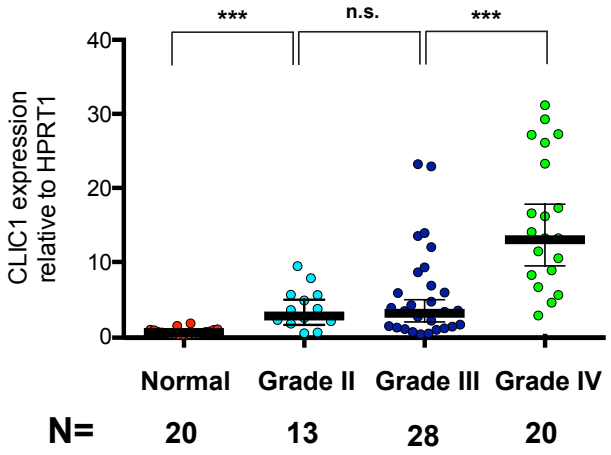

Figure 18. CLIC1 expression in astrocytic tumors. CLIC1 expression levels by qRT-PCR in normal brain specimens (n=20) and in astrocytic tumors of different grades (n=13 WHO grade II, n=28 WHO grade III and n=20 WHO Grade IV). The solid lines represent the mean value; Error bars represent 95% confidence intervals. *** $p < 0.0001$ of differences between averages of indicated pairs calculated by ANOVA with Tamhane's multiple comparison test; n.s.: not significant.

We isolated GBM stem/progenitor cells from surgically resected human GBM specimens and cultured them as neurospheres by using previously established conditions (Ortensi et al.). We next assessed CLIC1 expression level in GBM derived neurosphers. Similarly to the results obtained for brain tissues, GBM stem/progenitor cells expressed significantly higher level of CLIC1 mRNA compared to normal human progenitor cells (NPCs), with variable degrees among the tumor samples analyzed (Figure 19).

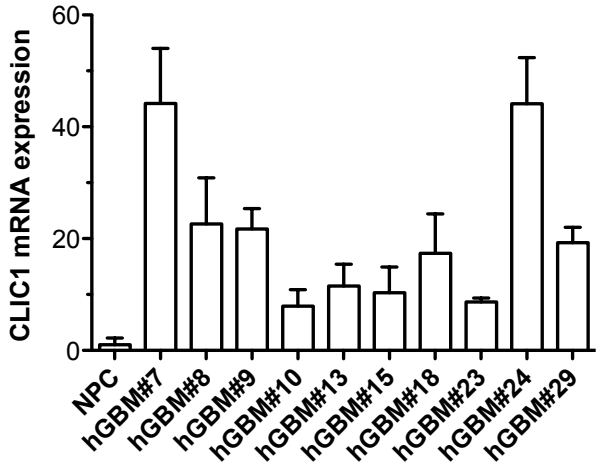

Figure 19. CLIC1 expression in patient-derived GBM neurospheres. CLIC1 expression levels by qRT-PCR in different patient-derived GBM neurospheres. Experiments were performed in triplicate; error bars represent 95% confidence intervals.

Considering that GBM-derived neurospheres are a mixed population of stem, progenitor and differentiated cells, we investigated CLIC1 localization within the neurosphere. A specific CLIC1 antibody (Figure 7) revealed a colocalization between CLIC1 and putative stem/progenitor cell markers (Sox2, Nestin) (Lee J et al., 2006), showing that CLIC1 is enriched in the stem/progenitor cell compartment of the neurosphere (Figure 20).

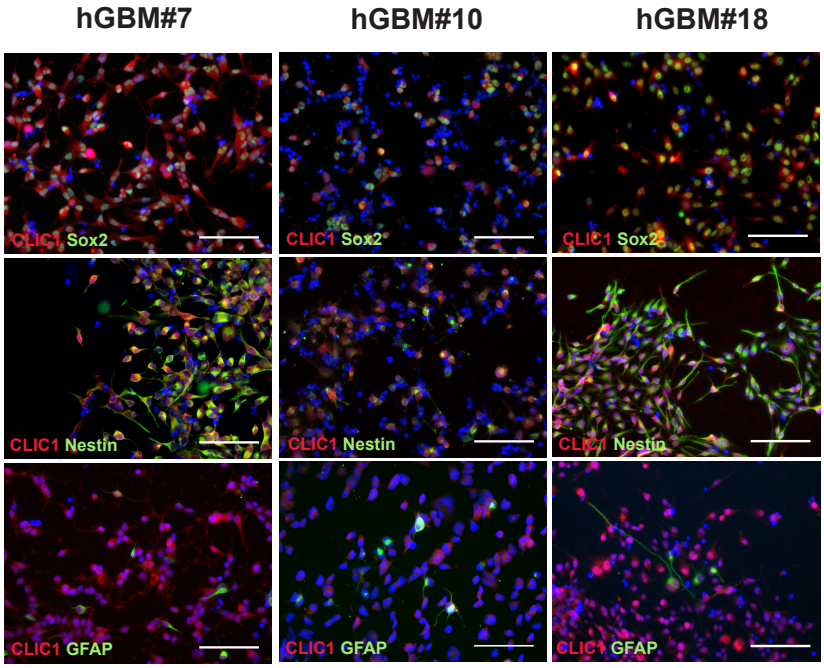

Figure 20. CLIC1 distribution within the neurosphere. Representative images of CLIC1 immunostaining in GBM-derived neurospheres. Dissociated neurospheres were fixed and processed for immunofluorescence (CLIC1, red; Sox2, Nestin and GFAP, green; DAPI, blue; merge, yellow). Scale bar = 50 μm.

The frequency of CLIC1 colocalization with either Sox2 or Nestin has been quantified and evaluated by Cohen's kappa index (Carletta J. et al., 1996) demonstrating that the frequency of co-localization observed was significantly higher (Cohen's kappa index close to 1.0) than what would be expected from stochastically behaving-markers (Cohen's kappa index close to 0.0) (Table 2).

	Marker I	Marker II	kappa index	Chi-square	p-value
GBM#7	CLIC1	Sox2	0,946	750,56	< 0,001
		Nestin	0,937	318,05	< 0,001
		GFAP	-0,014	18,33	< 0,001
GBM#10	CLIC1	Sox2	0,873	476,55	< 0,001
		Nestin	0,836	406,68	< 0,001
		GFAP	-0,007	0,23	0,634
GBM#18	CLIC1	Sox2	0,856	336,49	< 0,001
		Nestin	0,907	726,36	< 0,001
		GFAP	0,007	2,17	0,140

Table 2. . Cohen's K close to 1 for highly associated markers, close to 0 for unrelated markers. The significance of observed K values has been evaluated by means of Chi square test. Immunostained cells were counted at 20X magnification, five fields for each sample (average cell number per field was 150). Three independent experiments were performed.

To further characterize CLIC1 co-localization with putative stem cell markers we performed FACS analysis in two different patient derived neurospheres (GBM#7 and GBM#10), analysing CLIC1, Nestin and GFAP expression levels. We found that the majority of cells (85-95%) was nestin-positive, and only a small percentage of cells, as few as 10%, was GFAP-positive. Moreover, we detected a positive correlation between CLIC1 and Nestin expression (r = 0.8 and 0.6 in hGBM#7 and hGBM#10 respectively), on the other hand no correlation has been scored between CLIC1 and GFAP expression (r=0.2 and 0.05 respectively) (Figure 21).

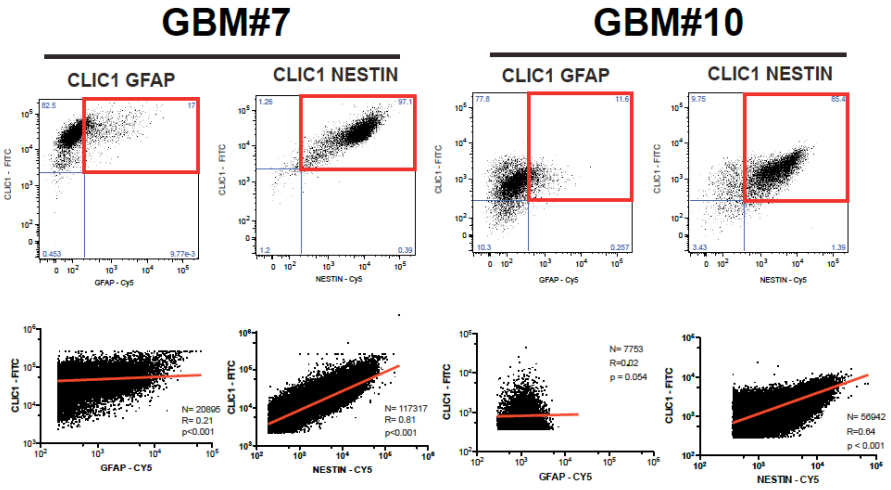

Figure 21. CLIC1 association with stem cell markers. GBM-derived neurospheres have been dissociated and labeled with CLIC1 antibody in association with either the neural stem cell marker Nestin or the astrocyte marker GFAP. Flow-cytometry analyses are depicted. Slopes of the fitting curves ($hGBM\#7_{NESTIN}$= 0.501, $hGBM\#7_{GFAP}$= 0.061, $hGBM\#10_{NESTIN}$= 0.531, $hGBM\#10_{GFAP}$= 0.016) and the reported correlation values (hGBM#7: R_{NESTIN}= 0.81, R_{GFAP}= 0.21; hGBM#10 R_{NESTIN}= 0.64, R_{GFAP}= 0.02), point out a better correlation of CLIC1 with Nestin than with GFAP.

3.3. CLIC1 chloride current in normal and tumoral neurospheres

CLIC1 can exist as both soluble globular protein and integral membrane protein with ion channel function depending on the tissue and on the oxidative status. After oxidative stress CLIC1 is able to translocate into plasma membrane where it acts as a Cl^- channel. Thus, we studied CLIC1 localization in normal human progenitor cells and GBM-derived neurospheres isolated from different patients. Immunofluorescent staining of not permeabilized cells revealed that CLIC1 is constitutively localized on the plasma membrane of GBM-derived neurospheres (Figure 22, upper panel); in contrast, NPCs did not show a plasma-membrane staining (Figure 22, lower panel).

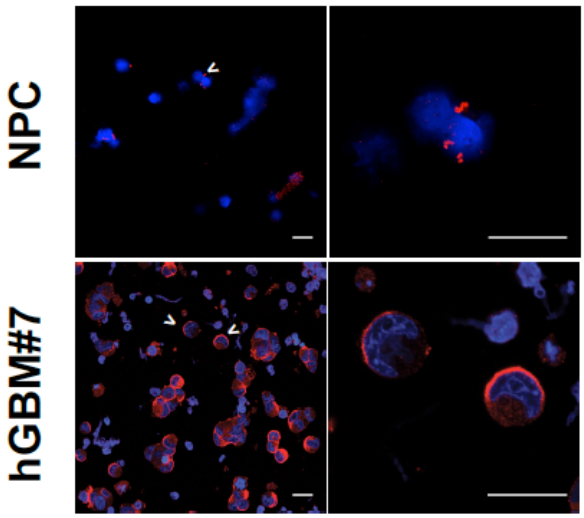

Figure 22. CLIC1 subcellular localization in normal and tumoral neurospheres. Representative images of CLIC1 immunostaining in not permeabilized normal and tumoral human neurospheres. Dissociated neurospheres were fixed and processed for immunofluorescence (CLIC1: red; DAPI: blue). Cells were analyzed using confocal laser scanning microscopy and a single optical x-y-plane section is shown. Scale bar = 10 µm. NPC: normal human progenitor cells; hGBM#7: neurospheres isolated from GBM#7 patient.

Western blotting analysis of cell fractions obtained from NPCs and hGBM#7 cells showed CLIC1 enrichment in the plasma membrane of human tumoral neurospheres (Figure 23), consistent with the result obtained in other GBM derived neurospheres (Figure 24).

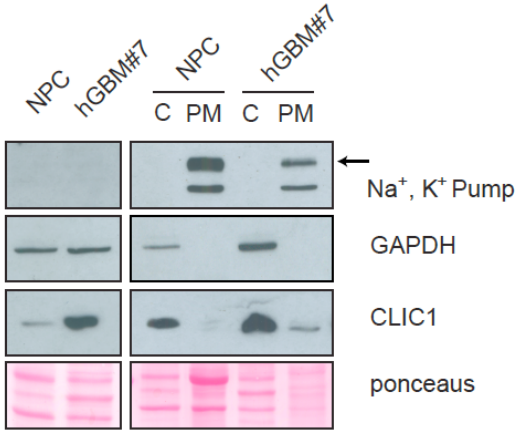

Figure 23. Plasma membrane localization in GBM- and neural stem cell-derived neurospheres. Western blotting analysis of CLIC1 expression levels in whole cell lysates (left panel) and plasma-membrane and cytoplasm-containing fractions (right panel) derived from normal (NPC) and tumoral neurospheres (hGBM#7). Na^+,K^+ Pump and GAPDH expression were examined to assess the purity of plasma-membrane and cytoplasmic fractions respectively. Reversible Ponceau staining was used as a control for equal protein loading.

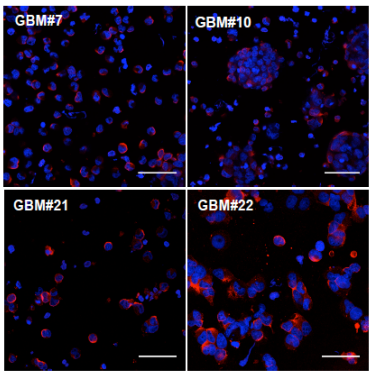

Figure 24. CLIC1 subcellular localization in several GBM-derived neurospheres. Representative images of CLIC1 immunostaining in not permeabilized normal and tumoral human neurospheres. Dissociated neurospheres were fixed and processed for immunofluorescence (CLIC1: red; DAPI: blue). Cells were analyzed using confocal laser scanning microscopy and a single optical x-y-plane section is shown. Scale bar = 20 µm. hGBM#7-22: neurospheres isolated from GBM#7-22 patient.

To unravel if CLIC1 constitutively localized on cell plasma membrane functions as ion channel, we measured CLIC1 ion channel activity by perforated patch clamp technique in NPCs and hGBM#7 cells. Cl^- currents mediated by CLIC1 were isolated using the specific inhibitor indanyloxyacetic acid–94 (IAA94), and normalized to the total current (I_{Tot}) in the corresponding cell (I_{IAA94} / I_{Tot}%). Interestingly, we found that CLIC1-mediated currents (IAA94-sensitive currents, I_{IAA94}) were more represented in tumoral cells (GLM: p-value < 0.001 related to cell type, and p=0.4311 related to membrane potential) (Figure 25). Taken together, these results demonstrate increased CLIC1 expression and activity in tumoral stem-progenitor cells compared to the normal counterparts.

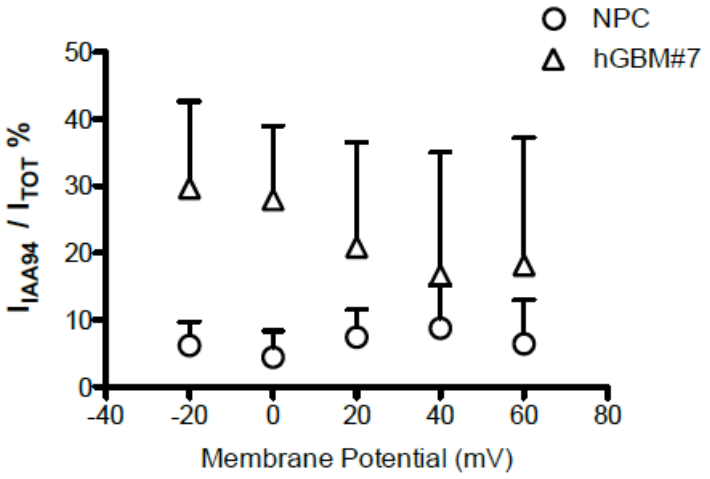

Figure 25. CLIC1 functional activity in GBM- and neural stem cell-derived neurospheres. CLIC1-mediated Cl^- currents measured by perforated patch clamp technique in normal (NPC) and tumoral (hGBM#7) neurospheres. Cl^- currents mediated by CLIC1 (I_{IAA94}) were isolated using the specific CLIC1 inhibitor indanyloxyacetic acid–94 (IAA94), and normalized to the total cell current (I_{Tot}) (I_{IAA94}/I_{Tot}%). Average values derived from five independent experiments were represented. Error bars represent 95% confidence intervals. GLM test of between-subjects effects: F for "potential" = 1.44, d. f. = 4, p = 0.235 (n. s.); F for "cell type" = 36.17, d. f. = 1, p = 0.001; F for variables interaction = 1.30, d. f. = 8, p = 0.266 n. s. No significance for interaction means a similar pattern of I_{IAA94} / I_{Tot} change for different cell types at different membrane potential values, even if average I_{IAA94} / I_{Tot} values are different between different cell types.

3.4. Chloride ion current upon CLIC1 knock-down in GBM-derived neurospheres.

To disclose CLIC1 role in GBM stem/progenitor cells, we silenced CLIC1 expression in patient-derived GBM neurospheres by cloning short-hairpin RNA oligonucleotides specific against human CLIC1 mRNA (sh) in a lentiviral vector containing green fluorescent protein (GFP) and puromycine resistance gene as reporters. The same vector containing an shRNA targeting the luciferase mRNA sequence was used as control (Non Targeting, NT). Interference efficiency was confirmed by western blot: CLIC1 was silenced by nearly 90% in different samples (Figure 26).

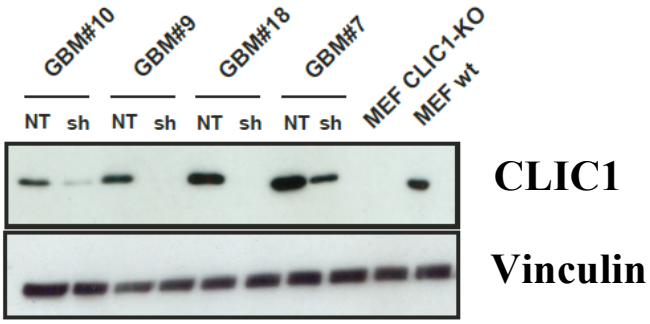

Figure 26. CLIC1 silencing in GBM-derived neurospheres. Western blotting analysis showing the efficiency of CLIC1 silencing in GBM neurospheres isolated from 4 patient samples. Dissociated neurospheres were transduced with lentivirus carrying either non-targeting shRNA (NT) or CLIC1 shRNA (sh). Mouse embryonic fibroblasts derived from CLIC1 knocked out mice (MEF CLIC1-KO) were used as negative controls. Vinculin was used as loading control.

In order to sort out whether the reduction in total CLIC1 protein level was associated with a modification in the amount of the Cl^- current mediated by this protein, we performed perforated patch clamp experiments in NT and CLIC1 silenced cells derived from two different patients (hGBM#7 and hGBM#10). Representative experiments from NT and sh cells are reported (Figure 27 A). Cell currents have been measured before (Total) and after IAA94 or 4,4'-Diisothiocyano-2,2'-stilbenedisulfonic acid (DIDS) addition to the bath solution. The corresponding Current/Voltage relationships clearly show a IAA94-sensitive current in NT cells but not in sh cells (Figure 27 B).

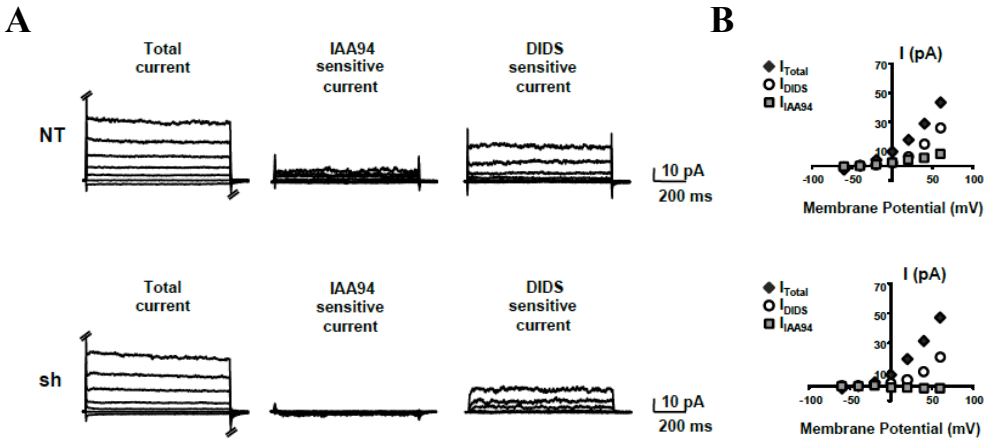

Figure 27. CLIC1 silencing and ion channel activity. Representative current traces (total, IAA94-sensitive and DIDS-sensitive currents) from control (NT) and CLIC1 silenced (sh) cells derived from hGBM#10 neurospheres, and elicited by different potential steps (from -60 mV to 60 mV).

In all the cells analyzed from both hGBM#7 and hGBM#10 neurospheres, we found that control cells always displayed a IAA94-sensitive current while CLIC1 silenced cells consistently showed the absence of a detectable CLIC1-mediated Cl^- current (Generalized Linear Model [GLM]: p-value < 0.0001 related to cell type, and p=0.979 related to membrane potential) (Figure 28 A). The other Cl^- currents in the cells, isolated using the inhibitor 4,4'-Diisothiocyano-2,2'-stilbenedisulfonic acid (DIDS-sensitive currents, I_{DIDS}), were comparable (GLM: p-value=0.068 related to cell type, and p=0.010 related to membrane potential) (Figure 28 B). These results corroborate the effects of CLIC1 silencing onto CLIC1 expression and ion channel activity, revealed as the lack of IAA94-sensitive current in CLIC1 silenced cells.

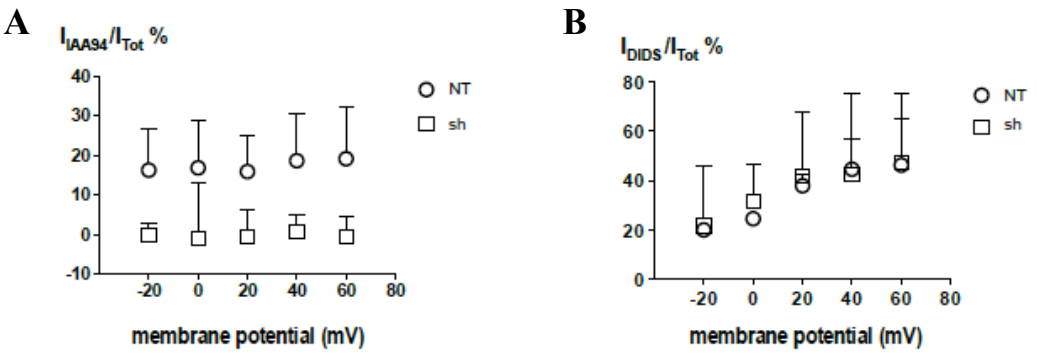

Figure 28. CLIC1 silencing and ion channel activity. The current-voltage relationships for the corresponding experiments in B and D. (A) CLIC1 sensitive currents (I_{IAA94}) were isolated using the specific CLIC1 inhibitor indanyloxyacetic acid–94 (IAA94), and normalized to the total cell current (I_{Tot}) (I_{IAA94}/I_{Tot}%). (B) The other Cl^- currents in the cells were evaluated by the inhibitor 4,4'-Diisothiocyano-2,2'-stilbenedisulfonic acid (I_{DIDS}) and normalized to the total cell current (I_{Tot}) (I_{DIDS}/I_{Tot}%). Average values derived from four independent experiments were represented. Error bars represent 95% confidence intervals. GLM test of between-subjects effects on I_{IAA94}/I_{Tot} values: F for "potential" = 0.108, d. f. = 4, p = 0.979 (n. s.); F for "cell type" = 50.038, d. f. = 1, p < 0.001; F for variables interaction = 0.058, d. f. = 4, p = 0.993 n. s. no significance for interaction means a similar pattern of I_{IAA94}/I_{Tot} change for different cell types at different membrane potential values, even if average I_{IAA94}/I_{Tot} values are different between different cell types. GLM test of between-subjects effects on I_{DIDS} / I_{Tot} values: F for "potential" = 4.031, d. f. = 4, p = 0.01; F for "cell type" = 3.590, d. f. = 1, p = 0.068; F for variables interaction = 0.085, d. f. = 4, p = 0.986. No significance for interaction means a similar pattern of I_{DIDS}/I_{Tot} change for different cell types at different membrane potential values.

3.5. Self-renewal and proliferative capacity of CLIC1 silenced neurospheres

We next investigated the role of CLIC1 in regulating the maintenance and the growth of GBM neurospheres. *In vitro* self-renewal capacity of CLIC1 silenced and control cells was evaluated

by methylcellulose assay. Single cells were plated in semi-solid medium, single clones counted after 15 days and the clonogenic cells were calculated as percentage of the total number of seeded cells. CLIC1 silenced cells formed significantly less (hGBM#7 NT: 11.63±5.23%, sh: 3.83±1.75%; hGBM#9 NT: 14.86±3.37%, sh: 3.20±0.71%; hGBM#10 NT: 14.00±3.23%, sh: 3.35±0.98%; p-value<0.01 in all experiments) (Figure 29 A) and smaller colonies (NT: 502.5±56.85 mm; sh: 264.0±13.50 mm. p-value < 0.01. N=5) (Figure 29 B), with a lower cellular content compared to control cells (NT: 830.00±119.22 cells, sh: 483.33±85.68 cells. p<0.01) (Figure 29 C).

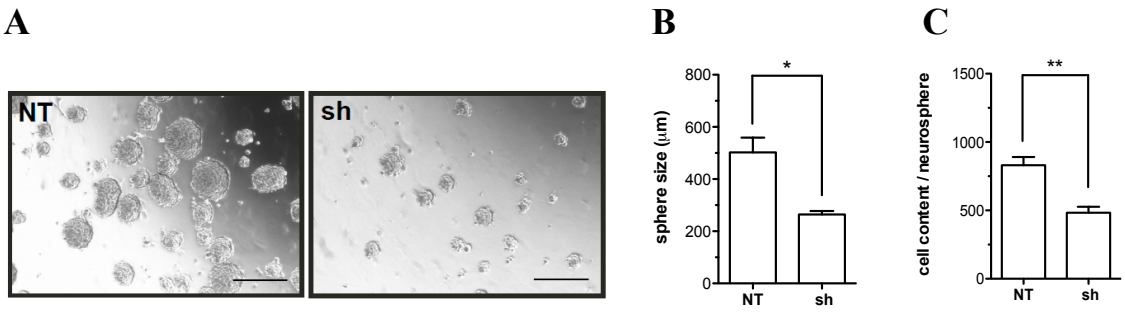

Figure 29. Effects of CLIC1 silencing on neurosphere size. (A) Representative microphotographs of control (NT) and CLIC1 silenced (sh) neurospheres formed in methilcellulose-containing medium after 15 days in culture. Scale bar = 300 μm. (B) Quantification of the maximal diameters of control (NT) and CLIC1 silenced (sh) hGBM#7 neurospheres. Ten neurospheres for each sample were analysed. (D) Quantification of hGBM#7 neurosphere cell number. Ten neurospheres for each sample were picked, dissociated and the cell number was determined.

When spheres generated at the first plating were dissociated and single cells were seeded on metyl-cellulose, control cells formed spheres with significantly high efficiency, while CLIC1 silenced cells generated only few small spheres, suggesting reduced self-renewal capacity (Figure 30 A). Interestingly, there was no difference in clonogenic capacity between CLIC1 silenced and control cells at the third re-plating when CLIC1 silenced cells re-expressed the protein (Figure 30 B and C).

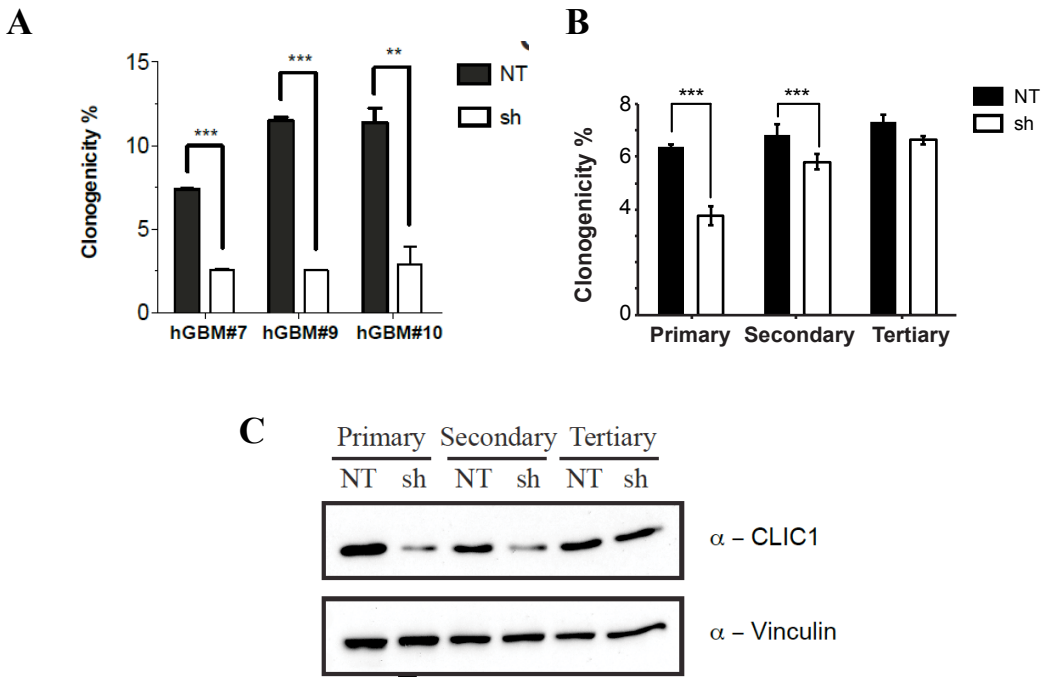

Figure 30. Effects of CLIC1 silencing on clonogenic potential. Neurosphere formation assay. (A) The clonogenic capacity of control (NT) and CLIC1 silenced (sh) cells was evaluated by plating cells in methilcellulose-containing medium. After 15 days, each plate was examined under a light microscope, and the total number of neurospheres was determined. (B) The clonogenic capacity og NT and sh neurospheres was assessed upon serial passaging. (C) Western Immunoblot of primary, secondary and tertiary colonies showed a marked reduction of shCLIC1 interference. Vinculin was exploited as loading control. Three independent experiments were performed; error bars represent 95% confidence intervals; * $p < 0.05$, ** $p < 0.001$, *** $p < 0.0001$.

Furthermore, CLIC1 silencing strongly reduced cellular growth kinetics in all patient-derived GBM neurospheres analyzed, as shown by MTT assay (hGBM#7: F=233.5, d.f.=1, p-value<0.001; hGBM#9: F=208.5, d.f.=1, p-value<0.001; hGBM#10: F=62.8, d.f.=1, p-value<0.001) (Figure 31).

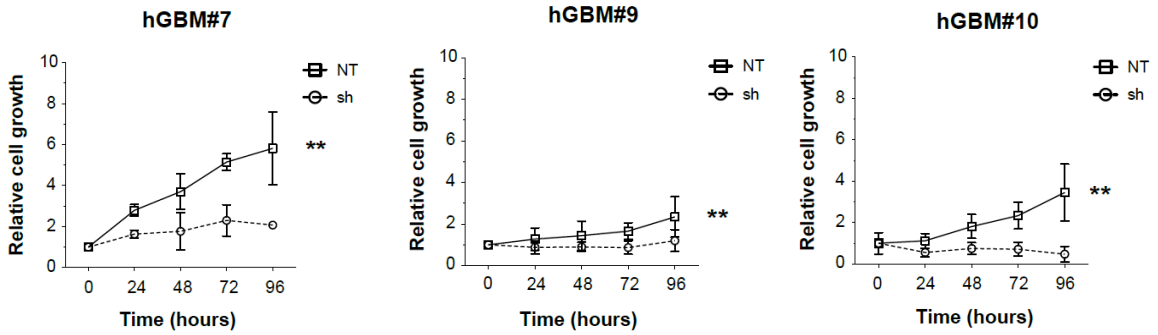

Figure 31. CLIC1 affects proliferation capacity of GBM-derived neurospheres. The growth of control (NT) and CLIC1 silenced (sh) cells isolated from 3 patient samples was measured by 3-(4, 5-dimethylthiazol-2-yl)-2, 5-diphenyltetrazolium bromide (MTT) assay. Three independent experiments

were performed; error bars represent 95% confidence intervals; ** p<0.001. GLM tests of between-subjects effects showed statistically significant difference in all patients for the relative cell growth according to the time, the interference, and the interaction between those two variables.

Consistent with cell proliferation data, CLIC1 silencing strongly reduced the percentage of BrdU positive cells in GBM derived neurospheres (hGBM#7 NT: 64.32±3.93%, sh: 12.09±2.25%; hGBM#9 NT: 28.58±2.58%, sh: 14.48±0.18%; hGBM#10 NT: 41.39±0.80%, sh: 18.61±1.32%. p-value<0.05 in all hGBM analyzed) (Figure 32).

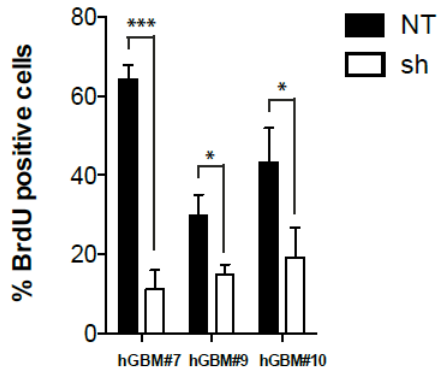

Figure 32. BrdU incorporation assay. Control (NT) and CLIC1 silenced (sh) neurospheres isolated from 3 patient samples were subjected to BrdU incorporation assay: BrdU-positive cells were quantified by immunofluorescence. Immunostained cells were counted at 20X magnification, five fields for each sample (average cell number per field was 150). Three independent experiments were performed; error bars represent 95% confidence intervals; * p < 0.05, ** p < 0.001, *** p < 0.0001.

However, cell cycle analysis showed no alteration in cell cycle progression (Figure 33 A). Moreover, no difference in the percentage of apoptotic cells between CLIC1 silenced and the control cells was detected (Figure 33 B and C). Together, these data indicate that CLIC1 downregulation affects the ability to steadily propagate GBM neurospheres.

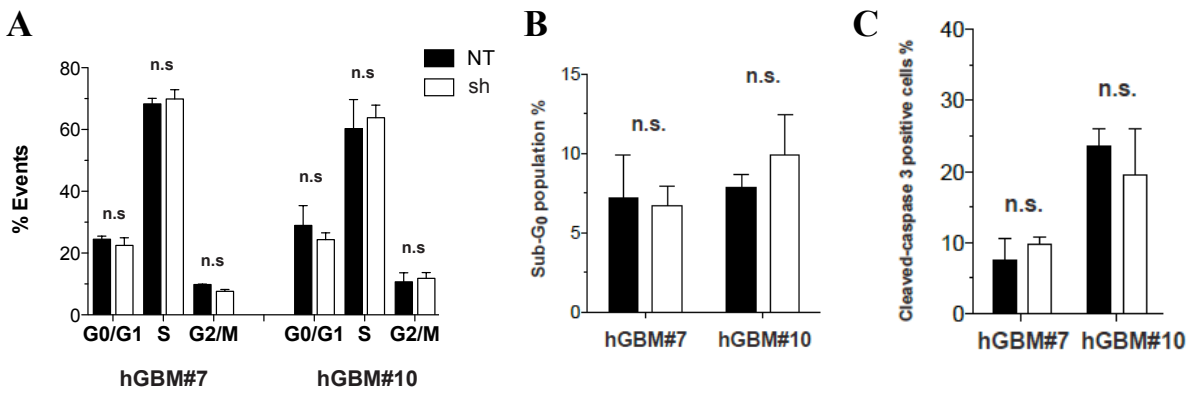

Figure 33. CLIC1 silencing and ion channel activity. (A) Cells were fixed and stained with PI for the DNA content analysis by using flow cytometry (FACS). The cell cycle distribution within the total cell population is shown as histograms with the percentage of cells in the cell cycle phases indicated for NT and CLIC1 silenced (sh) cells. The results are representative of three experiments. (B) Apoptosis detection in CLIC1 silenced (sh) and NT cells. The percentages of apoptotic cells in the cultures were analysed by PI staining for DNA content analysis by using flow cytometry (FACS) or (C) by immunofluorescent detection of cleaved caspase 3. Results shown are relative to three independent experiments; error bars represent 95% confidence intervals; p values are two-sided (Student t test).

3.6. GBM stem / progenitor cell proliferation and CLIC1-mediated chloride current

To determine whether the effect of CLIC1 silencing on GBM stem/progenitors' growth is dependent on its function as ion channel, we treated GBM neurospheres with a specific CLIC1 antibody. We performed electrophysiological recordings in perforated patch clamp configuration on cells derived by mechanically dissociated neurospheres, to test the antibody efficacy in blocking CLIC1-mediated Cl^- currents. Upon CLIC1 antibody addition, a reduction of total current was observed, but no further reduction was detected following IAA-94 addition (Figure 34 A and B upper panels); similar results were obtained by treating cells first with IAA-94 and then with the specific CLIC1 antibody (Figure 34 A and B middle panels) (ANOVA with Tamhane's multiple comparison test for IAA94/CLIC1 antibody treatment: p-value<<0.0001). No alteration in total current was measured treating the cells with a mouse isotype antibody (IgG) as control (Figure 34 A and B lower panels) (ANOVA with Tamhane's multiple comparison test for IgG antibody treatment: p-value=0.66). Overall, these data prove the efficacy and the specificity of CLIC1 antibody in blocking CLIC1-mediated Cl^- currents.

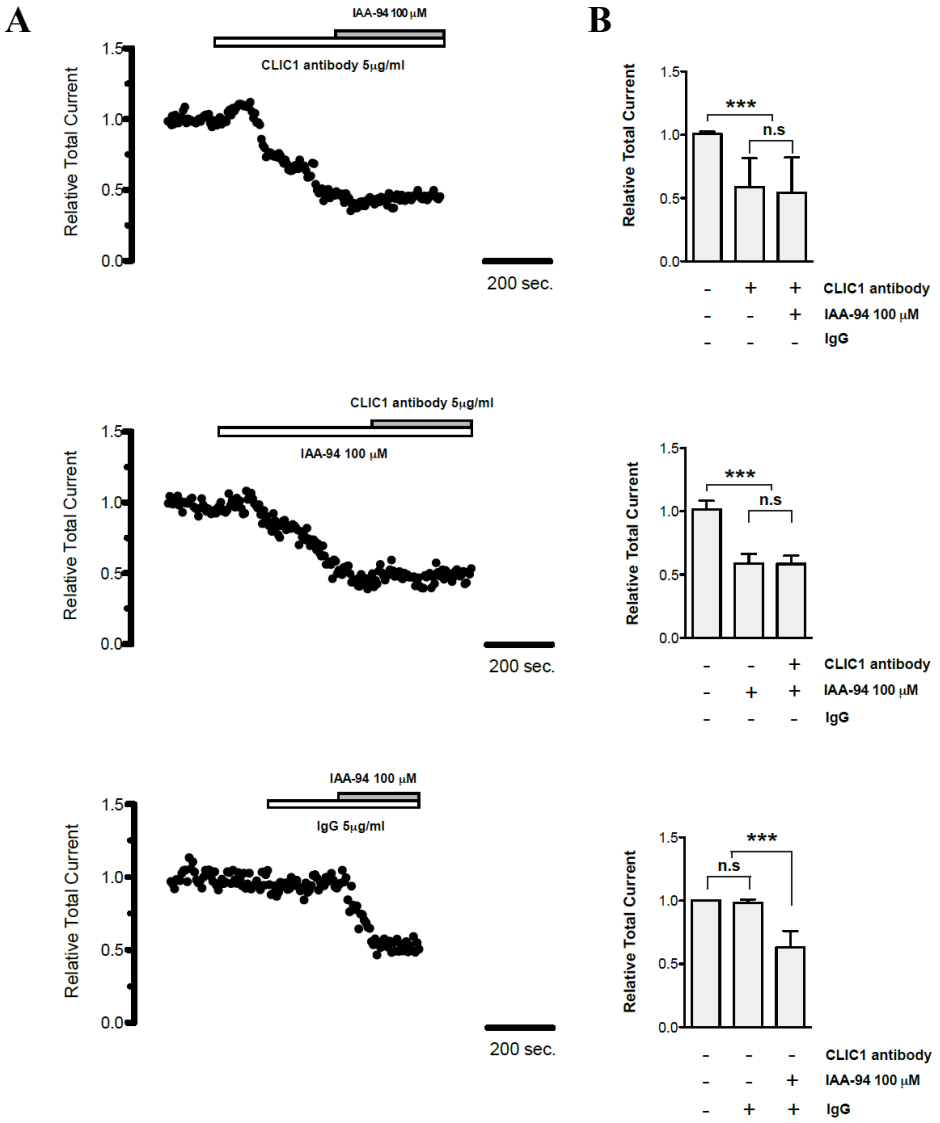

Figure 34. Effects of CLIC1 antibody treatment on GBM neurospheres. (A and B) The effect of CLIC1 antibody on CLIC1 currents has been assessed by perforated patch clamp technique. (A) Representative whole cell current traces recorded in the perforated patch configuration at 50 mV from NT and CLIC1 silenced (sh) cells derived from hGBM#10 cells are shown. (B) Quantification of the different treatments as in (A) on whole cell current traces. Average values derived from four independent experiments were represented. The significance of the differences in relative total current after Tahmane's test for disomogeneous variances is shown: n. s. = not significant, *** $p < 0.0001$.

We next treated GBM neurospheres with different doses of CLIC1 antibody (1, 5 and 10 mg/ml) and measured the percentage of viable cells after 72 hours. The blockage of CLIC1 activity decreased cell growth in a dose dependent manner (Figure 35).

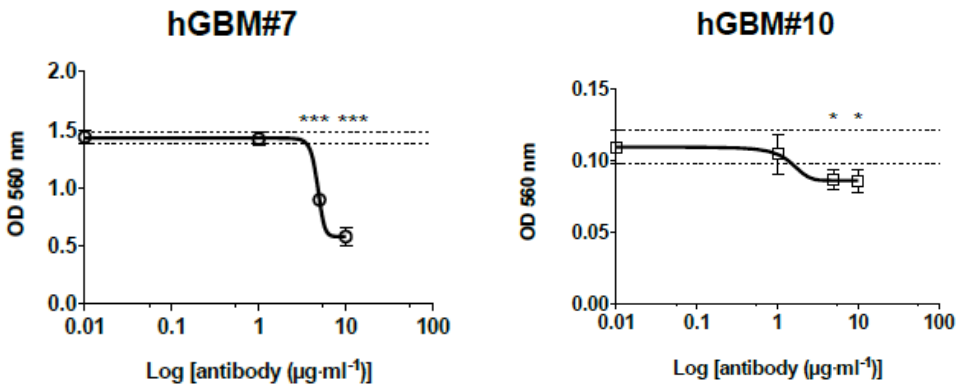

Figure 35. Effects of CLIC1 antibody treatment on GBM neurosphere viability. Effect of CLIC1 antibody on GBM neurospheres derived from hGBM#7 and hGBM#10 patients. GBM neurospheres were treated with increasing concentrations of CLIC1 antibody (1, 5 and 10 µg/ml) for 72 hours and cell viability was monitored by MTT assay; error bars represent 95% confidence intervals; three independent experiments were performed. The difference between cell viability at different antibody concentrations and reference average viability in control conditions has been evaluated by Bonferroni's test. The significance of the differences is shown: * $p < 0.05$, *** $p < 0.0001$.

The maximal biological effect was observed at the highest doses tested (10 µg/ml) in cells that express higher levels of CLIC1 (hGBM#7), while cells expressing lower levels of CLIC1 (hGBM#10) reached the maximal biological effect already at lower doses of CLIC1 antibody (5 mg/ml) (p-value<0.05 at 5 and 10 mg/ml of CLIC1 antibody). BrdU uptake was reduced in both cell lines after CLIC1 antibody treatment (NT: 30.6±6.90%, sh: 17.7±4.30%; p-value<0.05) while there were not differences in the percentage of apoptotic cells between treated and untreated cells (CLIC1 antibody: 23.1±4.2% and IgG: 21.0±3.6%; p-value=0.42) (Figure 36). These results recapitulate those obtained after CLIC1 silencing, demonstrating that CLIC1 ion channel activity is essential for the growth of GBM stem/progenitor cells.

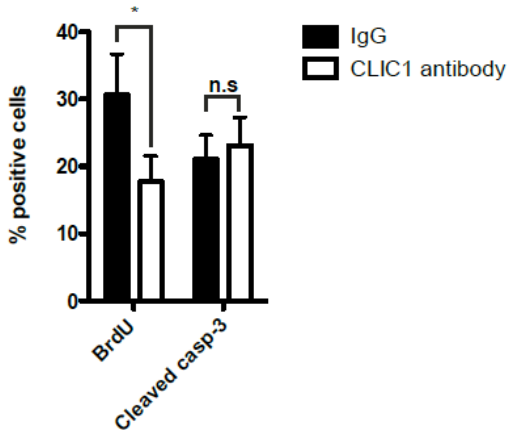

Figure 36. Effects of CLIC1 antibody treatment on neurosphere proliferation and apoptosis. Effect of CLIC1 antibody treatment on BrdU incorporation (left panel) and caspase-3 activation (right panel) in hGBM#7 neurospheres. BrdU- or cleaved caspase-3 positive cells were counted at 20X magnification, five fields for each sample (average cell number per field was 150). Three independent experiments were performed. An unpaired two-sided Student's test was used: * $p < 0.05$, n. s.: not significant.

3.7. CLIC1 involvement in GBM development *in vivo*

To determine the *in vivo* relevance of CLIC1 silencing, we performed an orthotopic transplantation assay. We stereotaxically implanted dissociated neurospheres infected with a lentivirus expressing either NT or shRNA specific for CLIC1 (sh) into the nucleus caudatus of immunodeficient mice. We monitored tumor formation and growth until the appearance of neurological signs. Survival of mice injected with CLIC1 silenced cells was prolonged in comparison with NT controls (Chi square = 6.21, d. f. 1, $p<0.05$) (Figure 37).

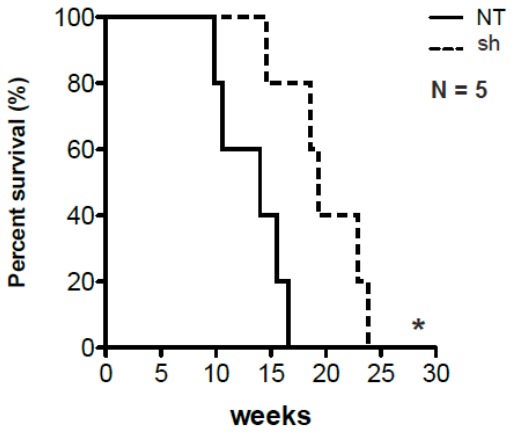

Figure 37. Evaluation of CLIC1 role in GBM development. Kaplan-Meier survival curve of mice intracranially transplanted with 10^5 control (NT) and CLIC1 silenced (sh) cells. Data are from one experiment with five mice per group. P-value was calculated with log rank test: * $p < 0.05$, Chi square = 6.27, d. f. 1.

Both control and CLIC1 silenced mice eventually developed GBMs according to WHO classification. When we sacrificed the transplanted mice at the same time, i.e. at the appearance of the neurologic signs in control mice, CLIC1 silenced mice (sh) were still presympthomatic (pre) and their tumors were significantly smaller than control ones (NT); however, when we analyzed CLIC1 silenced sympthomatic (sym) mice their tumors reached the size of control tumors (Figure 38 A and B; ANOVA with Tamhane's multiple comparison tests: NT vs pre

p<0.05; pre vs sym p<0.05; NT vs sym p = n.s). CLIC1 silenced xenografts lacked CLIC1 expression as detected by IHC at the early time point, while CLIC1 expression level became comparable between CLIC1 silenced (sh) tumors and controls (NT) at the late time point (Figure 38 A).

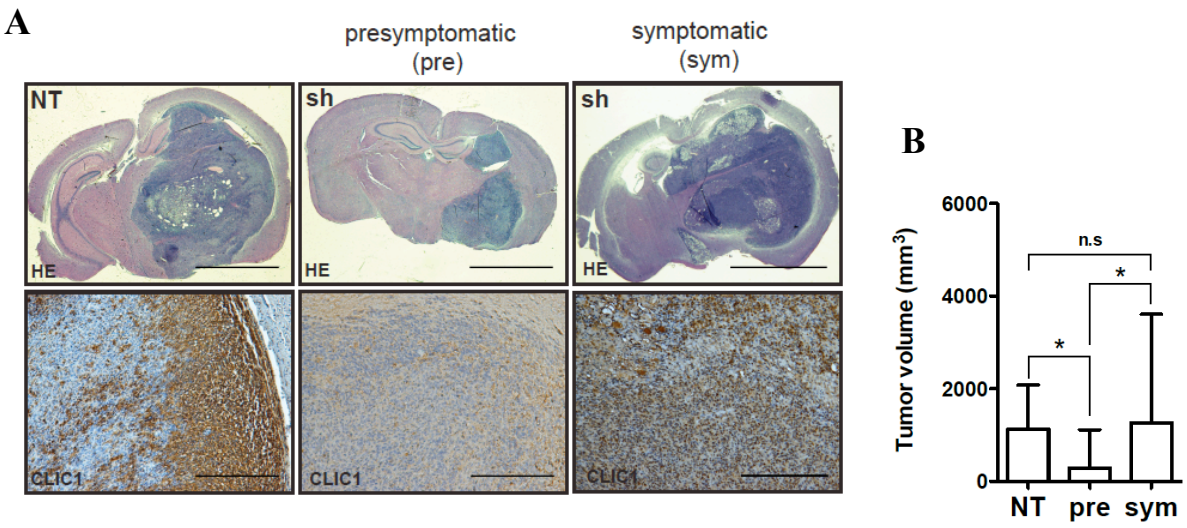

Figure 38. Effect of CLIC1 silencing on tumor volume (A) Representative brain images from mice intracranially injected with NT and CLIC1 silenced (sh) cells stained with hematoxylin and eosin (H&E) (top row, scale bar = 3mm) or CLIC1 (bottom row, scale bar = 300μm); pre: presympthomatic mice; sym: sympthomatic mice. (B) Tumor volume quantification, as indicated. Experiment was carried out using 3 mice per group. Error bars represent 95% confidence intervals; * p<0.05. One-way ANOVA with Bonferroni's correction was used.

Interestingly, when lower numbers of cells (10^2 and 10 for GBM#10 and 10^3, 10^2 and 10 for GBM#18) were injected in mice, none of the mice that received CLIC1 silenced cells developed tumors (Table 3). The calculated stem cell frequency by the ELDA algorithm was significantly lower in CLIC1 silenced cells (hGBM#10: Chi-square = 17.5, d.f = 1, p < 0.0001; hGBM#18: Chi-square = 34.2, d.f = 1, p<<0.0001) and was underestimated due to the observed CLIC1 re-expression in all formed tumors. Thus CLIC1 appears to be relevant in GBM-neurospheres to form tumors.

	hGBM#10		hGBM#18	
Number of cells	NT	sh	NT	sh
100000	3/3	3/3	5/5	5/5
10000	3/3	3/3	5/5	4/5
1000	3/3	1/3	5/5	0/5
100	2/3	0/3	2/5	0/5
10	2/3	0/3	2/5	0/5
Estimate	**1:47**	**1:2357**	**1:106**	**1:7854**

Table 3. Table representing the incidence of tumor formation of tumor bearing mice and the CSC frequency calculated in the hGBM neurospheres (estimate). hGBM#10: Chi-square = 17.5, $p < 0.0001$; hGBM#18: Chi-square = 34.2, *** $p < 0.0001$.

Given the ability of CLIC1 antibody to reduce the proliferation of patient-derived GBM neurospheres *in vitro*, we next explored a potentially translatable targeting of CLIC1 *in vivo*. To test this, we transplanted GBM derived neurospheres treated with CLIC1 antibody into the brains of immunodeficient mice. We sacrificed three mice every week, following tumor progression for a month. Cell treatment with CLIC1 antibody resulted in smaller tumours (Figure 39 A) and significantly improved overall mice survival (Figure 39 B) (n=6, Log-rank $p<0.01$). Thus, transient exposure to CLIC1 antibody produces a significant decrease in the *in vivo* tumorigenicity of GBM cells.

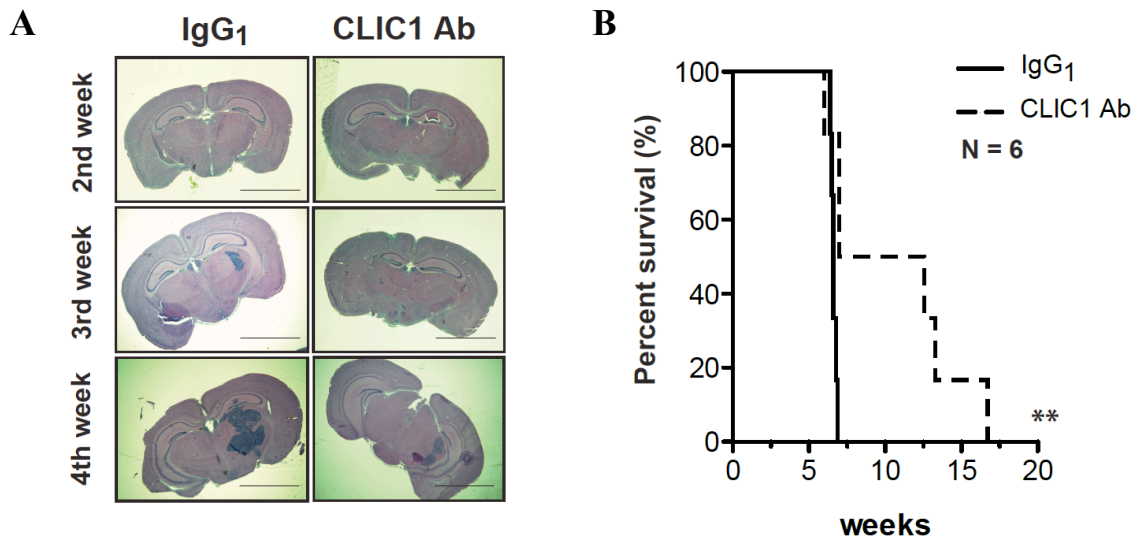

Figure 39. Effect of anti-CLIC1 antibody treatment on GBM development (A) Representative Hematoxylin and eosin stained histological images from mice intracranially injected with hGBM#7 cells treated with CLIC1 antibody or isotype control antibody (scale bar = 3 mm). Mice were killed at 2^{nd}, 3^{rd} and 4^{th} week, as shown. (B) Kaplan-Meier survival analysis of mice intracranially implanted with 10^5 hGBM#7 cells treated with CLIC1 antibody or isotype control antibody. Data are from one experiment with six mice per group. P-value was calculated with log rank test: * p = 0.012, Chi square = 6.36, d. f. 1.

CLIC1 is a protein whose presence has been already established in a variety of biological fluids like blood, urine and extracellular media. It has been shown that levels of circulating CLIC1 can be of prognostic value in pathological conditions like nasopharyngeal and ovarian carcinoma; given our data showing CLIC1 to be particularly expressed in malignant brain tumors and its proved role in regulating GBM cell proliferation and cancer stem cell self-renewal, we wish to propose CLIC1 as potential viable biomarker in human GBM, and therefore study its mechanism of action in vitro and in vivo.

3.8. CLIC1 protein is secreted by glioblastoma cells *in vitro*

CLIC1 was recently identified by proteomic screens in the supernatants of various cell lines (ref.) and in human fluids (i. e. serum, plasma, CSF) (ref.). These intriguing observations promted us to examine the possibility that CLIC1 protein could be released by gliobastoma cells as well. Specifically, we collected conditioned media from different glioblastoma cell lines, and evaluated CLIC1 protein level in the culture media by western immunoblot analysis. CLIC1 protein was expressed in the cell lysates of all samples analyzed and the examination of conditioned medium revealed that glioblastoma cells release CLIC1 protein (Figure 27 A). The culture medium was devoid of GAPDH suggesting that CLIC1 release in the conditioned medium was not a consequence of contamination by intracellular protein (Figure 40 A). Moreover, cell viability measured by PI incorporation was greater than 95%, providing that CLIC1 release was not due to cell death (Figure 40 B).

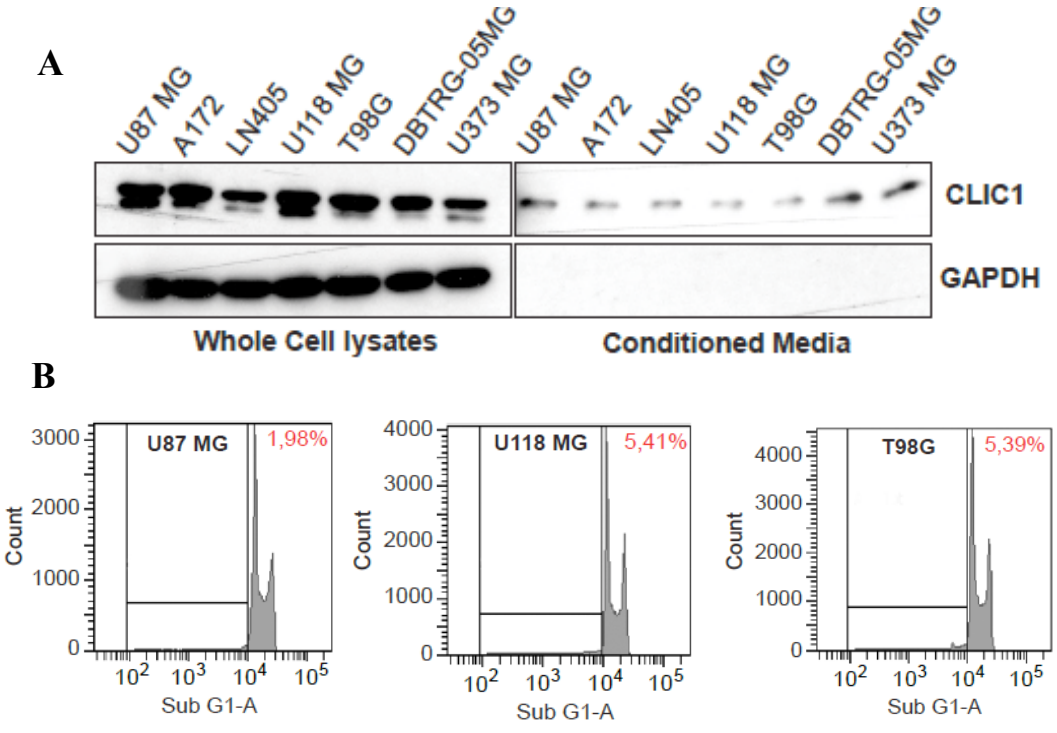

Figure 40. CLIC1 retrieval in culture media. (A) Western blotting analysis showing the expression of CLIC1 in several GBM cell lines (upper left) and in their respective media (upper right). GAPDH was used as loading control and to rule out release of cytoplasmic protein due to cell death. (B) The percentages of apoptotic cells in the cultures were analysed in three different cell lines by PI staining for DNA content analysis by using flow cytometry (FACS).

To further confirm CLIC1 protein release by glioblastoma cells, we took advantage of U87 MG glioblastoma cells overexpressing CLIC1 protein fused to Green Fluorescent Protein (GFP) at the N-terminal (CLIC1 GFP). 24 hours after cell plating, we collected culture medium and employed immunoprecipitation against GFP-tag to enrich CLIC1 GFP fusion protein from the culture medium. A single band of 50KDa corresponding to CLIC1 GFP fusion protein was detected in the medium from U87 MG overexpressing cells, confirming that exogenous CLIC1 GFP protein was released in the medium (Figure 41).

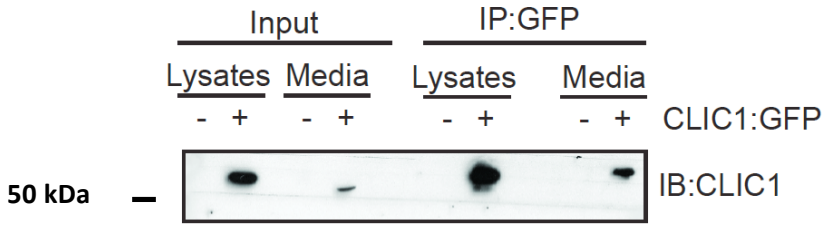

Figure 41. Exogenous CLIC1 GFP is secreted in culture medium. (A) Western blotting analysis showing the expression of CLIC1 in U87MG expressing (+) or not (-) a GFP-fused form of CLIC1. Input shows the expression of CLIC1 GFP in whole cell extracts (lysates) and in collected medium (media), while IP:GFP displays CLIC1 GFP expression in the same samples upon GFP immune-precipitation.

As a complementary approach, we co-cultured U87 MG glioblastoma cells expressing a FLAG-tagged isoform of CLIC1 (U87MG CLIC1 FLAG) with U87 MG glioblastoma cells expressing Green Fluorescent Protein (U87 MG GFP). After 24 hours, we detected by immunofluorescence studies FLAG-tagged isoform of CLIC1 in U87 MG GFP cells (Figure 42), indicating that CLIC1 protein has been transferred from cell to cell.

Colletively, the above observations demonstrate that CLIC1 protein is secreted by glioblastoma cells *in vitro*.

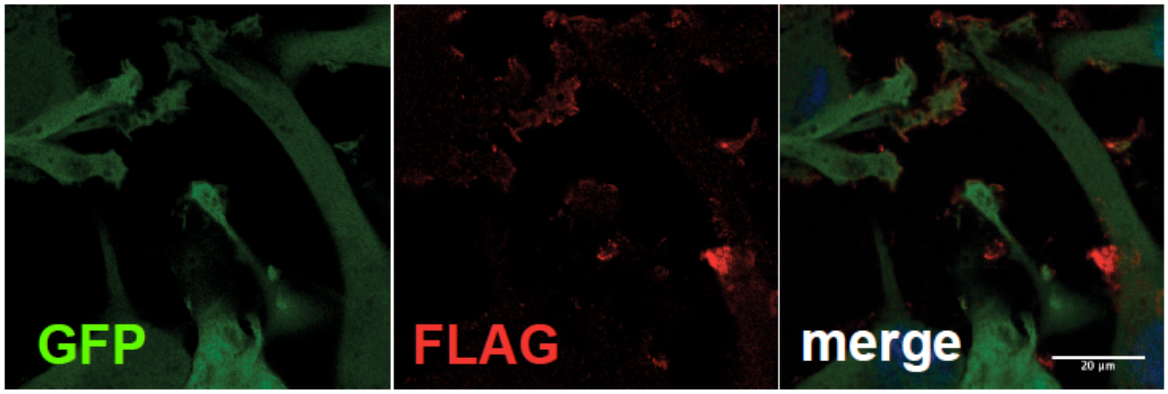

Figure 42. Exogenous CLIC1 is secreted and uptaken by recipient cells. Representative images of U87MG GFP cells (left panel) expressing CLIC1 FLAG variant (mid panel) onto several protrusions (right panel). U87MG cells were fixed and processed for immunofluorescence (GFP, green; CLIC1 FLAG, red). Scale bar = 20 µm.

3.9. CLIC1 protein is secreted via extracellular vesicles (EVs)

In order to understand the mechanism of CLIC1 protein release from glioblastoma cells, we checked the one based on EVs. Interestingly, CLIC1 protein contains a PPxL motif for binding of Nedd4 type E3 ubiquitine ligases, and a dileucine cluster motif that facilitate endocytosis and intracellular trafficking. Moreover, analysis of ExoCarta database revealed that CLIC1 protein resides in EVs, comprising exosomes and microvesicles based on their composition and biophysical properties, released from different cell types. To investigate whether CLIC1 secreted protein is contained in EVs derived from glioblastoma cells, we chose to study the well-characterized U87 MG glioblastoma cell line, which is known to produce significant amounts of EVs. EVs were isolated from U87 MG conditioned media according to an established protocol based on serial centrifugation (Théry C et al., 2006). Nanoparticle Tracking Analysis (NTA) revealed the presence of an heterogeneous population of vesicles, which possesses an average mean diameter of 146 $\pm$ 3.4 nm and comprises smaller EVs, ranging in size from 10 to 150 nm (60% of the total), and larger EVs, with a diameter larger than 150nm (40% of the total) (Figure 43 A and B).

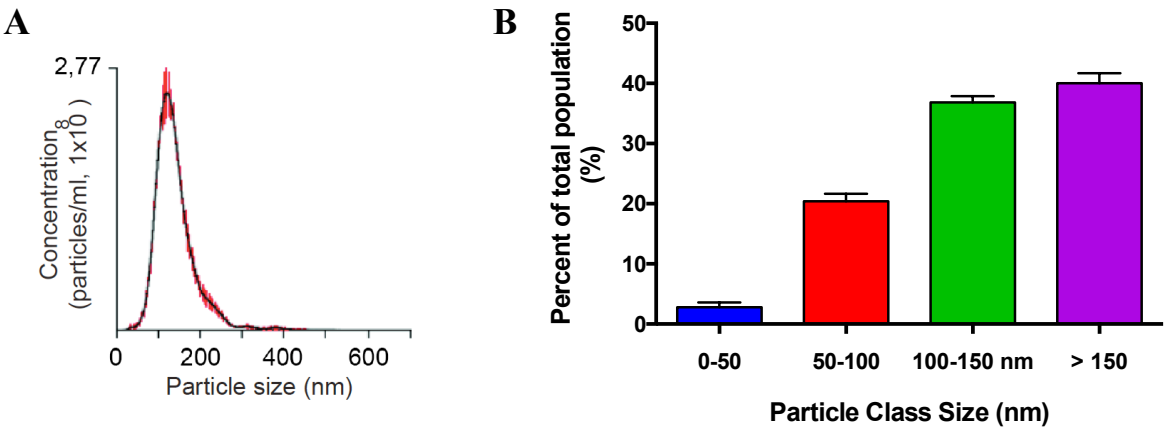

Figure 43. Nanoparticle tracking analysis. (A) Graph displaying size and yield of particles detected in our EV preparations by Nanosight. (B) Graph showing percentual size distribution. Mean values are depicted. Error bars represent standard error.

Characterization by electron microscopy showed bilayered vesicles (Figure 44 A) positive for CD63, a tetraspanin strongly enriched in late endosomes and EVs (Figure. 44 B).

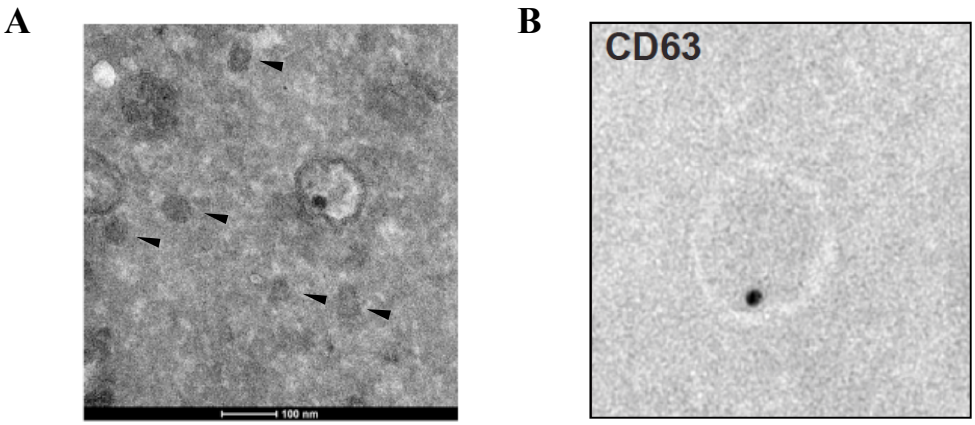

Figure 44. Morphological analysis of EVs. (A) Electron micrograph of U87MG EVs. Picture shows membrane bound vesicles of 50-100 nm (arrowheads). (B) Immunogold labeling showing a vesicle positive for the vesicular marker CD63.

Purified EVs were enriched in the exosome specific proteins CD63 and tsg101 (tumor susceptibility gene 101), with respect to whole cell lysates wich were immuno-negative for both proteins (Figure 45 A). Notably, GM130 *cis*-Golgi marker was absent, demonstrating the purity of the isolated fractions (Figure 45 A). Interestingly, CLIC1 protein was expressed in EVs derived from U87 MG cells, as demonstrated by western immunoblot analysis (Figure 45

A) and immuno-electron microscopy (Figure 45 B). In agreement with the experiments performed in U87 MG cells, we confirmed CLIC1 protein expression in EVs derived from two other glioblastoma cell lines (i. e. U118 MG and T98G) (Figure 45 A).

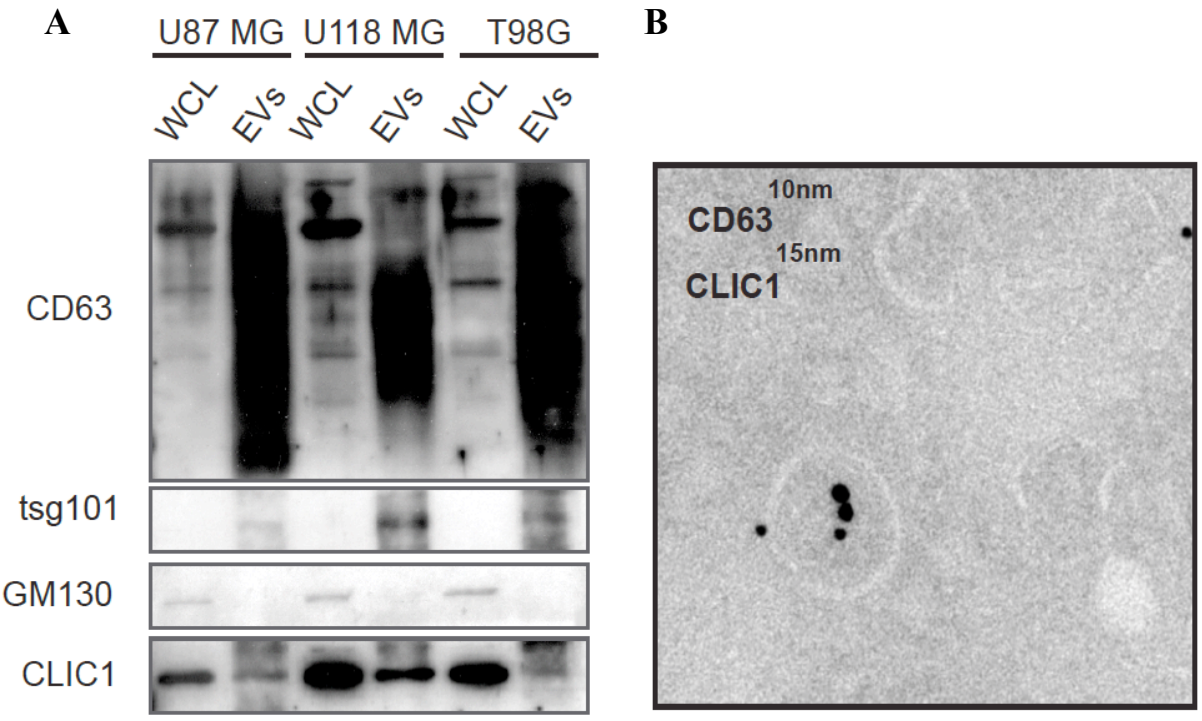

Figure 45. CLIC1 expression within EVs. (A) Western immunoblot of whole cell lysates (WCL) and respective EVs of different GBM cell lines. Endocytic markers (CD63, tsg101) are expressed in EVs while GM130 expression, a cis-Golgi protein, is not detectable in EVs samples. (B) EVs are immunogold labeled with CD63 (10 nm gold bead) and CLIC1 (15 nm gold bead).

To further support CLIC1 sorting to EVs, we visualized the colocalization between CLIC1 and CD63 protein at the cellular level, by applying the *in situ* proximal ligation assay (PLA). The PLA exploits antibodies to which single stranded DNA oligonucleotides are attached; when target antigens resides 10-50 nm close, oligonucleotide strands can hybridize and, following ligation, a circular DNA is formed. Specific fluorescent probes and several round of PCR amplification are then exploited to amplify the signal. The *in situ* PLA revealed a large number of fluorescence spots in cell cytoplasm, indicating that a substantial fraction of CLIC1 protein was located in CD63 positive compartments of the cell (Figure 46, left panel). The possibility

that the PLA signals were derived from non-specific binding of PLA probes was excluded by the absence of fluorescence PLA spots analysing CLIC1 silenced cells (Figure 46, right panel). Taken together, our data provide evidence that CLIC1 protein is secreted from glioblastoma cells in EVs.

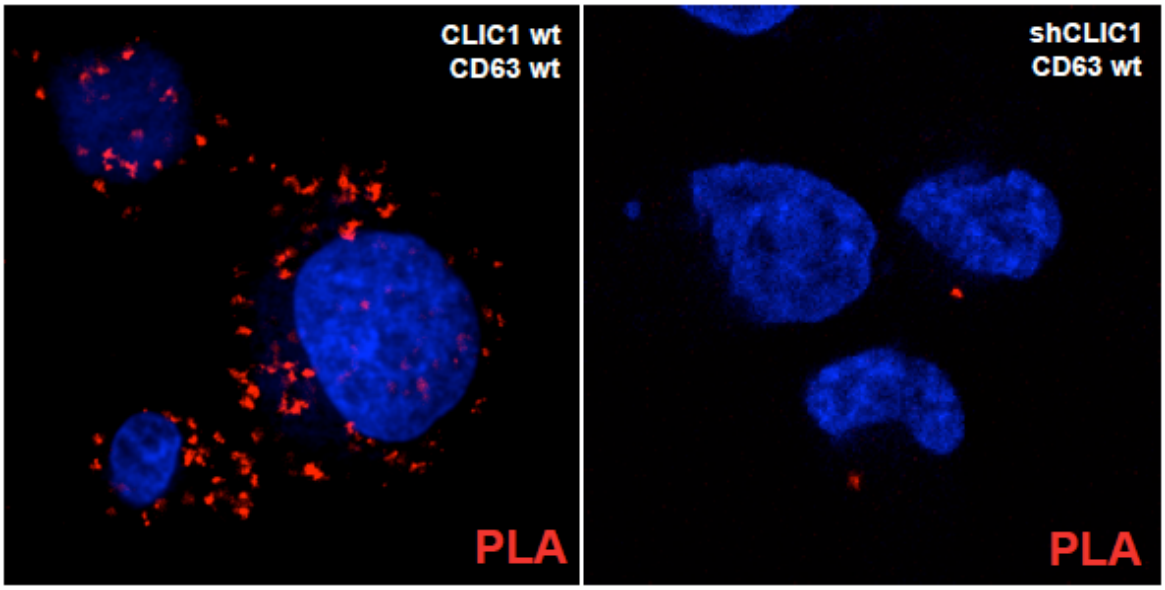

Figure 46. CLIC1 co-expression with CD63. The co-expression of CLIC1 with CD63 has been assessed by proximity ligation assay in U87MG wt cells (left panel). The degree of interaction is proportional to the number of foci (red); to rule out the specificity of the assay, U87MG shCLIC1 cells have been analyzed (right panel).

3.10. CLIC1-containing EVs regulate the proliferative response of glioblastoma cells

We have previously described the role of CLIC1 protein in GBM progression through the modulation of GBM CSC self-renewal and proliferation. We then sought to determine if CLIC1-containing EVs might influence the proliferative response of GBM cells as well. In order to exert their effect, EVs must be internalized by recipient cells. We labeled U87 MG cell-derived EVs with the lipid-associating fluorescent dye PKH26. When PKH26 positive EVs were incubated with human embryonic kidney 293T cells, we observed a rapid uptake of labeled EVs into the recipient cells, as indicated by confocal microscopy (Figure 47 A). Labeled EVs displayed a time-dependent uptake kinetic, which reached the maximum 24 hours after incubation, when PKH26 fluorescence was observed in more then 80% of

recipient cells (Figure 47 B). Moreover, incubation at 4 °C abolished EV uptake (Figure 47 C).

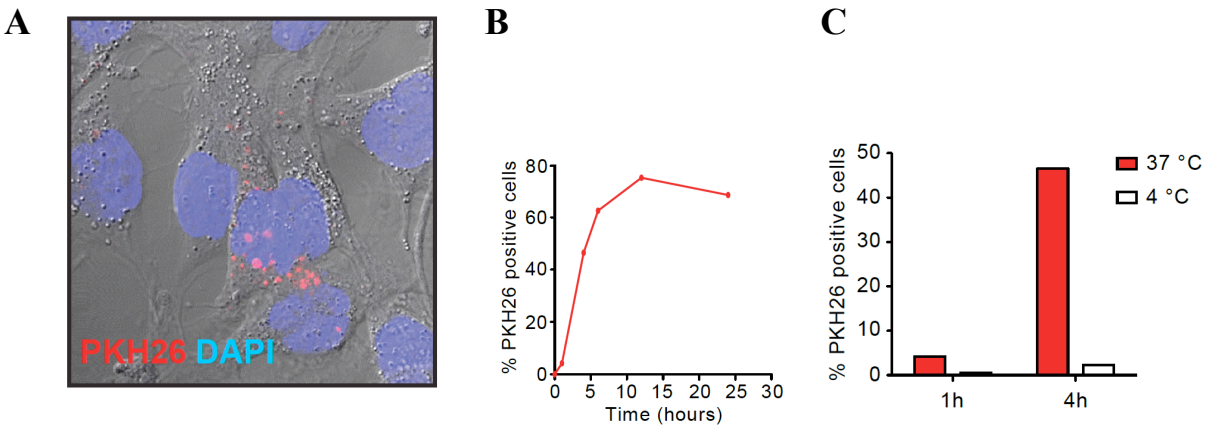

Figure 47. EV functional uptake. Collected EVs are actively uptaken by recipient cells. (A) Representative confocal image of 293T cells treated with EVs labeled by PKH-26. (B) Quantification of PKH-26 positivity of 293T cells treated with labeled EVs for 0-24 hours; the uptake of EVs is time-dependent and reaches its peak at 12 hours. (C) Quantification of 293T cell PKH-26 positivity after 1 and 4 hours of treatment with labeled EVs; EV uptake has been analyzed both in normal conditions (37°C) and at 4°C. Reduced EV internalization rules out passive diffusion through the cell.

To assess the effects of CLIC1-containing EVs, we took advantage from U87 glioblastoma cell line, which normally express CLIC1 protein, and we used it either to silence CLIC1 expression (U87 shCLIC1) or to overexpress a FLAG-tagged version of CLIC1 protein (U87 CLIC1 FLAG). We collected conditioned media from the same amount of control (U87 NT), U87 siCLIC1 and U87 CLIC1 FLAG cells and isolated EVs through serial centrigutations. Western immunoblot analysis confirmed that CLIC1 protein was present in the EVs derived from the three cell lines. Notably, CLIC1 expression level in EVs mirrored CLIC1 cellular level. Moreover, the three EV groups expressed the known exosomal markers CD63 and tsg101 at the same level (Figure 48).

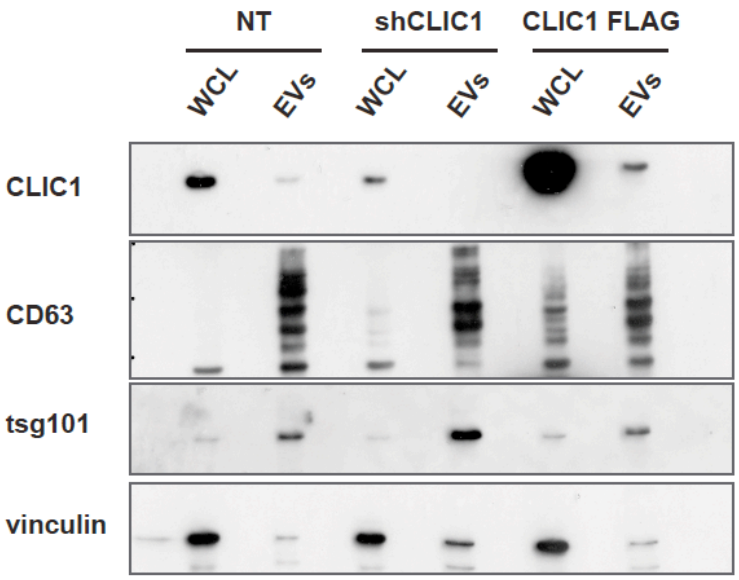

Figure 48. Characterization of EVs isolated upon CLIC1 modulation. Western immunoblot of whole cell lysates (WCL) obtained from NT, shCLIC1 and CLIC1 FALG U87MG cells; respective EVs have been analyzed as well. CD63 and tsg101 have been used as endocytic markers; vinculin is the loading control.

Funcionally active EVs isolated from U87 NT, U87 shCLIC1 or U87 CLIC1 FLAG cells were added to U87 MG recipient cells and cell proliferation was evaluated. EVs have been shown to sustain glioblastoma cell growth *in vitro*. In line with these findings, proliferation was increased after treatment with EVs isolated from U87MG NT cells (NT EVs). Administration of an equal amount of EVs isolated from CLIC1 overexpressing U87 MG cells (CLIC1 FLAG EVs) showed a robust proliferative response of U87 MG recipient cells, resulting in more then three-fold stimulation of proliferation compared to untreated cells. Intriguingly, the mitogenic stimulus was strongly impaired upon treatment with EVs derived from CLIC1 silenced U87 MG cells (shCLIC1 EVs) (Figure 49). Comprehensively, these data demonstrate that CLIC1-containing EVs modulate glioblastoma proliferative response in a CLIC1-dependent fashion.

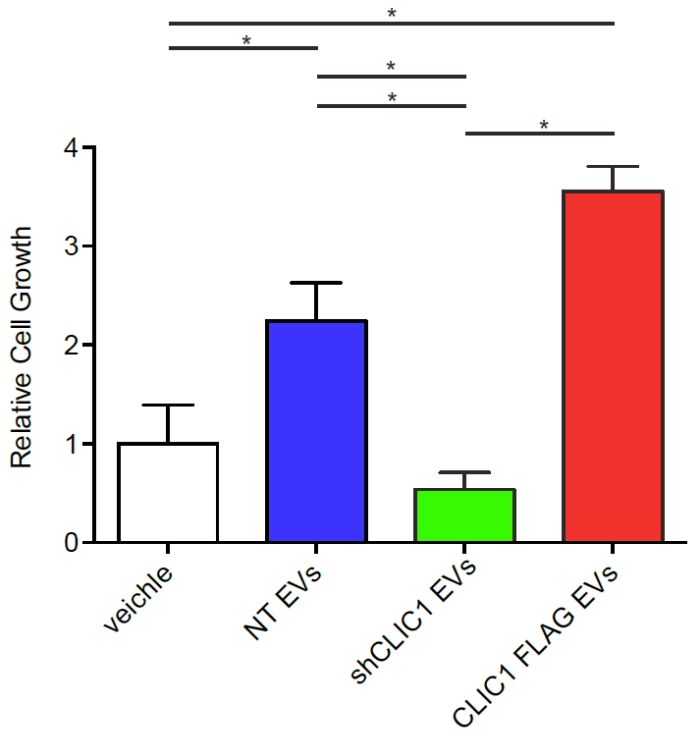

Figure 49. Vesicular CLIC1 levels and cell proliferation *in vitro*. The growth of U87MG wt cells was measured by 3-(4, 5-dimethylthiazol-2-yl)-2, 5-diphenyltetrazolium bromide (MTT) assay after the treatment with NT, shCLIC1, CLIC1 FLAG EVs (50μg/ml) or PBS (vehicle); it is depicted cell viability following 120 hours of treatment. Three independent experiments were performed; error bars represent standard error; * $p<0.05$.

3.11. CLIC1 regulates EV proliferative potential *in vivo*

To disclose whether the effect of CLIC1-containging EVs were maintained also *in vivo*, we subcutaneously injected U87 MG cells treated with NT EVs, siCLIC1 EVs and CLIC1 FLAG EVs, or PBS as control, into one flank of nude mice and monitored tumor growth over time. In agreement with the *in vitro* results, we measured a m arked boost of tumor growth upon treatment with NT EVs. Interestingly, co-injecting U87MG cells together with CLIC1 FLAG EVs resulted in a massive increase of the tumor growth. On the other hand, cell treatment with shCLIC1 EVs resulted in the total abolishment of such enhancement (Figure 50 A). At the onset of epidermic lesions, we surgically resected subcutaneous tumors and weighted them. As shown in Figure 37 A, the mean tumor weights were significantly higher in mice bearing tumors derived from U87 MG cells treated with CLIC1 FLAG EVs (Figure 50 B).

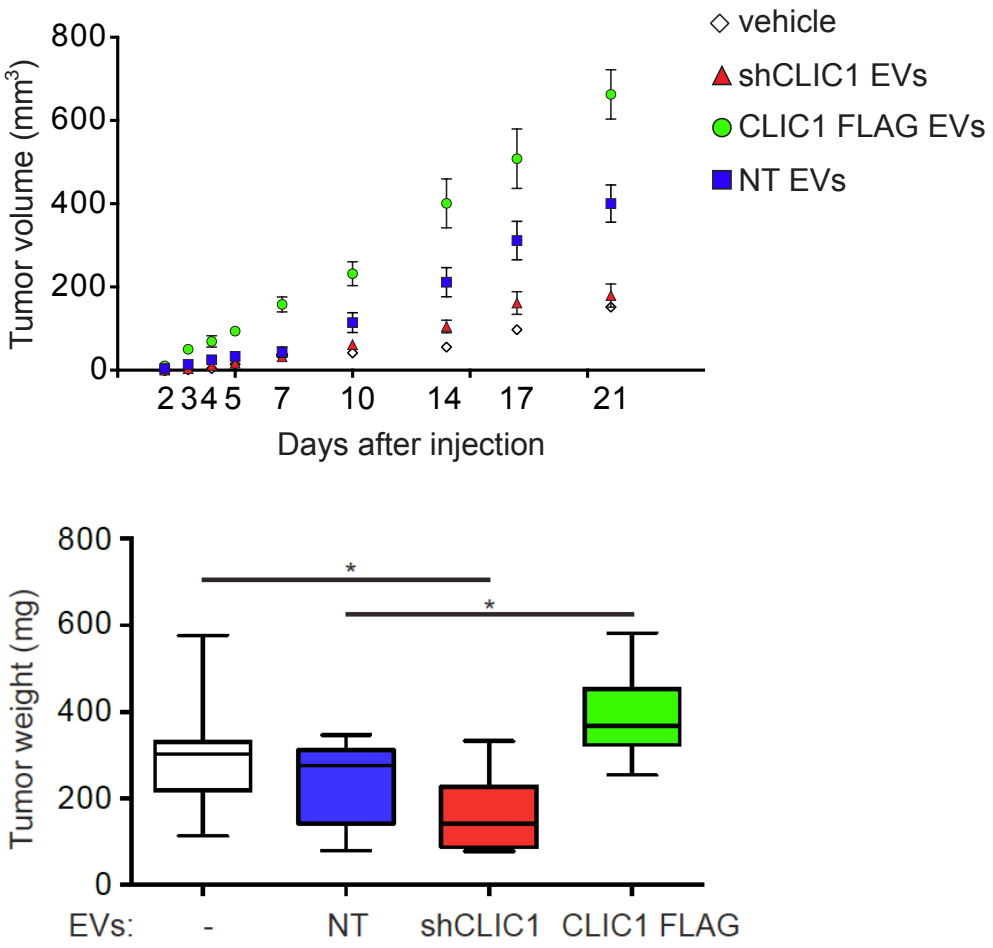

Figure 50. Vesicular CLIC1 levels and tumor development *in vivo*. (A) The volume of subcutaneously injected U87MG tumors has been measured after treatment with NT, shCLIC1, CLIC1 FLAG EVs or PBS (vehicle). (B) Surgically resected tumors have been weighted. Three independent experiments were performed; error bars in A represent standard errors; solid lines in B are median values while error bars stand for minimum and maximum values.. GLM tests of between-subjects effects showed statistically significant difference for the relative tumor growth according to the time, the treatment, and the interaction between those two variables. * $p<0.05$

We next established orthotopic xenografts by injecting into nude mice brains U87 MG cells together with NT EVs, shCLIC1 EVs, CLIC1 FLAG EVs, or PBS as control. We sacrificed nude mice after one and three weeks and evaluated tumor incidence. The results indicated that EVs with low-CLIC1 content (shCLIC1 EVs), formed tumors with lower incidence (Table 4). These results collectively suggest that CLIC1 modulation influences EV-mediated tumorigenic potential of glioblastoma cells.

Treatment	Engrafted tumors	
	1st week	3rd week
Vehicle	2/10	9/10
NT EVs	5/10	8/10
siCLIC1 EVs	1/10	2/10
CLIC1 FLAG EVs	8/10	10/10

Table 4. Table representing the incidence of tumor formation in nude mice intra-cranially injected with U87MG treated with NT, shCLIC1, CLIC1 FLAG EVs or PBS (vehicle).

3.12. GBM Cancer Stem Cells-derived EVs contain CLIC1 protein

Glioblastoma is mainteined by a sub-population of cancer stem cells (GBM CSCs) that survives traditional therapies, allowing tumor regrowth, and explains intratumoral cellular heterogeneity typical of this tumor (Reya, 2011). We verified whether CLIC1 protein could be secreted from GBM CSCs, and whether its release occurred via EVs. GBM CSCs have been isolated from human GBM specimen and cultured in serum-free medium. Examination of conditioned medium 48 hours after cell plating revealed that GBM CSCs secrete CLIC1 protein (Figure 51 A). Notably, CLIC1 protein detected in the medium was not released as a consequence of cell death, as demonstrated by the absence of GAPDH in the culture medium (Figure 51 A) and by the low percentage of cell death measured by PI incorporation method (Figure 51 B).

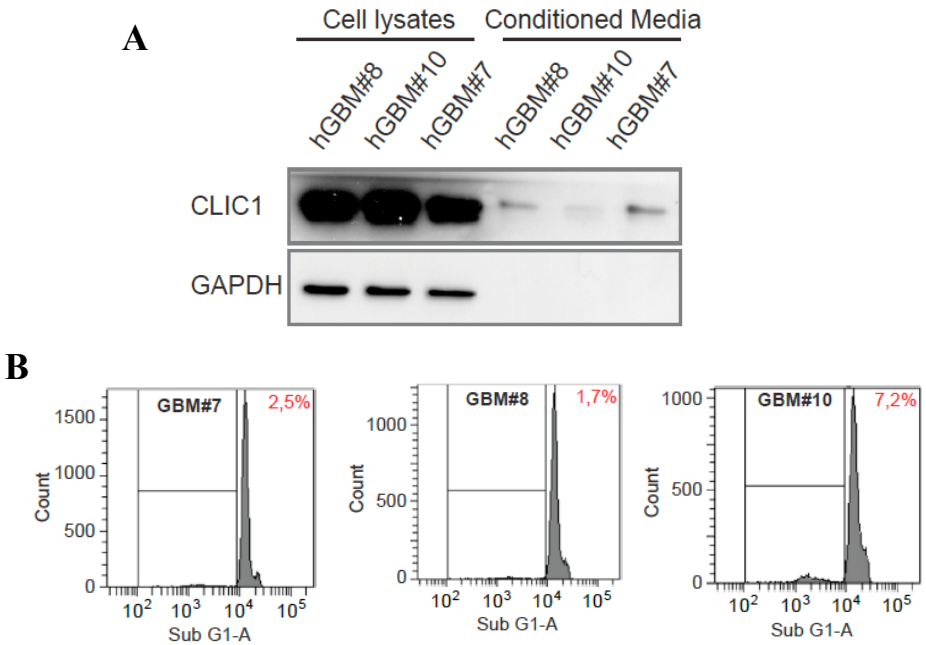

Figure 51. CLIC1 retrieval in culture media of GBM-derived neurospheres. (A) Western blotting analysis showing the expression of CLIC1 in three different GBM-derived neurospheres and in their respective media. GAPDH was used as loading control and to rule out release of cytoplasmic proteins due to cell death. (B) The percentages of apoptotic cells in the cultures were analysed by PI staining for DNA content analysis.

Next, we isolated EVs from the conditioned medium of GBM CSCs. The size of the isolated EVs was confirmed using NTA with an average peak at 120 nm (Figure 52).

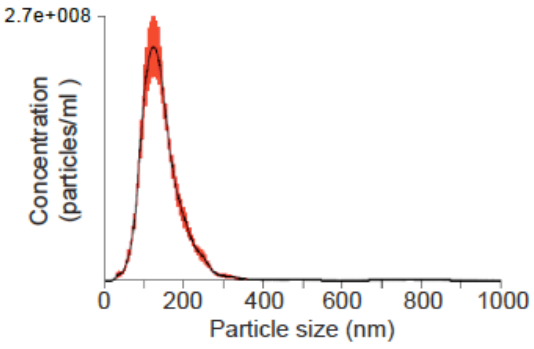

Figure 52. Nanoparticle tracking analysis in GBM-derived neurospheres. Graph displaying size and yield of particles detected in hGBM#22 EV preparations by Nanosight.

Western immunoblot analysis performed on EV extracts confirmed the enrichment of the exosomal markers CD63 and tsg101 and the lack of expression of GM130 *cis*-Golgi marker compared to the corresponding whole cell lysates (Figure 4053 In agreement with data obtained from glioblastoma cell lines, we confirmed that CLIC1 protein was expressed in GBM CSC-

derived EVs (Figure 53).

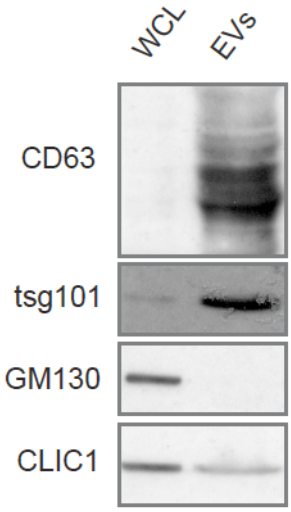

Figure 53. CLIC1 expression within EVs. (A) Western immunoblot of whole cell lysates (WCL) of hGBM#22 neurosphere and respective EVs. Endocytic markers (CD63, tsg101) are expressed in EVs while GM130 expression, a cis-Golgi protein, is not detectable in EVs sample.

To investigate the role of CLIC1 in GBM CSC-derived EVs, we silenced CLIC1 expression in GBM CSCs and purified EVs from culture medium by differential centrifugation. We observed a significant decrease of CLIC1 protein content in either CLIC1 silenced GBM CSCs and in the corresponding EVs (shCLIC1 EVs) (Figure 54). In contrast, no major alterations in CD63 and tsg101 expression were detected between shCLIC1 EVs and NT EVs (Figure 54).

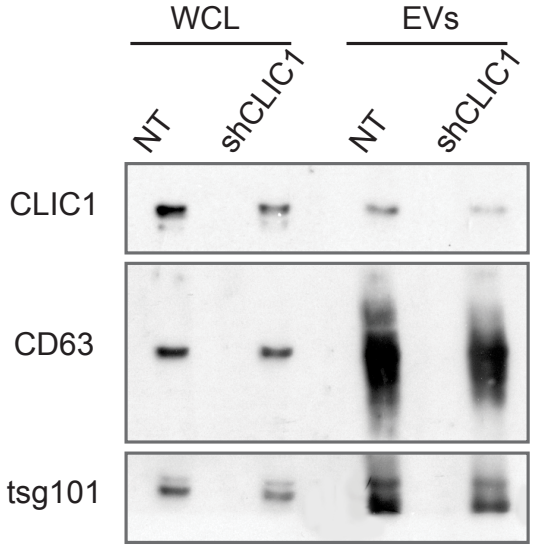

Figure 54. CLIC1 modulation in EVs derived from GBM neurospheres. Western immunoblot of whole cell lysates (WCL) obtained from NT and shCLIC1 hGBM#22 neurospheres; respective EVs have been analyzed as well. CD63 and tsg101 have been used as endocytic markers; vinculin is the loading control.

To determine if CLIC1-containg EVs secreted by GBM CSCs were able to exert a pro-proliferative effect, we incubated GBM CSCs with their own shCLIC1 EVs and NT EVs. In agreement with the results obtained with GBM cells lines, CLIC1 depletion in EVs resulted in a significant reduction of GBM CSCs growth compared to control (Figure 55).

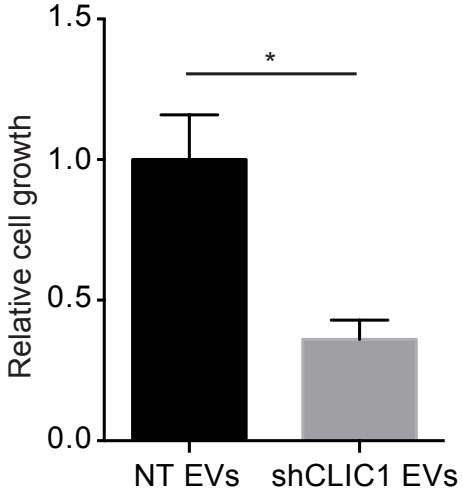

Figure 55. Vesicular CLIC1 levels and cell proliferation *in vitro*. The growth of hGBM#22 wt cells was measured by 3-(4, 5-dimethylthiazol-2-yl)-2, 5-diphenyltetrazolium bromide (MTT) assay after the treatment with NT and shCLIC1 EVs (50μg/ml); it is depicted cell viability following 120 hours of treatment. Three independent experiments were performed; error bars represent standard error; An unpaired two-sided Student's test was used. * $p<0.05$.

In the same way, intracranial injection of GBM CSCs treated with siCLIC1 EVs resulted in a significant reduction of tumor incidence at the early time point analysed (i. e. 2 week after cell injection). However, the absence of any difference in tumor incidence at the end point of the experiment (i. e. 4 week after cell injection) could reflect a delay in tumor formation (Table 5).

Treatment	Engrafted tumors	
	2nd week	4th week
NT EVs	6/10	4/5
shCLIC1 EVs	3/10	5/5

Table 5. Table representing the incidence of tumor formation in nude mice intra-cranially injected with hGBM#22 treated with NT and shCLIC1 EVs.

3.13 CLIC1 modulation in the cell does not alter EV features

We next sought to define whether the difference in EV stimulatory capacity might be due to alteration in EV features. EVs purified from the same amount of U87 NT, U87 shCLIC1 and U87 CLIC1 FLAG cells were analysed by NTA. Neither CLIC1 silencing nor CLIC1 overexpression in glioblastoma cells had any effect on EV size distribution (Figure 56 A and B).

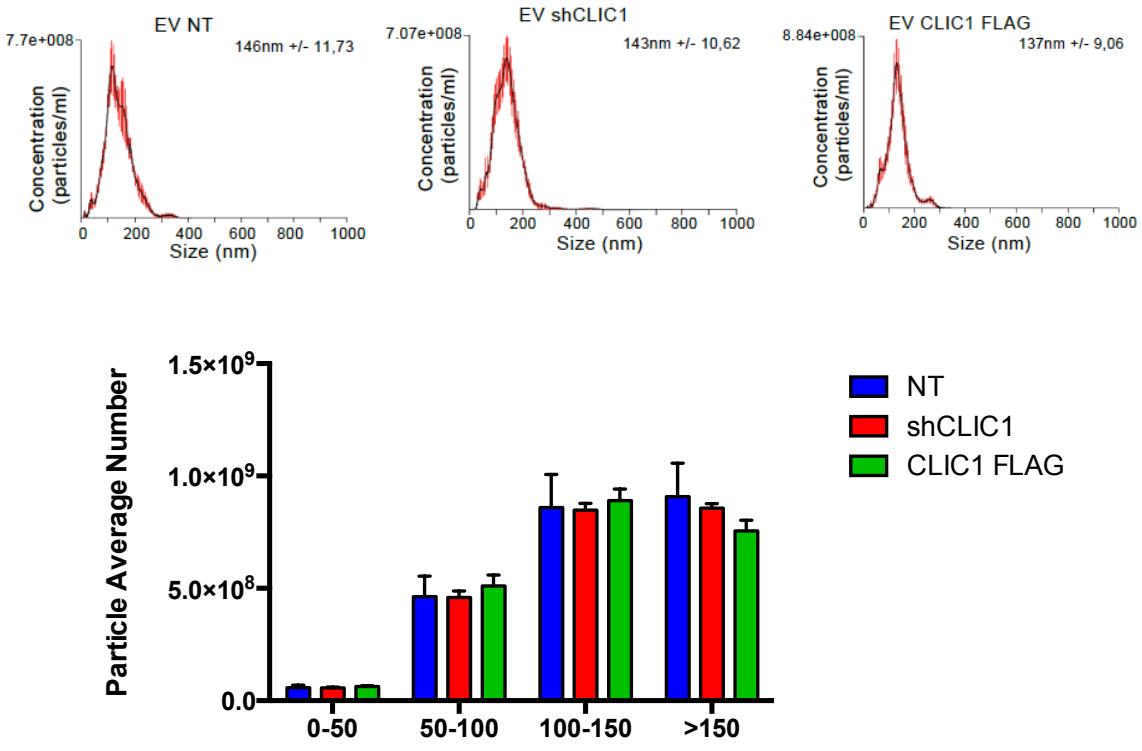

Figure 56. EVs dimensional classes are not affected by CLIC1 modulation. (A) Graph displaying size and yield of particles detected in hGBM#22 EV preparations by Nanosight. (B) Vesicles have been divided in four different dimensional classes. Error bars represents standard errors.

Also the yield of EVs secreted by U87 siCLIC1 and U87 CLIC1 FLAG was identical to that of EVs produced by control cells (Figure 57).

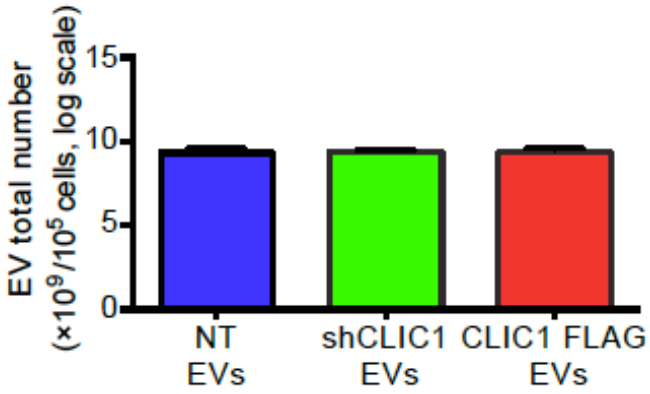

Figure 57. EVs yield is not affected by CLIC1 modulation. (A) Graph displaying size and yield of particles detected in hGBM#22 EV preparations by Nanosight. (B) Vesicles have been divided in four different dimensional classes. Error bars represents standard errors.

Moreover, CD63 and tsg101 exosome markers were equally expressed either in EVs or in the corresponding U87MG cells they had been derived from (Figure 58). These data show that CLIC1 modulation in glioblastoma cells does not affect EV phenotypic features or EV secretion.

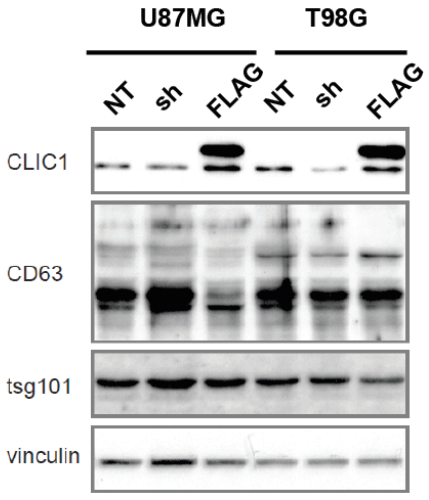

Figure 58. CLIC1 modulation does not alter the expression of endocytic markers. Western immunoblot of whole cell lysates obtained from NT, shCLIC1 and CLIC1 FLAG U87MG and T98G; CD63 and tsg101 have been used as endocytic markers; vinculin as loading control.

In addition, PKH26 labeled EVs from control, CLIC1 silenced and CLIC1 overexpressing cells were equally taken up into U87 MG recipient cells, thus excluding the possibility that the differences in the proliferative responses observed could be due to differences in EV uptake efficiency (Figure 59).

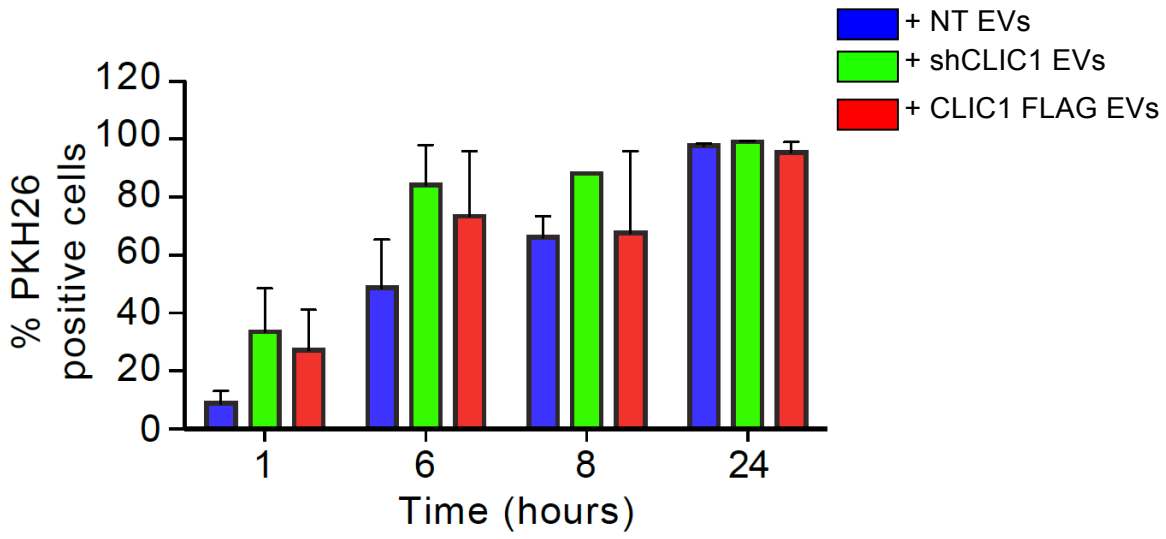

Figure 59. CLIC1 modulation within the EV does not alter its uptake. Cell positivity to PKH-26 after treatment with PKH-26 labeled NT, shCLIC1 and CLIC1 FLAG EVs. Two-way ANOVA. Contribution of "treatment" and the consequent interaction with "time": $P > 0.05$. Three independent experiments have been carried out.

Next, we determined the protein composition of purified EVs and whether this content could account for the differences in the proliferative response of glioblastoma cells. To do this, *we took advantage of CLIC1 FLAG EVs, which induced the strongest pro-prolifetive response both in vitro and in vivo.* Three independent preparations of either CLIC1 FLAG or NT EVs were analysed by label-free quantitative proteomic analysis. The peak intensity observed for the two samples (CLIC1 FLAG and NT EVs) was very similar, reflecting that the same amount of protein was loaded (data not shown). Interestingly, we identified in both NT and CLIC1 FLAG EVs 20 out of 25 of the top canonical EV proteins reported in Exocarta database. Proteins classification based on Gene Ontology (GO) annotations for cellular localization and biological processes (Figure 60) revealed that both CLIC1 FLAG and NT EVs shared characteristics of

bona fide EVs. We identified a total of 611 proteins in CLIC1 FLAG EVs, the majority of these are not altered (557) compared to NT EVs, with only 54 proteins differentially expressed (APPENDIX I). The nice overlapping in the protein content of EVs isolated from CLIC1 overexpressing with NT EVs paves the way to the possibility that the pro-proliferative response induced by CLIC1 FLAG EVs might be CLIC1-dependant.

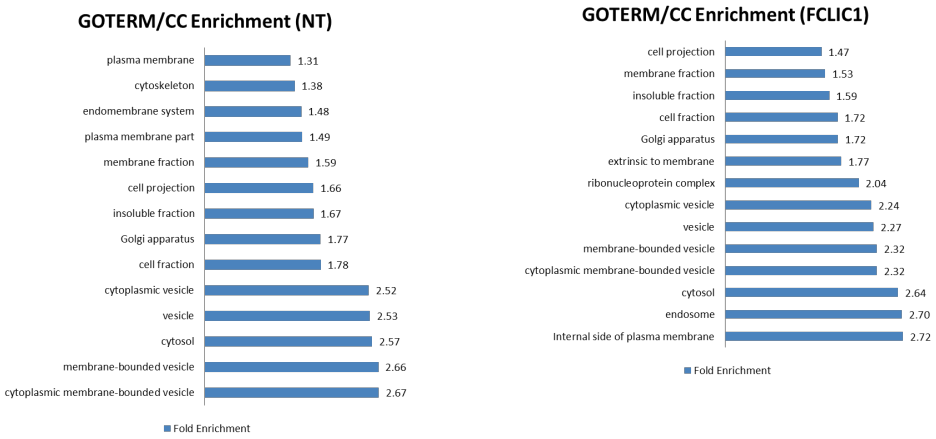

Figure 60. Gene Ontology (GO) enrichment analysis of proteins detected in CLIC1 FLAG EVs (FCLIC1) and in control EVs (NT). Significant GO terms found in exosomes derived from CLIC1 FLAG EVs and in NT EVs.

4. DISCUSSION

4.1. CLIC1 is a functionally relevant prognostic marker in human GBMs

In this thesis we analyzed the functional role of CLIC1 in gliomagenesis. By investigating different on line available expression microarray data sets, we identified CLIC1 to be over-expressed in brain tumors compared to normal brains, with its expression increasing along with WHO tumor grades, reaching the highest expression level in GBMs. Moreover, among GBMs, we identified CLIC1 to cluster within GBM mesenchymal subtype, which is considered of poorer prognostic status, due to high infiltration rate and marked vascularization, higher necrosis and associated inflammatory infiltrates (Veraak R.G. et al., 2010) and increased treatment resistance. Importantly, our study also pointed out that CLIC1 expression inversely associates with patient survival and therefore it could be of potential prognostic value in monitoring glioma progression. CLIC1 overexpression has been demonstrated in wide variety of tumor types (Wang J.W. et al., 2009; Petrova D.T. et al., 2008), including gliomas (Wang L. et al., 2012; Setti M. et al., 2013). Taken together, these studies demonstrate that CLIC1 expression confers proliferative advantage, it is required for cancer cell migration and invasion, and sustains cancer cell tumorigenicity. Recently, chloride channels have been involved in the chemotherapeutic resistance of glioma stem-like cells (Kand M.K. and Kang S.K., 2008). Here, we demonstrate that CLIC1 silencing in stem/progenitor cells derived from GBM patients negatively influences both proliferative capacity and self-renewal properties *in vitro*, and impairs their *in vivo* tumorigenic potential. GBMs are the most frequent brain tumors and despite different treatment modalities, overall results have remained unchanged over the last 25 years. GBM patients have less than 30% of probability to survive more than two years also with optimal therapy. Thus, the finding of a good target for patient-specific therapy would be of paramount importance from a clinical standpoint. GBMs contain a subpopulation of cancer stem cells with intrinsic resistance to therapy that can repopulate the tumor after treatment. Therefore, a new approach to cancer therapy might focus on specific targeting of the resistant CSC populations. In our study we show that CLIC1 is enriched in cancer stem/progenitor cells

compared to the cells that make up the bulk of the tumor. In physiological conditions, CLIC1 exists usually in a soluble form in the cytoplasm, but following oxidative stimuli it translocates to the plasma membrane, where it acts as a chloride-selective ion channel (Littler D.R. et al., 2004). CLIC1 localization on the plasma membrane has been associated to cells in G2/M stage of the cell cycle (Valenzuela S.M. et al., 2000) and alteration of CLIC1 levels by RNA interference has been demonstrated to impair cell cycle progression *in vitro* (Tung J.J. et al., 2010). We found that CLIC1 is constitutively localized on the plasma membrane of GBM stem/progenitor cells compared to the normal counterpart. This different localization of CLIC1 in tumoral versus normal stem/progenitor cells could allow the specific targeting of cancer cells. Moreover, we demonstrate that CLIC1 silencing affects proliferation, clonogenicity and tumorigenic potential of GBM stem/progenitor cells. Given that CLIC1 is constitutively expressed on the plasma membrane of GBM stem/progenitor cells conferring them a growth advantage, our results aim to pursuit CLIC1 as a molecular target for therapeutic purpose during the insurgence and progression of the tumorigenic process. Notably the treatment of human GBM stem/progenitor cells with the specific CLIC1 antibody mimics the biological effects of CLIC1 silencing, being able to reduce tumor cell growth both *in vitro* and *in vivo* and demonstrating that CLIC1 biological effect is dependent on its function as ion channel on the plasma-membrane. Small molecules that specifically inhibit CLIC1 expression or functions are yet to be identified. The investigation of the molecular players mediating the functional effects of CLIC1 in GBM stem cells would permit to set up new therapeutic strategies to block GBM. The investigation of these molecules on inhibiting GBM progression in human patients is therefore highly warranted.

4.2. Vesicular CLIC1 contributes to EV-mediated proliferative response

A great limitation to GBM successful treatment resides in tardiness of diagnosis; this is due to the time frame between the appearance of the first oncogenic hit, with the consequent cellular transformation, and the unveiling starting neurological signs, often related to an advanced, hence incurable, stage of the pathology. For this and other reasons, many efforts have been

made to identify viable biomarkers that could recapitulate or disclose glioma progression, as easily as a blood sample. In this study we showed that CLIC1 is actually secreted by GBM cells together with EVs where it plays a role in the EV-mediated proliferative response. Unlikely the majority of ion channels, CLIC1 behaves as both soluble and membrane-spanning protein; soluble-to-transmembrane transition is usually regulated by changes in the redox cellular status that, through the formation of an intra-monomeric disulfide bond, allows the morphological rearrangement required to membrane insertion. The vast majority of CLIC1 protein is kept in the cytoplasm in its soluble form, as shown from protein extractions carried out with digitonin; digitonin-resistant CLIC1 is either PM-bound or bound to cytosolic vesicles (Ulmasov et al., 2007). CLIC1 vesicular localization is endorsed by CLIC1 expression pattern itself, scattered and dotted as many studies reported in several human cell lines (PancI, HeLa, macrophages) (Tulk et al., 1998; Ulmasov et al., 2007; Jiang et al., 2012). These observations are consistent with CLIC1 lack of typical transmembrane-signal peptide, thus suggesting that CLIC1 might exploit mechanisms of export alternative to canonical endoplasmic reticulum (ER) /Golgi apparatus secretion pathways (Valenzuela M.S. et al., 1997); moreover, this evidence is even strengthened by CLIC1 mislocalization with most of ER/Golgi/lysosome markers (Ulmasov et al., 2007). Different recent studies identified CLIC1 secreted protein as a potential biomarker in nasopharyngeal (Ying-Hwa C. et al., 2009) and ovarian carcinoma (Hsin-Yao Tang et al., 2012). Accordingly with these results, in the first part of our study we inquired about CLIC1 secretion carried out by GBM cells. Three different and independent lines of evidence showed CLIC1 to be secreted by GBM cells: culture medium analysis by western immunoblot, immunoprecipitation of a GFP-tagged form of CLIC1 from collected supernatants, uptake/secretion assay using traceable CLIC1 variants. Afterwards, we focused on the mechanism of secretion adopted by GBM cells to export CLIC1 to the extracellular environment. A significant part of secreted proteins exploits ER/trans-Golgi pathway; to do that target protein has to show a specific signal peptide that fate it to the exocytic pathway (Nickel et al., 2005). CLIC1 in not endowed with such region; moreover it is synthetized by cytosolic

ribosomes (Jiang et al., 2012). Literature data mining documented CLIC1 expression within exosomes released by a plethora of cell types and biological fluids (Pisitkun T et al., 2004; Valadi et al., 2007; Buschow et al., 2010; Welton et al., 2010; Staubach et al., 2009); furthermore, CLIC1 is listed as a top-scored protein in *ExoCarta* database. It is commonly acknowledged that ubiquitin dynamics represent a major signal triggering the recruitment of ESCRT machinery and cargo incorporation within exosomes (Baietti et al., 2012; Henne W.M. et al., 2014). CLIC1 primary structure harbors a PPxY motif, recognized by the WW domain of the Nedd4 E3 ubiquitin-ligase (Jolliffe et al., 2000; Shirk et al., 2005); in addition, CLIC1 displays two dileucine motifs that are thought to support its enrollment into endocytic pathway (Bernard TK et al., 2008; Behnke J et al., 2011). These structural hints, together with our biochemical data showing ubiquitinated CLIC1 in GBM cells and its affinity for Nedd4 protein, prompted us to pursue CLIC1 expression within exosomes isolated by human GBMs. It has been already reported that both GBM cell lines and primary samples release exosomes in vitro (Skog J. et al., 2008); we then retrieved exosomes by high speed serial centrifugation (Théry C. et al., 2006) from the growing medium of different GBM cell lines and GBM derived cancer stem/progenitor cells. Sample purity was assessed by: (1) western blot, showing a significant enrichment of the common endocytic markers like CD63, CD9, tsg101, (2) Nanoparticle Tracking Analysis (NTA, Nanosight) testing our vesicle sizes so that they fall in the 50-150 nm range, (3) EM analysis proving the existence of morphologically heterogeneous, bilayer-enclosed vesicles, (4) label-free mass spectrometry actually identifying the most common players involved in endocytosis rather that PM-associated proteins. Although data collected are in agreement with previous characterizations reported in literature (Raposo and Stoorvogel, 2013; Skog et al., 2008), the lack of a broadly acknowledged and reproducible methodology to achieve homogeneous preparations, persuaded us to drop the term “exosome” in favor of the most accepted “extracellular vesicle” (EV) (Colombo M et al., 2014).

Our work demonstrated that CLIC1 is actually expressed within EVs released by GBM cells. Indeed, EM analysis unveiled CLIC1 distribution in EVs expressing high levels of the

endocytic protein CD63; to better pinpoint CLIC1 pattern of expression in GBM cells we took advantage of PLA technique, confirming CLIC1 localization together with CD63. The second part of our study aimed to characterize CLIC1 involvement in defining EV-driven GBM physiopathology. Given our previous study showing CLIC1 involvement in regulating GBM cell biology in vitro and in vivo (Setti M. et al., 2013), we wanted to test whether these traits could be passed in vitro and in vivo by EVs. It is reported that EVs released by GBM cells are able to enhance proliferation both autochrinously and parachrinously (Skog et al., 2008).

We proved that by tuning CLIC1 levels within EVs, it was actually possible to abolish (shCLIC1) or to boost (CLIC1 FLAG) GBM cell proliferation *in vitro*; in agreement with in vitro experiments, mice subcutaneously injected with U87MG treated with CLIC1 FLAG EVs developed markedly bigger tumors while cells treated with shCLIC1 EVs behaved as untreated U87MG. Notably, while U87MG wt cells were positively stimulated in vitro with as much as EVs 50 mg/ml (0.5 ng EVs/cell in 100 ml), we observed a remarkable response in vivo (almost 10'000-fold stronger) with as few as 1 mg/ml (0.06 pg EVs/cell in 100 ml), thus making plausible to hypothesize that other biological forces beyond cell proliferation were driving tumor expansion (e.g. angiogenesis, tumor associated macrophages). Comprehensively, data collected so far suggest that CLIC1 is actually secreted within EVs where CLIC1 is involved in regulating EV-mediated pro-tumorigenic response. It is then conceivable that the aforementioned CLIC1 pro-tumorigenic phenotype (Setti et al., 2013) might rely on EV fraction other than CLIC1 cytoplasmic levels: secreted CLIC1 may induce tumor proliferation either directly by mediating the expansion of the neoplasia or by manipulating cells of tumoral niche. Label-free proteomic approaches suggested no-major differences other than CLIC1 in the composition of the EVs, thus making us wonder about the involvement of other non-proteic components of the vesicle, like microRNAs. More effort must be done in order to shed light on the molecular mechanism adopted by EVs to achieve their pro-tumorigenic effect, as well as the role of CLIC1 in this poorly understood and characterized mechanism of action.

5. Future Perspectives

- **Stable isotope labeling with amino acids in cell culture (SILAC) proteomic analysis.**

  Our experiments have shown that CLIC1 levels within the EV affect the proliferative status of recipient cells. Label-free MS experiments resulted in a "no-difference" output, thus leading us to the conclusion that EVs underwent no major proteomic changes upon CLIC1 modulation. Label-free mass spectrometry technology has several limitations that may affect the final outcome, like not discriminating below 2.5-fold differences and being less sensitive. To gain a deeper and more reliable insight about the proteomic status of the three subpopulations, we are going to perform SILAC assay on the EVs purified by U87MG NT, shCLIC1 and FLAG cells; it could be possible that mild changes in several candidates belonging to the same pathways might drive or contribute to the proliferative phenotype.

- **RNA-sequencing analysis**

  In parallel with the proteomic approach, we are going to analyze the RNA content (both long and small RNAs) of U87MG NT, shCLIC1 and CLIC1 FLAG cells and respective EVs. By analyzing RNA content within the cell, we could identify the alterations responsible of the phenotype described in Results (pg. 71-74); the same kind of information will be retrieved for NT, shCLIC1 and CLIC1 FLAG EVs thus possibly allowing the identification of targets and players different from the ones involved inside the cell. Finally, combining the data collected from both cell and EV transcriptome, we will be able to assess the correlation index between cell and respective EV and eventually identify new hits that might be differentially enriched in EVs derived from NT, shCLIC1 and CLIC1 FLAG cells.

- **Electrophysiological role of U87MG derived EVs.**

  We have already shown how CLIC1-mediated currents are responsible of regulating proliferative and tumorigenic response in GBM-derived cancer stem/progenitor cells (Results pg. 75-76 and 79-80). It is also known from literature that several cell types exploit EVs to transfer surface markers to recipient cells, thus making us wondering whether U87MG cells might take advantage of EVs to transfer transmembrane-CLIC1 on the plasma membrane of recipient cells. We are going to patch U87MG cells before and after the treatment with NT, shCLIC1 and CLIC1 FLAG EVs and CLIC1-mediated currents will be evaluated; it would be of extreme interest to treat U87MG cells with anti-CLIC1 antibody, to collect EVs from anti-CLIC1 treated cells (EVs*), and to test whether EVs* and shCLIC1 EVs trigger the same phenotypic response. The transcriptome of EVs* and shCLIC1 EVs will be eventually sequenced to distinguish candidates that rely on CLIC1 physical presence from the ones influenced by CLIC1-mediated chloride current.

- **CLIC1 as a viable biomarker in GBM**

  To effectively assess CLIC1 viability as biomarker in patients affected by GBM, we are going to exploit a syngenic mouse model where murine-derived GBM cells will be othotopically injected into the brain of mice of the same strain (C57B6). First, we are going to assess CLIC1 basal levels in plasma samples of C57B6 tumor-free mice; variability in CLIC1 levels will influence sample size but a cohort as large as ten mice will likely pander to both feasibility and statistical significance. To establish a proper basal line, we will take blood samples every 5 days for 15 days from tumor-free mice. Mice will be injected with 100’000 cells of a syngenic GBM cell line (GL261) and we will periodically take blood samples every 5 days. To monitor CLIC1 fluctuations in response to GBM volume, we are going to induce tumor shrinkage by treating GBM-bearing mice with a standard alkylating chemotherapeutic agent (temozolomide

270mg/kg) and we will keep on taking blood samples every 5 days until tumor recurrance. GBM progression, shrinkage and relapse will be followed up by magnetic resonance imaging (MRI) and CLIC1 levels will be eventually evaluated by ELISA assay.

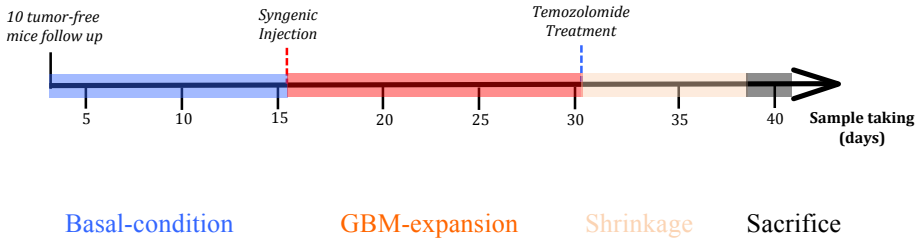

APPENDIX I

Gene names	t-test p value	t-test Difference
CLIC1	7.784E-09	2.523
TFG	4.669E-04	1.630
COL6A3	5.771E-04	1.481
SLC16A3	2.940E-04	1.146
RAP2A	2.899E-04	1.088
TIMP2	1.146E-03	1.087
NT5E	6.512E-05	1.075
PTPN23	2.259E-04	1.031
CACNA1D	1.364E-03	0.985
HLA-DRB1	2.034E-04	0.927
CD9	4.507E-06	0.924
SLC4A2	1.627E-03	0.874
CHMP3	2.262E-03	0.858
HLA-DPB1	1.635E-04	0.835
SLC6A6	1.246E-03	0.831
VTA1	3.047E-04	0.772
VPS4A	1.955E-06	0.763
SH3GL1	1.563E-06	0.758
RALB	6.370E-04	0.738
FLOT1	1.730E-04	0.714
VPS28	8.921E-04	0.677
S100A11	1.231E-03	0.666
IST1	5.284E-06	0.641
FLOT2	1.739E-04	0.634
ARRDC1	5.595E-08	0.616
VPS4B	6.927E-04	0.611
PDCD6IP	1.793E-03	0.594
ENO1	1.355E-03	0.586
CHMP1B	1.177E-03	0.583
HSPA8	2.830E-07	0.564
RAB22A	9.508E-06	0.551
RAB5C	1.886E-03	0.532
BROX	1.175E-03	0.522
MYOF	4.641E-04	0.498
ANXA1	2.463E-03	0.482
RAB7A	2.889E-04	0.444
DNAJA2	2.288E-03	0.404
CPD	7.929E-04	0.395
JAK1	5.918E-04	0.368
C3	1.156E-03	-0.529
PKM2	1.703E-03	-0.756
VCP	3.484E-05	-0.841
SERPINE2	7.037E-04	-0.996
HNRNPH1	5.060E-04	-1.015
QSOX1	1.175E-03	-1.089
RPL8	1.761E-03	-2.446

KEGG pathway Enrichment analysis

Category	Term	Count	%	P-Value	Benjamini
KEGG_PATHWAY	Endocytosis	9	20.9	2.7E-4	1.0E-2

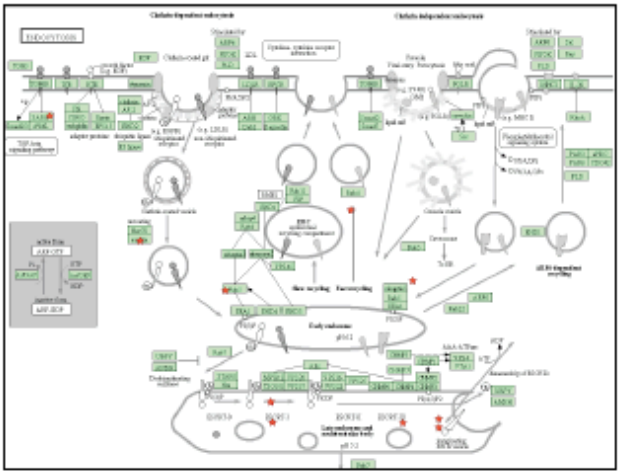

Appendix I. KEGG Pathway Analysis of CLIC1 FLAG EVs (FCLIC1) compared to NT EVs (NT). List of proteins differentially expressed in FCLIC1 versus NT; 54 candidates out of 611 proteins (8%) were found differentially expressed, among these 20% (9 proteins) were identified as endocytic proteins.

REFERENCES

Abounader, R., and Laterra, J. (2005). Scatter factor/hepatocyte growth factor in brain tumor growth and angiogenesis. Neuro Oncol 7, 436-451.

Admyre, C., S. M. Johansson, K. R. Qazi, J. J. Filen, R. Lahesmaa, M. Norman, E. P. Neve, A. Scheynius and S. Gabrielsson. "Exosomes with Immune Modulatory Features Are Present in Human Breast Milk." J Immunol 179, no. 3 (2007): 1969-78.

Aimone, J.B., Wiles, J., and Gage, F.H. (2006). Potential role for adult neurogenesis in the encoding of time in new memories. Nat Neurosci 9, 723-727.

Al-Hajj, M., Wicha, M.S., Benito-Hernandez, A., Morrison, S.J., and Clarke, M.F. (2003). Prospective identification of tumorigenic breast cancer cells. Proc Natl Acad Sci U S A 100, 3983-3988.

Al-Nedawi K, Meehan B, Micallef J, et al. (2008) Intercellular transfer of the oncogenic receptor EGFRvIII by microvesicles derived from tumour cells. Nat Cell Biol;10(5):619–624.

Anido J, Sáez-Borderías A, Gonzàlez-Juncà A, Rodón L, Folch G, Carmona MA, Prieto-Sánchez RM, Barba I, Martínez-Sáez E, Prudkin L, Cuartas I, Raventós C, Martínez-Ricarte F, Poca MA, García-Dorado D, Lahn MM, Yingling JM, Rodón J, Sahuquillo J, Baselga J,Seoane J. (2010). TGF-β Receptor Inhibitors Target the CD44(high)/Id1(high) Glioma-Initiating Cell Population in Human Glioblastoma. Cancer Cell. 2010 Dec 14;18(6):655-68.

Antonyak, Marc A., Bo Li, Lindsey K. Boroughs, Jared L. Johnson, Joseph E. Druso, Kirsten L. Bryant, David A. Holowka and Richard A. Cerione. "Cancer Cell-Derived Microvesicles Induce Transformation by Transferring Tissue Transglutaminase and Fibronectin to Recipient Cells." Proceedings of the National Academy of Sciences, (2011).

Arscott WT, Tandle AT, Zhao S, Shabason JE, Gordon IK, Schlaff CD, Zhang G, Tofilon PJ, Camphausen KA. (2013) Ionizing radiation and glioblastoma exosomes: implications in tumor biology and cell migration. Transl Oncol. 6(6):638-48.

Asea, A., C. Jean-Pierre, P. Kaur, P. Rao, I. M. Linhares, D. Skupski and S. S. Witkin. "Heat Shock Protein-Containing Exosomes in Mid-Trimester Amniotic Fluids." J Reprod Immunol 79, no. 1 (2008): 12-7.

Averaimo S, Milton RH, Duchen MR, Mazzanti M. Chloride intracellular channel 1 (CLIC1): Sensor and effector during oxidative stress. FEBS Lett. 2010 May 17;584(10):2076-84.

Bachoo, R.M., Maher, E.A., Ligon, K.L., Sharpless, N.E., Chan, S.S., You, M.J., Tang, Y., DeFrances, J., Stover, E., Weissleder, R., et al. (2002). Epidermal growth factor receptor and Ink4a/Arf: convergent mechanisms governing terminal differentiation and transformation along the neural stem cell to astrocyte axis. Cancer Cell 1, 269-277.

Bao, S., Wu, Q., McLendon, R.E., Hao, Y., Shi, Q., Hjelmeland, A.B., Dewhirst, M.W., Bigner, D.D., and Rich, J.N. (2006). Glioma stem cells promote radioresistance by preferential activation of the DNA damage response. Nature 444, 756-760.

Barabe, F., Kennedy, J.A., Hope, K.J., and Dick, J.E. (2007). Modeling the initiation and progression of human acute leukemia in mice. Science 316, 600-604.

Batagov, A. O., V. A. Kuznetsov and I. V. Kurochkin. "Identification of Nucleotide Patterns Enriched in Secreted Rnas as Putative Cis-Acting Elements Targeting Them to Exosome Nano-Vesicles." BMC Genomics 12 Suppl 3, (2011): S18.

Batchelor, T.T., Sorensen, A.G., di Tomaso, E., Zhang, W.T., Duda, D.G., Cohen, K.S., Kozak, K.R., Cahill, D.P., Chen, P.J., Zhu, M., et al. (2007). AZD2171, a pan-VEGF receptor tyrosine kinase inhibitor, normalizes tumor vasculature and alleviates edema in glioblastoma patients. Cancer Cell 11, 83-95.

Bergenheim T[1], Malmström A, Bolander H, Michanek A, Stragliotto G, Damber L, Björ O, Henriksson R. (2007). Registration on regional basis of patients with primary brain tumors. Regional differences disclosed. Lakartidningen. 2007 Jan 31-Feb 6;104(5):332-8, 340-1

Beckmann, J., Scheitza, S., Wernet, P., Fischer, J.C., and Giebel, B. (2007). Asymmetric cell division within the human hematopoietic stem and progenitor cell compartment: identification of asymmetrically segregating proteins. Blood 109, 5494-5501.

Berryman, M. and A. Bretscher. "Identification of a Novel Member of the Chloride Intracellular Channel Gene Family (Clic5) That Associates with the Actin Cytoskeleton of Placental Microvilli." Mol Biol Cell 11, no. 5 (2000): 1509-21.

Berryman MA[1], Goldenring JR. (2003). CLIC4 is enriched at cell-cell junctions and colocalizes with AKAP350 at the centrosome and midbody of cultured mammalian cells. Cell Motil Cytoskeleton. 2003 Nov;56(3):159-72

Bredel M, Scholtens DM, Harsh GR, Bredel C, Chandler JP, Renfrow JJ, Yadav AK, Vogel H, Scheck AC, Tibshirani R, Sikic BI. (2009). A network model of a cooperative genetic landscape in brain tumors. JAMA. 2009 Jul 15;302(3):261-75.

Brennan, C.W., Verhaak, R.G., McKenna, A., Campos, B., Noushmehr, H., Salama, S.R., Zheng, S., Chakravarty, D., Sanborn, J.Z., Berman, S.H., et al. (2013) The somatic genomic landscape of glioblastoma. Cell.155(2):462-477.

Bleau, A.M., Hambardzumyan, D., Ozawa, T., Fomchenko, E.I., Huse, J.T., Brennan, C.W., and Holland, E.C. (2009). PTEN/PI3K/Akt pathway regulates the side population phenotype and ABCG2 activity in glioma tumor stem-like cells. Cell Stem Cell 4, 226-235.

Bonnefoix, T., Bonnefoix, P., Verdiel, P., and Sotto, J.J. (1996). Fitting limiting dilution experiments with generalized linear models results in a test of the single-hit Poisson assumption. J Immunol Methods 194, 113-119.

Bonnet, D., and Dick, J.E. (1997). Human acute myeloid leukemia is organized as a hierarchy that originates from a primitive hematopoietic cell. Nat Med 3, 730-737.

Booth, A. M., Y. Fang, J. K. Fallon, J. M. Yang, J. E. Hildreth and S. J. Gould. "Exosomes and Hiv Gag Bud from Endosome-Like Domains of the T Cell Plasma Membrane." J Cell Biol 172, no. 6 (2006): 923-35.

Brennan, C., Momota, H., Hambardzumyan, D., Ozawa, T., Tandon, A., Pedraza, A., and Holland, E. (2009). Glioblastoma subclasses can be defined by activity among signal transduction pathways and associated genomic alterations. PLoS One 4, e7752.

Brescia, P., Richichi, C., and Pelicci, G. (2011). Identification of glioma stem cells: what is already known and how far do we still need to go? The biomarkers dilemma. JCM in press.

Bronisz A, Wang Y, Nowicki MO, et al. Extracellular vesicles modulate the glioblastoma microenvironment via a tumor suppression signaling network directed by miR-1. Cancer Res. 2014;74(3):738–750.

Buschow, S. I., B. W. van Balkom, M. Aalberts, A. J. Heck, M. Wauben and W. Stoorvogel. "Mhc Class Ii-Associated Proteins in B-Cell Exosomes and Potential Functional Implications for Exosome Biogenesis." Immunol Cell Biol 88, no. 8 (2010): 851-6.

Caby, M. P., D. Lankar, C. Vincendeau-Scherrer, G. Raposo and C. Bonnerot. "Exosomal-Like Vesicles Are Present in Human Blood Plasma." Int Immunol 17, no. 7 (2005): 879-87.

Cairncross JG, Ueki K, Zlatescu MC, Lisle DK, Finkelstein DM, Hammond RR, Silver JS, Stark PC, Macdonald DR, Ino Y, Ramsay DA, Louis DN. (1998). Specific genetic predictors of chemotherapeutic response and survival in patients with anaplastic oligodendrogliomas. J Natl Cancer Inst. 90(19):1473-9.

Calabrese, C., Poppleton, H., Kocak, M., Hogg, T.L., Fuller, C., Hamner, B., Oh, E.Y., Gaber, M.W., Finklestein, D., Allen, M., et al. (2007). A perivascular niche for brain tumor stem cells. Cancer Cell 11, 69-82.

Cameron, H.A., and McKay, R.D. (2001). Adult neurogenesis produces a large pool of new granule cells in the dentate gyrus. J Comp Neurol 435, 406-417.
Campbell, L.L., and Polyak, K. (2007). Breast tumor heterogeneity: cancer stem cells or clonal evolution? Cell Cycle 6, 2332-2338.

Carletta J. Assessing agreement on classification tasks: the kappa statistic. . Computational Linguistics 1996;22(2):249-254.

Carro, M.S., Lim, W.K., Alvarez, M.J., Bollo, R.J., Zhao, X., Snyder, E.Y., Sulman, E.P., Anne, S.L., Doetsch, F., Colman, H., et al. (2010). The transcriptional network for mesenchymal transformation of brain tumours. Nature 463, 318-325.

Castillo, L., Etienne-Grimaldi, M.C., Fischel, J.L., Formento, P., Magne, N., and Milano, G. (2004). Pharmacological background of EGFR targeting. Ann Oncol 15, 1007-1012.

Chaichana, K., Zamora-Berridi, G., Camara-Quintana, J., and Quinones-Hinojosa, A. (2006). Neurosphere assays: growth factors and hormone differences in tumor and nontumor studies. Stem Cells 24, 2851-2857.

Chang, Y. H., C. C. Wu, K. P. Chang, J. S. Yu, Y. C. Chang and P. C. Liao. "Cell Secretome Analysis Using Hollow Fiber Culture System Leads to the Discovery of Clic1 Protein as a Novel Plasma Marker for Nasopharyngeal Carcinoma." J Proteome Res 8, no. 12 (2009): 5465-74.

Chen, R., Nishimura, M.C., Bumbaca, S.M., Kharbanda, S., Forrest, W.F., Kasman, I.M., Greve, J.M., Soriano, R.H., Gilmour, L.L., Rivers, C.S., et al. (2010). A hierarchy of self-renewing tumor-initiating cell types in glioblastoma. Cancer Cell 17, 362-375.

Chen, C. D., C. S. Wang, Y. H. Huang, K. Y. Chien, Y. Liang, W. J. Chen and K. H. Lin. "Overexpression of Clic1 in Human Gastric Carcinoma and Its Clinicopathological

Significance." Proteomics 7, no. 1 (2007): 155-67.

Clarke, I.D., and Dirks, P.B. (2003). A human brain tumor-derived PDGFR-alpha deletion mutant is transforming. Oncogene 22, 722-733.

Clayton A, Turkes A, Dewitt S, Steadman R, Mason MD, Hallett MB. (2004) Adhesion and signaling by B cell-derived exosomes: the role of integrins. FASEB J;18(9):977-9.

Cocucci, E., G. Racchetti and J. Meldolesi. "Shedding Microvesicles: Artefacts No More." Trends Cell Biol 19, no. 2 (2009): 43-51.

Colman, H., Zhang, L., Sulman, E.P., McDonald, J.M., Shooshtari, N.L., Rivera, A., Popoff, S., Nutt, C.L., Louis, D.N., Cairncross, J.G., et al. (2010). A multigene predictor of outcome in glioblastoma. Neuro Oncol 12, 49-57.

Colombo M, Raposo G, Théry C. (2014). Exosomes and Other Extracellular Vesicles. Annu. Rev. Cell Dev. Biol. 2014. 30:255–89

Costello, J.F., Plass, C., Arap, W., Chapman, V.M., Held, W.A., Berger, M.S., Su Huang, H.J., and Cavenee, W.K. (1997). Cyclin-dependent kinase 6 (CDK6) amplification in human gliomas identified using two-dimensional separation of genomic DNA. Cancer Res 57, 1250-1254.

Curtis, M.A., Kam, M., Nannmark, U., Anderson, M.F., Axell, M.Z., Wikkelso, C., Holtas, S., van Roon-Mom, W.M., Bjork-Eriksson, T., Nordborg, C., et al. (2007). Human neuroblasts migrate to the olfactory bulb via a lateral ventricular extension. Science 315, 1243-1249.

Dalerba, P., Dylla, S.J., Park, I.K., Liu, R., Wang, X., Cho, R.W., Hoey, T., Gurney, A., Huang, E.H., Simeone, D.M., et al. (2007). Phenotypic characterization of human colorectal cancer stem cells. Proc Natl Acad Sci U S A 104, 10158-10163.

Denzer, K., M. van Eijk, M. J. Kleijmeer, E. Jakobson, C. de Groot and H. J. Geuze. "Follicular Dendritic Cells Carry Mhc Class Ii-Expressing Microvesicles at Their Surface." J Immunol 165, no. 3 (2000): 1259-65.

Dolecek T.A., Propp J.M., Stroup N..E, Kruchko C. (2012) CBTRUS statistical report: primary brain and central nervous system tumors diagnosed in the United States in 2005-2009. Neuro Oncol. 14(suppl 5):v1-v49.

Emmanouilidou, Evangelia, Katerina Melachroinou, Theodoros Roumeliotis, Spiros D. Garbis, Maria Ntzouni, Lukas H. Margaritis, Leonidas Stefanis and Kostas Vekrellis. "Cell-Produced A-Synuclein Is Secreted in a Calcium-Dependent Manner by Exosomes and Impacts Neuronal Survival." The Journal of Neuroscience 30, no. 20 (2010): 6838-6851.

Eramo, A., Lotti, F., Sette, G., Pilozzi, E., Biffoni, M., Di Virgilio, A., Conticello, C., Ruco, L., Peschle, C., and De Maria, R. (2008). Identification and expansion of the tumorigenic lung cancer stem cell population. Cell Death Differ 15, 504-514.

Faury D, Nantel A, Dunn SE, Guiot MC, Haque T, Hauser P, Garami M, Bognár L, Hanzély Z, Liberski PP, Lopez-Aguilar E, Valera ET, Tone LG, Carret AS, Del Maestro RF, Gleave M, Montes JL, Pietsch T, Albrecht S, Jabado N. (2007). Molecular profiling identifies prognostic

subgroups of pediatric glioblastoma and shows increased YB-1 expression in tumors. J Clin Oncol. 25(10):1196-208.

Fevrier, Benoit, Didier Vilette, Fabienne Archer, Damarys Loew, Wolfgang Faigle, Michel Vidal, Hubert Laude and Graça Raposo. "Cells Release Prions in Association with Exosomes." Proceedings of the National Academy of Sciences of the United States of America 101, no. 26 (2004): 9683-9688.

Frederick, L., Eley, G., Wang, X.Y., and James, C.D. (2000). Analysis of genomic rearrangements associated with EGRFvIII expression suggests involvement of Alu repeat elements. Neuro Oncol 2, 159-163.

Freije, W.A., Castro-Vargas, F.E., Fang, Z., Horvath, S., Cloughesy, T., Liau, L.M., Mischel, P.S., and Nelson, S.F. (2004). Gene expression profiling of gliomas strongly predicts survival. Cancer Res 64, 6503-6510.

Fuller, G.N., Hess, K.R., Rhee, C.H., Yung, W.K., Sawaya, R.A., Bruner, J.M., and Zhang, W. (2002). Molecular classification of human diffuse gliomas by multidimensional scaling analysis of gene expression profiles parallels morphology-based classification, correlates with survival, and reveals clinically-relevant novel glioma subsets. Brain Pathol 12, 108-116.

Furnari, F.B., Fenton, T., Bachoo, R.M., Mukasa, A., Stommel, J.M., Stegh, A., Hahn, W.C., Ligon, K.L., Louis, D.N., Brennan, C., et al. (2007). Malignant astrocytic glioma: genetics, biology, and paths to treatment. Genes Dev 21, 2683-2710.

Galli, R., Binda, E., Orfanelli, U., Cipelletti, B., Gritti, A., De Vitis, S., Fiocco, R., Foroni, C., Dimeco, F., and Vescovi, A. (2004). Isolation and characterization of tumorigenic, stem-like neural precursors from human glioblastoma. Cancer Res 64, 7011-7021.

Giebel, B., and Beckmann, J. (2007). Asymmetric cell divisions of human hematopoietic stem and progenitor cells meet endosomes. Cell Cycle 6, 2201-2204.

Godard, S., Getz, G., Delorenzi, M., Farmer, P., Kobayashi, H., Desbaillets, I., Nozaki, M., Diserens, A.C., Hamou, M.F., Dietrich, P.Y., et al. (2003). Classification of human astrocytic gliomas on the basis of gene expression: a correlated group of genes with angiogenic activity emerges as a strong predictor of subtypes. Cancer Res 63, 6613-6625.

Godlewski J, Krichevsky AM, Johnson MD, Chiocca EA, Bronisz A. (2014) Belonging to a network-microRNAs, extracellular vesicles, and the glioblastoma microenvironment. Neuro Oncol. [Epub ahead of print] Review.

Gomes, Catarina, Sascha Keller, Peter Altevogt and Júlia Costa. "Evidence for Secretion of Cu,Zn Superoxide Dismutase Via Exosomes from a Cell Model of Amyotrophic Lateral Sclerosis." Neuroscience Letters 428, no. 1 (2007): 43-46.

Gomez-Manzano, C., Holash, J., Fueyo, J., Xu, J., Conrad, C.A., Aldape, K.D., de Groot, J.F., Bekele, B.N., and Yung, W.K. (2008). VEGF Trap induces antiglioma effect at different stages of disease. Neuro Oncol 10, 940-945.

Griffon N, Jeanneteau F, Prieur F, Diaz J, Sokoloff P. (2003) CLIC6, a member of the intracellular chloride channel family, interacts with dopamine D(2)-like receptors. Brain Res Mol Brain Res.117(1):47-57.

Grossman, S.A., Phuphanich, S., Lesser, G., Rozental, J., Grochow, L.B., Fisher, J., and Piantadosi, S. (2001). Toxicity, efficacy, and pharmacology of suramin in adults with recurrent high-grade gliomas. J Clin Oncol 19, 3260-3266.

Halatsch, M.E., Schmidt, U., Unterberg, A., Vougioukas, V.I., Anticancer Res. 2006 Nov-Dec;26(6B):4191-4.

Hanahan, D., and Weinberg, R.A. (2000). The hallmarks of cancer. Cell 100, 57-70.

Harding, C., J. Heuser and P. Stahl. "Endocytosis and Intracellular Processing of Transferrin and Colloidal Gold-Transferrin in Rat Reticulocytes: Demonstration of a Pathway for Receptor Shedding." Eur J Cell Biol 35, no. 2 (1984): 256-63.

Harris, M.A., Yang, H., Low, B.E., Mukherjee, J., Guha, A., Bronson, R.T., Shultz, L.D., Israel, M.A., and Yun, K. (2008). Cancer stem cells are enriched in the side population cells in a mouse model of glioma. Cancer Res 68, 10051-10059.

Harrop, S. J., M. Z. DeMaere, W. D. Fairlie, T. Reztsova, S. M. Valenzuela, M. Mazzanti, R. Tonini, M. R. Qiu, L. Jankova, K. Warton, A. R. Bauskin, W. M. Wu, S. Pankhurst, T. J. Campbell, S. N. Breit and P. M. Curmi. "Crystal Structure of a Soluble Form of the Intracellular Chloride Ion Channel Clic1 (Ncc27) at 1.4-a Resolution." J Biol Chem 276, no. 48 (2001): 44993-5000.

Hartmann, C., Hentschel, B., Wick, W., Capper, D., Felsberg, J., Simon, M., Westphal, M., Schackert, G., Meyermann, R., Pietsch, T., et al. (2010). Patients with IDH1 wild type anaplastic astrocytomas exhibit worse prognosis than IDH1-mutated glioblastomas, and IDH1 mutation status accounts for the unfavorable prognostic effect of higher age: implications for classification of gliomas. Acta Neuropathol 120, 707-718.

Hartmann, C., Meyer, J., Balss, J., Capper, D., Mueller, W., Christians, A., Felsberg, J., Wolter, M., Mawrin, C., Wick, W., et al. (2009). Type and frequency of IDH1 and IDH2 mutations are related to astrocytic and oligodendroglial differentiation and age: a study of 1,010 diffuse gliomas. Acta Neuropathol 118, 469-474.

Hegi, M.E., Diserens, A.C., Gorlia, T., Hamou, M.F., de Tribolet, N., Weller, M., Kros, J.M., Hainfellner, J.A., Mason, W., Mariani, L., et al. (2005). MGMT gene silencing and benefit from temozolomide in glioblastoma. N Engl J Med 352, 997-1003.

Heimberger AB, Sampson JH. (2009). The PEPvIII-KLH (CDX-110) vaccine in glioblastoma multiforme patients. Expert Opin Biol Ther. 9(8):1087-98.

Hemler, M. E. "Tetraspanin Proteins Mediate Cellular Penetration, Invasion, and Fusion Events and Define a Novel Type of Membrane Microdomain." Annu Rev Cell Dev Biol 19, (2003): 397-422.

Hemmati, H.D., Nakano, I., Lazareff, J.A., Masterman-Smith, M., Geschwind, D.H., Bronner-Fraser, M., and Kornblum, H.I. (2003). Cancerous stem cells can arise from pediatric brain tumors. Proc Natl Acad Sci U S A 100, 15178-15183.

Henson, J.W., Schnitker, B.L., Correa, K.M., von Deimling, A., Fassbender, F., Xu, H.J., Benedict, W.F., Yandell, D.W., and Louis, D.N. (1994). The retinoblastoma gene is involved in malignant progression of astrocytomas. Ann Neurol 36, 714-721.

Holland, E.C., Celestino, J., Dai, C., Schaefer, L., Sawaya, R.E., and Fuller, G.N. (2000). Combined activation of Ras and Akt in neural progenitors induces glioblastoma formation in mice. Nat Genet 25, 55-57.

Huang, J. S., C. C. Chao, T. L. Su, S. H. Yeh, D. S. Chen, C. T. Chen, P. J. Chen and Y. S. Jou. "Diverse Cellular Transformation Capability of Overexpressed Genes in Human Hepatocellular Carcinoma." Biochem Biophys Res Commun 315, no. 4 (2004): 950-8.

Hurley, James H. "The Escrt Complexes." Critical Reviews in Biochemistry and Molecular Biology 45, no. 6 (2010): 463-487.

Huse, J.T., and Holland, E.C. (2009). Genetically engineered mouse models of brain cancer and the promise of preclinical testing. Brain Pathol 19, 132-143.

Huse, J.T., Phillips, H.S., and Brennan, C.W. (2011). Molecular subclassification of diffuse gliomas: seeing order in the chaos. Glia 59, 1190-1199.

Ignatova, T.N., Kukekov, V.G., Laywell, E.D., Suslov, O.N., Vrionis, F.D., and Steindler, D.A. (2002). Human cortical glial tumors contain neural stem-like cells expressing astroglial and neuronal markers in vitro. Glia 39, 193-206.

Irion, U. and D. St Johnston. "Bicoid Rna Localization Requires Specific Binding of an Endosomal Sorting Complex." Nature 445, no. 7127 (2007): 554-8.

Kang, M. K. and S. K. Kang. "Pharmacologic Blockade of Chloride Channel Synergistically Enhances Apoptosis of Chemotherapeutic Drug-Resistant Cancer Stem Cells." Biochem Biophys Res Commun 373, no. 4 (2008): 539-44.

Kern, S.E., and Shibata, D. (2007). The fuzzy math of solid tumor stem cells: a perspective. Cancer Res 67, 8985-8988.

Kilic, T., Alberta, J.A., Zdunek, P.R., Acar, M., Iannarelli, P., O'Reilly, T., Buchdunger, E., Black, P.M., and Stiles, C.D. (2000). Intracranial inhibition of platelet-derived growth factor-mediated glioblastoma cell growth by an orally active kinase inhibitor of the 2-phenylaminopyrimidine class. Cancer Res 60, 5143-5150.

Kraus, J.A., Glesmann, N., Beck, M., Krex, D., Klockgether, T., Schackert, G., Schlegel, U., J Neurooncol. 2000 Jun;48(2):89-94.

Kucharzewska P, Christianson HC, Welch JE, et al. (2013) Exosomes reflect the hypoxic status of glioma cells and mediate hypoxia-dependent activation of vascular cells during tumor development. Proc Natl Acad Sci U S A;110(18):7312–7317.

Lachenal G., Karin P.G., Chivet M., Fiona J. Hemming, Agnès Belly, Gilles Bodon, Béatrice Blot, Georg Haase, Yves Goldberg and Rémy Sadoul. "Release of Exosomes from Differentiated Neurons and Its Regulation by Synaptic Glutamatergic Activity." Molecular and Cellular Neuroscience 46, no. 2 (2011): 409-418.

Ladner JE, Parsons JF, Rife CL, Gilliland GL, Armstrong RN. (2004). Parallel evolutionary pathways for glutathione transferases: structure and mechanism of the mitochondrial class kappa enzyme rGSTK1-1. Biochemistry. 2004 Jan 20;43(2):352-61.

Laks, D.R., Masterman-Smith, M., Visnyei, K., Angenieux, B., Orozco, N.M., Foran, I., Yong, W.H., Vinters, H.V., Liau, L.M., Lazareff, J.A., et al. (2009). Neurosphere formation is an independent predictor of clinical outcome in malignant glioma. Stem Cells 27, 980-987.

Lapidot, T., Sirard, C., Vormoor, J., Murdoch, B., Hoang, T., Caceres-Cortes, J., Minden, M., Paterson, B., Caligiuri, M.A., and Dick, J.E. (1994). A cell initiating human acute myeloid leukaemia after transplantation into SCID mice. Nature 367, 645-648.

Lathia, J.D., Gallagher, J., Heddleston, J.M., Wang, J., Eyler, C.E., Macswords, J., Wu, Q., Vasanji, A., McLendon, R.E., Hjelmeland, A.B., et al. (2010). Integrin alpha 6 regulates glioblastoma stem cells. Cell Stem Cell 6, 421-432.

Lee, J., Kotliarova, S., Kotliarov, Y., Li, A., Su, Q., Donin, N.M., Pastorino, S., Purow, B.W., Christopher, N., Zhang, W., et al. (2006). Tumor stem cells derived from glioblastomas cultured in bFGF and EGF more closely mirror the phenotype and genotype of primary tumors than do serum-cultured cell lines. Cancer Cell 9, 391-403.

Lee, J., Son, M.J., Woolard, K., Donin, N.M., Li, A., Cheng, C.H., Kotliarova, S., Kotliarov, Y., Walling, J., Ahn, S., et al. (2008). Epigenetic-mediated dysfunction of the bone morphogenetic protein pathway inhibits differentiation of glioblastoma-initiating cells. Cancer Cell 13, 69-80.

Li Y, Li D, Zeng Z, Wang D. (2006). Trimeric structure of the wild soluble chloride intracellular ion channel CLIC4 observed in crystals. Biochem Biophys Res Commun. 343(4):1272-8.

Li, A., Walling, J., Ahn, S., Kotliarov, Y., Su, Q., Quezado, M., Oberholtzer, J.C., Park, J., Zenklusen, J.C., and Fine, H.A. (2009). Unsupervised analysis of transcriptomic profiles reveals six glioma subtypes. Cancer Res 69, 2091-2099.

Li Y, Guessous F, Zhang Y, et al. (2009) MicroRNA-34a inhibits glioblastoma growth by targeting multiple oncogenes. Cancer Res;69(19): 7569–7576.

Libermann TA, Nusbaum HR, Razon N, Kris R, Lax I, Soreq H, Whittle N, Waterfield MD, Ullrich A, Schlessinger J. (1985). Amplification, enhanced expression and possible rearrangement of EGF receptor gene in primary human brain tumours of glial origin. Nature. 313(5998):144-7.

Ligon, K.L., Huillard, E., Mehta, S., Kesari, S., Liu, H., Alberta, J.A., Bachoo, R.M., Kane, M., Louis, D.N., Depinho, R.A., et al. (2007). Olig2-regulated lineage-restricted pathway controls replication competence in neural stem cells and malignant glioma. Neuron 53, 503-517.

Liu, C., Sage, J.C., Miller, M.R., Verhaak, R.G., Hippenmeyer, S., Vogel, H., Foreman, O., Bronson, R.T., Nishiyama, A., Luo, L., et al. (2011). Mosaic analysis with double markers reveals tumor cell of origin in glioma. Cell 146, 209-221.

Liu, Q., Nguyen, D.H., Dong, Q., Shitaku, P., Chung, K., Liu, O.Y., Tso, J.L., Liu, J.Y., Konkankit, V., Cloughesy, T.F., et al. (2009). Molecular properties of CD133+ glioblastoma stem cells derived from treatment-refractory recurrent brain tumors. J Neurooncol 94, 1-19.

Littler, D. R., S. J. Harrop, W. D. Fairlie, L. J. Brown, G. J. Pankhurst, S. Pankhurst, M. Z. DeMaere, T. J. Campbell, A. R. Bauskin, R. Tonini, M. Mazzanti, S. N. Breit and P. M. Curmi. "The Intracellular Chloride Ion Channel Protein Clic1 Undergoes a Redox-Controlled Structural
Transition." J Biol Chem 279, no. 10 (2004): 9298-305.

Littler, D. R., Stephen J. Harrop, Sophia C. Goodchild, Juanita M. Phang, Andrew V. Mynott, Lele Jiang, Stella M. Valenzuela, Michele Mazzanti, Louise J. Brown, Samuel N. Breit and Paul M. G. Curmi. "The Enigma of the Clic Proteins: Ion Channels, Redox Proteins, Enzymes, Scaffolding Proteins?" FEBS Letters 584, no. 10 (2010): 2093-2101.

Lois, C., Garcia-Verdugo, J.M., and Alvarez-Buylla, A. (1996). Chain migration of neuronal precursors. Science 271, 978-981.

Louis, D.N. (1994). The p53 gene and protein in human brain tumors. J Neuropathol Exp Neurol 53, 11-21.

Louis, D.N., Ohgaki, H., Wiestler, O.D., Cavenee, W.K., Burger, P.C., Jouvet, A., Scheithauer, B.W., and Kleihues, P. (2007). The 2007 WHO classification of tumours of the central nervous system. Acta Neuropathol 114, 97-109.

Louis, S.A., Rietze, R.L., Deleyrolle, L., Wagey, R.E., Thomas, T.E., Eaves, A.C., and Reynolds, B.A. (2008). Enumeration of neural stem and progenitor cells in the neural colony-forming cell assay. Stem Cells 26, 988-996.

Luskin, M.B. (1993). Restricted proliferation and migration of postnatally generated neurons derived from the forebrain subventricular zone. Neuron 11, 173-189.

Madhavan S ZJ, Kotliarov Y, Sahni H, Fine HA, Buetow K. Rembrandt: helping personalized medicine become a reality through integrative translational research. Mol Cancer Res 2009;7(2):157-67

Mallegol, Julia, Guillaume Van Niel, Corinne Lebreton, Yves Lepelletier, Céline Candalh, Christophe Dugave, Joan K. Heath, Graça Raposo, Nadine Cerf–Bensussan and Martine Heyman. "T84-Intestinal Epithelial Exosomes Bear Mhc Class Ii/Peptide Complexes Potentiating Antigen Presentation by Dendritic Cells." Gastroenterology 132, no. 5 (2007): 1866-1876.

Mathivanan S, Simpson RJ. ExoCarta: A compendium of exosomal proteins and RNA. (2009). Proteomics. 9(21):4997-5000.

Martin J.L. Thioredoxin--a fold for all reasons. (1995). Structure. 3(3):245-50.

Masyuk, A. I., B. Q. Huang, C. J. Ward, S. A. Gradilone, J. M. Banales, T. V. Masyuk, B. Radtke, P. L. Splinter and N. F. LaRusso. "Biliary Exosomes Influence Cholangiocyte Regulatory Mechanisms and Proliferation through Interaction with Primary Cilia." Am J Physiol
Gastrointest Liver Physiol 299, no. 4 (2010): G990-9.

Matsuda M, Imaoka T, Vomachka AJ, Gudelsky GA, Hou Z, Mistry M, Bailey JP, Nieport KM, Walther DJ, Bader M, Horseman ND. (2004). Serotonin regulates mammary gland development via an autocrine-paracrine loop. Dev Cell. 6(2):193-203.
Mayer-Proschel, M., Kalyani, A.J., Mujtaba, T., and Rao, M.S. (1997). Isolation of lineage-restricted neuronal precursors from multipotent neuroepithelial stem cells. Neuron 19, 773-785.

Menon, S. G. and P. C. Goswami. "A Redox Cycle within the Cell Cycle: Ring in the Old with the New." Oncogene 26, no. 8 (2007): 1101-9.

Miller, C.R., and Perry, A. (2007). Glioblastoma. Arch Pathol Lab Med 131, 397-406.

Milton, R. H., R. Abeti, S. Averaimo, S. DeBiasi, L. Vitellaro, L. Jiang, P. M. Curmi, S. N. Breit, M. R. Duchen and M. Mazzanti. "Clic1 Function Is Required for Beta-Amyloid-Induced Generation of Reactive Oxygen Species by Microglia." J Neurosci 28, no. 45 (2008): 11488-99.

Mittelbrunn M, Gutiérrez-Vázquez C, Villarroya-Beltri C, González S, Sánchez-Cabo F, González MÁ, Bernad A, Sánchez-Madrid F. Unidirectional transfer of microRNA-loaded exosomes from T cells to antigen-presenting cells. (2011). Nat Commun. 2011;2:282.

Mobius, W., Y. Ohno-Iwashita, E. G. van Donselaar, V. M. Oorschot, Y. Shimada, T. Fujimoto, H. F. Heijnen, H. J. Geuze and J. W. Slot. "Immunoelectron Microscopic Localization of Cholesterol Using Biotinylated and Non-Cytolytic Perfringolysin O." J Histochem Cytochem 50, no. 1 (2002): 43-55.

Montecalvo A, Larregina AT, Shufesky WJ, et al. (2012) Mechanism of transfer of functional microRNAs between mouse dendritic cells via exosomes. Blood;119(3):756–766.

Moore, K.A., and Lemischka, I.R. (2006). Stem cells and their niches. Science 311, 1880-1885.

Nigro, J.M., Misra, A., Zhang, L., Smirnov, I., Colman, H., Griffin, C., Ozburn, N., Chen, M., Pan, E., Koul, D., et al. (2005). Integrated array-comparative genomic hybridization and expression array profiles identify clinically relevant molecular subtypes of glioblastoma. Cancer Res 65, 1678-1686.

Norden, A.D., Drappatz, J., and Wen, P.Y. (2008). Novel anti-angiogenic therapies for malignant gliomas. Lancet Neurol 7, 1152-1160.

Noushmehr, H., Weisenberger, D.J., Diefes, K., Phillips, H.S., Pujara, K., Berman, B.P., Pan, F., Pelloski, C.E., Sulman, E.P., Bhat, K.P., et al. (2010). Identification of a CpG island methylator phenotype that defines a distinct subgroup of glioma. Cancer Cell 17, 510-522.

Nowell, P.C. (1976). The clonal evolution of tumor cell populations. Science 194, 23-28.

Nutt, C.L., Mani, D.R., Betensky, R.A., Tamayo, P., Cairncross, J.G., Ladd, C., Pohl, U., Hartmann, C., McLaughlin, M.E., Batchelor, T.T., et al. (2003). Gene expression-based classification of malignant gliomas correlates better with survival than histological classification. Cancer Res 63, 1602-1607.

Ogawa, Y., Y. Miura, A. Harazono, M. Kanai-Azuma, Y. Akimoto, H. Kawakami, T. Yamaguchi, T. Toda, T. Endo, M. Tsubuki and R. Yanoshita. "Proteomic Analysis of Two Types of Exosomes in Human Whole Saliva." Biol Pharm Bull 34, no. 1 (2011): 13-23.

Ohgaki, H., and Kleihues, P. (2007). Genetic pathways to primary and secondary glioblastoma. Am J Pathol 170, 1445-1453.

Omuro A., DeAngelis L. (2013). Glioblastoma and Other Malignant Gliomas. JAMA 310(17):1842-1850.

Pallini, R., Ricci-Vitiani, L., Banna, G.L., Signore, M., Lombardi, D., Todaro, M., Stassi, G., Martini, M., Maira, G., Larocca, L.M., et al. (2008). Cancer stem cell analysis and clinical outcome in patients with glioblastoma multiforme. Clin Cancer Res 14, 8205-8212.

Pan BT, Teng K, Wu C, Adam M, Johnstone RM. 1985. Electron microscopic evidence for externalization of the transferrin receptor in vesicular form in sheep reticulocytes. J. Cell Biol. 101:942–48

Parsons, D.W., Jones, S., Zhang, X., Lin, J.C., Leary, R.J., Angenendt, P., Mankoo, P., Carter, H., Siu, I.M., Gallia, G.L., et al. (2008). An integrated genomic analysis of human glioblastoma multiforme. Science 321, 1807-1812.

Pelloski, C.E., Ballman, K.V., Furth, A.F., Zhang, L., Lin, E., Sulman, E.P., Bhat, K., McDonald, J.M., Yung, W.K., Colman, H., et al. (2007). Epidermal growth factor receptor variant III status defines clinically distinct subtypes of glioblastoma. J Clin Oncol 25, 2288-2294.

Petrova, D. T., A. R. Asif, V. W. Armstrong, I. Dimova, S. Toshev, N. Yaramov, M. Oellerich and D. Toncheva. "Expression of Chloride Intracellular Channel Protein 1 (Clic1) and Tumor Protein D52 (Tpd52) as Potential Biomarkers for Colorectal Cancer." Clin Biochem 41, no. 14-15 (2008): 1224-36.

Phillips, H.S., Kharbanda, S., Chen, R., Forrest, W.F., Soriano, R.H., Wu, T.D., Misra, A., Nigro, J.M., Colman, H., Soroceanu, L., et al. (2006). Molecular subclasses of high-grade glioma predict prognosis, delineate a pattern of disease progression, and resemble stages in neurogenesis. Cancer Cell 9, 157-173.

Piccirillo, S.G., Reynolds, B.A., Zanetti, N., Lamorte, G., Binda, E., Broggi, G., Brem, H., Olivi, A., Dimeco, F., and Vescovi, A.L. (2006). Bone morphogenetic proteins inhibit the tumorigenic potential of human brain tumour-initiating cells. Nature 444, 761-765.

Pisitkun, Trairak, Rong-Fong Shen and Mark A. Knepper. "Identification and Proteomic Profiling of Exosomes in Human Urine." Proceedings of the National Academy of Sciences of the United States of America 101, no. 36 (2004): 13368-13373.

Prados, M.D., Lamborn, K.R., Chang, S., Burton, E., Butowski, N., Malec, M., Kapadia, A., Rabbitt, J., Page, M.S., Fedoroff, A., et al. (2006). Phase 1 study of erlotinib HCl alone and combined with temozolomide in patients with stable or recurrent malignant glioma. Neuro Oncol 8, 67-78.

Quintana, E., Shackleton, M., Sabel, M.S., Fullen, D.R., Johnson, T.M., and Morrison, S.J. (2008). Efficient tumour formation by single human melanoma cells. Nature 456, 593-598.

Rajendran, Lawrence, Masanori Honsho, Tobias R. Zahn, Patrick Keller, Kathrin D. Geiger, Paul Verkade and Kai Simons. "Alzheimer's Disease B-Amyloid Peptides Are Released in Association with Exosomes." Proceedings of the National Academy of Sciences 103, no. 30 (2006): 11172-11177.

Rao, M.S., Noble, M., and Mayer-Proschel, M. (1998). A tripotential glial precursor cell is present in the developing spinal cord. Proc Natl Acad Sci U S A 95, 3996-4001.

Raposo G, Nijman HW, Stoorvogel W, Liejendekker R, Harding CV, et al. 1996. B lymphocytes secrete antigen-presenting vesicles. J. Exp. Med. 183:1161–72

Raposo G, Stoorvogel W. Extracellular vesicles: exosomes, microvesicles, and friends. (2013). J Cell Biol. 200(4):373-83.

Ratajczak, J., M. Wysoczynski, F. Hayek, A. Janowska-Wieczorek and M. Z. Ratajczak. Membrane-Derived Microvesicles: Important and Underappreciated Mediators of Cell-to-Cell Communication. Leukemia 20, no. 9 (2006): 1487-95.

Raymond, E., Brandes, A.A., Dittrich, C., Fumoleau, P., Coudert, B., Clement, P.M., Frenay, M., Rampling, R., Stupp, R., Kros, J.M., et al. (2008). Phase II study of imatinib in patients with recurrent gliomas of various histologies: a European Organisation for Research and Treatment of Cancer Brain Tumor Group Study. J Clin Oncol 26, 4659-4665.

Reya, T., Morrison, S.J., Clarke, M.F., and Weissman, I.L. (2001). Stem cells, cancer, and cancer stem cells. Nature 414, 105-111.

Reynolds, B.A., and Rietze, R.L. (2005). Neural stem cells and neurospheres--re-evaluating the relationship. Nat Methods 2, 333-336.

Reynolds, B.A., and Weiss, S. (1992). Generation of neurons and astrocytes from isolated cells of the adult mammalian central nervous system. Science 255, 1707-1710.
Reynolds, B.A., and Weiss, S. (1996). Clonal and population analyses demonstrate that an EGF-responsive mammalian embryonic CNS precursor is a stem cell. Dev Biol 175, 1-13.

Ricci-Vitiani, L., Lombardi, D.G., Pilozzi, E., Biffoni, M., Todaro, M., Peschle, C., and De Maria, R. (2007). Identification and expansion of human colon-cancer-initiating cells. Nature 445, 111-115.

Ricci-Vitiani, L., Pallini, R., Biffoni, M., Todaro, M., Invernici, G., Cenci, T., Maira, G., Parati, E.A., Stassi, G., Larocca, L.M., et al. (2010). Tumour vascularization via endothelial differentiation of glioblastoma stem-like cells. Nature 468, 824-828.

Rich, J.N., Reardon, D.A., Peery, T., Dowell, J.M., Quinn, J.A., Penne, K.L., Wikstrand, C.J., Van Duyn, L.B., Dancey, J.E., McLendon, R.E., et al. (2004). Phase II trial of gefitinib in recurrent glioblastoma. J Clin Oncol 22, 133-142.

Rickman, D.S., Bobek, M.P., Misek, D.E., Kuick, R., Blaivas, M., Kurnit, D.M., Taylor, J., and Hanash, S.M. (2001). Distinctive molecular profiles of high-grade and low-grade gliomas based on oligonucleotide microarray analysis. Cancer Res 61, 6885-6891.

Rietze, R.L., and Reynolds, B.A. (2006). Neural stem cell isolation and characterization. Methods Enzymol 419, 3-23.

Ronquist, G. and I. Brody. "The Prostasome: Its Secretion and Function in Man." Biochim Biophys Acta 822, no. 2 (1985): 203-18.

Sampson, J.H., Archer, G.E., Mitchell, D.A., Heimberger, A.B., and Bigner, D.D. (2008). Tumor-specific immunotherapy targeting the EGFRvIII mutation in patients with malignant glioma. Semin Immunol 20, 267-275.

Sanai, N., Tramontin, A.D., Quinones-Hinojosa, A., Barbaro, N.M., Gupta, N., Kunwar, S., Lawton, M.T., McDermott, M.W., Parsa, A.T., Manuel-Garcia Verdugo, J., et al. (2004). Unique astrocyte ribbon in adult human brain contains neural stem cells but lacks chain migration. Nature 427, 740-744.

Scadden, D.T. (2006). The stem-cell niche as an entity of action. Nature 441, 1075-1079.

Seaberg RM, Smukler SR, Kieffer TJ, Enikolopov G, Asghar Z, Wheeler MB, Korbutt G, van der Kooy D. (2004) Clonal identification of multipotent precursors from adult mouse pancreas that generate neural and pancreatic lineages. Nat Biotechnol. 22(9):1115-24.

Sennino, B., Falcon, B.L., McCauley, D., Le, T., McCauley, T., Kurz, J.C., Haskell, A., Epstein, D.M., and McDonald, D.M. (2007). Sequential loss of tumor vessel pericytes and endothelial cells after inhibition of platelet-derived growth factor B by selective aptamer AX102. Cancer Res 67, 7358-7367.

Shackleton, M., Quintana, E., Fearon, E.R., and Morrison, S.J. (2009). Heterogeneity in cancer: cancer stem cells versus clonal evolution. Cell 138, 822-829.

Shah, N.P., Skaggs, B.J., Branford, S., Hughes, T.P., Nicoll, J.M., Paquette, R.L., and Sawyers, C.L. (2007). Sequential ABL kinase inhibitor therapy selects for compound drug-resistant BCR-ABL mutations with altered oncogenic potency. J Clin Invest 117, 2562-2569.

Shai, R., Shi, T., Kremen, T.J., Horvath, S., Liau, L.M., Cloughesy, T.F., Mischel, P.S., and Nelson, S.F. (2003). Gene expression profiling identifies molecular subtypes of gliomas. Oncogene 22, 4918-4923.

Shen, B., Y. Fang, N. Wu and S. J. Gould. "Biogenesis of the Posterior Pole Is Mediated by the Exosome/Microvesicle Protein-Sorting Pathway." J Biol Chem 286, no. 51 (2011): 44162-76.

Shirahata, M., Iwao-Koizumi, K., Saito, S., Ueno, N., Oda, M., Hashimoto, N., Takahashi, J.A., and Kato, K. (2007). Gene expression-based molecular diagnostic system for malignant gliomas is superior to histological diagnosis. Clin Cancer Res 13, 7341-7356.

Simons, M. and G. Raposo. "Exosomes--Vesicular Carriers for Intercellular Communication." Curr Opin Cell Biol 21, no. 4 (2009): 575-81.

Simpson RJ, Lim JW, Moritz RL, Mathivanan S. Exosomes: proteomic insights and diagnostic potential. Expert Rev Proteomics. 6(3):267-83.

Singh SK, Hawkins C, Clarke ID, Squire JA, Bayani J, Hide T, Henkelman RM, Cusimano MD, Dirks PB. (2004). Identification of human brain tumour initiating cells. Nature. 432(7015):396-401

Singh SK, Clarke ID, Terasaki M, Bonn VE, Hawkins C, Squire J, Dirks PB. (2003). Identification of a cancer stem cell in human brain tumors. Cancer Res. 63(18):5821-8.

Singh, H., M. A. Cousin and R. H. Ashley. "Functional Reconstitution of Mammalian 'Chloride Intracellular Channels' Clic1, Clic4 and Clic5 Reveals Differential Regulation by Cytoskeletal Actin." Febs j 274, no. 24 (2007): 6306-16.

Skog J, Würdinger T, Rijn Sjoerd van, H. Meijer Dimphna, Gainche Laura, T. Curry William, S. Carter Bob, M. Krichevsky Anna and O. Breakefield Xandra. "Glioblastoma Microvesicles Transport Rna and Proteins That Promote Tumour Growth and Provide Diagnostic Biomarkers." Nature Cell Biology 10, no. 12 (2008): 1470-1476.

Sobo, K., Le Blanc, I., Luyet, P.P., Fivaz, M., Ferguson, C., Parton, R.G., Gruenberg, J., and van der Goot, F.G. (2007). Late endosomal cholesterol accumulation leads to impaired intra-endosomal trafficking. PLoS One 2, e851.

Son, M.J., Woolard, K., Nam, D.H., Lee, J., and Fine, H.A. (2009). SSEA-1 is an enrichment marker for tumor-initiating cells in human glioblastoma. Cell Stem Cell 4, 440-452.

Soroceanu, L., Kharbanda, S., Chen, R., Soriano, R.H., Aldape, K., Misra, A., Zha, J., Forrest, W.F., Nigro, J.M., Modrusan, Z., et al. (2007). Identification of IGF2 signaling through phosphoinositide-3-kinase regulatory subunit 3 as a growth-promoting axis in glioblastoma. Proc Natl Acad Sci U S A 104, 3466-3471.

Staubach, S., H. Razawi and F. G. Hanisch. "Proteomics of Muc1-Containing Lipid Rafts from Plasma Membranes and Exosomes of Human Breast Carcinoma Cells Mcf-7." Proteomics 9, no. 10 (2009): 2820-35.

Stiles, C.D., and Rowitch, D.H. (2008). Glioma stem cells: a midterm exam. Neuron 58, 832-846.

Stupp, R., Hegi, M.E., Gilbert, M.R., and Chakravarti, A. (2007). Chemoradiotherapy in malignant glioma: standard of care and future directions. J Clin Oncol 25, 4127-4136.

Stupp, R., Mason, W.P., van den Bent, M.J., Weller, M., Fisher, B., Taphoorn, M.J., Belanger, K., Brandes, A.A., Marosi, C., Bogdahn, U., et al. (2005). Radiotherapy plus concomitant and adjuvant temozolomide for glioblastoma. N Engl J Med 352, 987-996.

Suslov, O.N., Kukekov, V.G., Ignatova, T.N., and Steindler, D.A. (2002). Neural stem cell heterogeneity demonstrated by molecular phenotyping of clonal neurospheres. Proc Natl Acad Sci U S A 99, 14506-14511.harding

Tang, H. Y., L. A. Beer, T. Chang-Wong, R. Hammond, P. Gimotty, G. Coukos and D. W. Speicher. "A Xenograft Mouse Model Coupled with in-Depth Plasma Proteome Analysis Facilitates Identification of Novel Serum Biomarkers for Human Ovarian Cancer." J Proteome Res 11, no. 2 (2012): 678-91.

Taylor RE, Bailey CC, Robinson KJ, Weston CL, Walker DA, Ellison D, Ironside J, Pizer BL, Lashford LS. (2005). Outcome for patients with metastatic (M2-3) medulloblastoma treated with SIOP/UKCCSG PNET-3 chemotherapy. Eur J Cancer. 41(5):727-34.

TCGA (2008). Comprehensive genomic characterization defines human glioblastoma genes and core pathways. Nature 455, 1061-1068.

Thery, C., M. Boussac, P. Veron, P. Ricciardi-Castagnoli, G. Raposo, J. Garin and S. Amigorena. "Proteomic Analysis of Dendritic Cell-Derived Exosomes: A Secreted Subcellular Compartment Distinct from Apoptotic Vesicles." J Immunol 166, no. 12 (2001): 7309-18.

Thery, C., M. Ostrowski and E. Segura. "Membrane Vesicles as Conveyors of Immune Responses." Nat Rev Immunol 9, no. 8 (2009): 581-93.

Toma, J.G., Akhavan, M., Fernandes, K.J., Barnabe-Heider, F., Sadikot, A., Kaplan, D.R., and Miller, F.D. (2001). Isolation of multipotent adult stem cells from the dermis of mammalian skin. Nat Cell Biol 3, 778-784.

Trajkovic, Katarina, Chieh Hsu, Salvatore Chiantia, Lawrence Rajendran, Dirk Wenzel, Felix Wieland, Petra Schwille, Britta Brügger and Mikael Simons. "Ceramide Triggers Budding of Exosome Vesicles into Multivesicular Endosomes." Science 319, no. 5867 (2008): 1244-1247.

Trams, E. G., C. J. Lauter, N. Salem, Jr. and U. Heine. "Exfoliation of Membrane Ecto-Enzymes in the Form of Micro-Vesicles." Biochim Biophys Acta 645, no. 1 (1981): 63-70.

Tulk, B. M. and J. C. Edwards. "Ncc27, a Homolog of Intracellular Cl- Channel P64, Is Expressed in Brush Border of Renal Proximal Tubule." Am J Physiol 274, no. 6 Pt 2 (1998): F1140-9.

Tung, J. J. and J. Kitajewski. "Chloride Intracellular Channel 1 Functions in Endothelial Cell Growth and Migration." J Angiogenes Res 2, (2010): 23.

Turcan, S., Rohle, D., Goenka, A., Walsh, L.A., Fang, F., Yilmaz, E., Campos, C., Fabius, A.W., et al., Nature. 2012 Feb 15;483(7390):479-83. doi: 10.1038/nature10866.

Uchida N, Buck DW, He D, Reitsma MJ, Masek M, Phan TV, Tsukamoto AS, Gage FH, Weissman IL. Direct isolation of human central nervous system stem cells. Proc Natl Acad Sci U S A. 97(26):14720-5.

Uhrbom, L., Dai, C., Celestino, J.C., Rosenblum, M.K., Fuller, G.N., and Holland, E.C. (2002). Ink4a-Arf loss cooperates with KRas activation in astrocytes and neural progenitors to generate glioblastomas of various morphologies depending on activated Akt. Cancer Res 62, 5551-5558.

Ulmasov, B., J. Bruno, P. G. Woost and J. C. Edwards. "Tissue and Subcellular Distribution of Clic1." BMC Cell Biol 8, (2007): 8.

Valadi, H., K. Ekstrom, A. Bossios, M. Sjostrand, J. J. Lee and J. O. Lotvall. "Exosome-Mediated Transfer of Mrnas and Micrornas Is a Novel Mechanism of Genetic Exchange between Cells." Nat Cell Biol 9, no. 6 (2007): 654-9.

Valenzuela, Stella M., Donald K. Martin, Suzanne B. Por, Joan M. Robbins, Kristina Warton, Michelle R. Bootcov, Peter R. Schofield, Terence J. Campbell and Samuel N. Breit. "Molecular Cloning and Expression of a Chloride Ion Channel of Cell Nuclei." Journal of Biological Chemistry 272, no. 19 (1997): 12575-12582.

Valenzuela, S. M., M. Mazzanti, R. Tonini, M. R. Qiu, K. Warton, E. A. Musgrove, T. J.

Campbell and S. N. Breit. "The Nuclear Chloride Ion Channel Ncc27 Is Involved in Regulation of the Cell Cycle." J Physiol 529 Pt 3, (2000): 541-52.

van den Boom, J., Wolter, M., Kuick, R., Misek, D.E., Youkilis, A.S., Wechsler, D.S., Sommer, C., Reifenberger, G., and Hanash, S.M. (2003). Characterization of gene expression profiles associated with glioma progression using oligonucleotide-based microarray analysis and real-time reverse transcription-polymerase chain reaction. Am J Pathol 163, 1033-1043.

van Niel, G., I. Porto-Carreiro, S. Simoes and G. Raposo. "Exosomes: A Common Pathway for a Specialized Function." J Biochem 140, no. 1 (2006): 13-21.

Vella, L. J., R. A. Sharples, V. A. Lawson, C. L. Masters, R. Cappai and A. F. Hill. "Packaging of Prions into Exosomes Is Associated with a Novel Pathway of Prp Processing." J Pathol 211, no. 5 (2007): 582-90.

Verhaak, R.G., Hoadley, K.A., Purdom, E., Wang, V., Qi, Y., Wilkerson, M.D., Miller, C.R., Ding, L., Golub, T., Mesirov, J.P., et al. (2010). Integrated genomic analysis identifies clinically relevant subtypes of glioblastoma characterized by abnormalities in PDGFRA, IDH1, EGFR, and NF1. Cancer Cell 17, 98-110.

Vescovi, A.L., Galli, R., and Reynolds, B.A. (2006). Brain tumour stem cells. Nat Rev Cancer 6, 425-436.

Vik-Mo, E.O., Sandberg, C., Olstorn, H., Varghese, M., Brandal, P., Ramm-Pettersen, J., Murrell, W., and Langmoen, I.A. (2010). Brain tumor stem cells maintain overall phenotype and tumorigenicity after in vitro culturing in serum-free conditions. Neuro Oncol.

Vital, A.L., Tabernero, M.D., Castrillo, A., Rebelo, O., Tao, H., Gomes, F., Nieto, A.B., Resende Oliveira, C., Lopes, M.C., and Orfao, A. (2010). Gene expression profiles of human glioblastomas are associated with both tumor cytogenetics and histopathology. Neuro Oncol 12, 991-1003.

von Deimling, A., Korshunov, A., and Hartmann, C. (2011). The next generation of glioma biomarkers: MGMT methylation, BRAF fusions and IDH1 mutations. Brain Pathol 21, 74-87.

Vredenburgh, J.J., Desjardins, A., Herndon, J.E., 2nd, Marcello, J., Reardon, D.A., Quinn, J.A., Rich, J.N., Sathornsumetee, S., Gururangan, S., Sampson, J., et al. (2007). Bevacizumab plus irinotecan in recurrent glioblastoma multiforme. J Clin Oncol 25, 4722-4729.

Wang, R., Chadalavada, K., Wilshire, J., Kowalik, U., Hovinga, K.E., Geber, A., Fligelman, B., Leversha, M., Brennan, C., and Tabar, V. (2010). Glioblastoma stem-like cells give rise to tumour endothelium. Nature 468, 829-833.

Wang Z, Liu H, Gu Y, Chapman ER. (2011). Reconstituted synaptotagmin I mediates vesicle docking, priming, and fusion. J Cell Biol. 195(7):1159-70.

Weis, S.M., and Cheresh, D.A. (2005). Pathophysiological consequences of VEGF-induced vascular permeability. Nature 437, 497-504.

Wen, P.Y., and Kesari, S. (2008). Malignant gliomas in adults. N Engl J Med 359, 492-507.

Westermark, B., Heldin, C.H., and Nister, M. (1995). Platelet-derived growth factor in human glioma. Glia 15, 257-263.

Westermark B, Nistér M. (1995). Molecular genetics of human glioma. Curr Opin Oncol. 7(3):220-5. Review.

White, I. J., L. M. Bailey, M. R. Aghakhani, S. E. Moss and C. E. Futter. "Egf Stimulates Annexin 1 Dependent Inward Vesiculation in a Multivesicular Endosome Subpopulation." Embo j 25, no. 1 (2006): 1-12.

Wang S., Cesca F., Loers G, Michaela Schweizer, Friedrich Buck, Fabio Benfenati, Melitta Schachner and Ralf Kleene. "Synapsin I Is an Oligomannose-Carrying Glycoprotein, Acts as an Oligomannose-Binding Lectin, and Promotes Neurite Outgrowth and Neuronal Survival When Released Via Glia-Derived Exosomes." The Journal of Neuroscience 31, no. 20 (2011): 7275-7290.

Wang, P., C. Zhang, P. Yu, B. Tang, T. Liu, H. Cui and J. Xu. "Regulation of Colon Cancer Cell Migration and Invasion by Clic1-Mediated Rvd." Mol Cell Biochem 365, no. 1-2 (2012): 313-21.

Welton, J. L., S. Khanna, P. J. Giles, P. Brennan, I. A. Brewis, J. Staffurth, M. D. Mason and A. Clayton. "Proteomics Analysis of Bladder Cancer Exosomes." Mol Cell Proteomics 9, no. 6 (2010): 1324-38

Wubbolts, R., R. S. Leckie, P. T. Veenhuizen, G. Schwarzmann, W. Mobius, J. Hoernschemeyer, J. W. Slot, H. J. Geuze and W. Stoorvogel. "Proteomic and Biochemical Analyses of Human B Cell-Derived Exosomes. Potential Implications for Their Function and Multivesicular Body Formation." J Biol Chem 278, no. 13 (2003): 10963-72.

Yan, H., Parsons, D.W., Jin, G., McLendon, R., Rasheed, B.A., Yuan, W., Kos, I., Batinic-Haberle, I., Jones, S., Riggins, G.J., et al. (2009). IDH1 and IDH2 mutations in gliomas. N Engl J Med 360, 765-773.

Yuan, H., Corbi, N., Basilico, C., and Dailey, L. (1995). Developmental-specific activity of the FGF-4 enhancer requires the synergistic action of Sox2 and Oct-3. Genes Dev 9, 2635-2645.

Yuan, X., Curtin, J., Xiong, Y., Liu, G., Waschsmann-Hogiu, S., Farkas, D.L., Black, K.L., and Yu, J.S. (2004). Isolation of cancer stem cells from adult glioblastoma multiforme. Oncogene 23, 9392-9400.

Zoller, M. "Tetraspanins: Push and Pull in Suppressing and Promoting Metastasis." Nat Rev Cancer 9, no. 1 (2009): 40-55.